



UNIVERSITÀ DEGLI STUDI DI SALERNO
DIPARTIMENTO DI FARMACIA



Francesco Pagano

Dottorato di ricerca
in Scienze Farmaceutiche
Ciclo NS XIII - 2012-2015

*Characterization and biological properties
of Citrus industrial derivatives and waste products
for the formulation of nutraceuticals*

*Characterization and biological properties
of Citrus industrial derivatives and waste products
for the formulation of nutraceuticals*



Francesco Pagano



Dipartimento di Farmacia
Via Giovanni Paolo II, 132 84084
Fisciano, Salerno



UNIVERSITÀ DEGLI STUDI DI SALERNO



UNIVERSITÀ DEGLI STUDI DI SALERNO

Dipartimento di Farmacia

Dottorato di ricerca

in Scienze Farmaceutiche

Ciclo XIII NS – 2012-2015

Coordinatore: Chiar.mo Prof. *Gianluca Sbardella*

***Characterization and biological properties of Citrus
industrial derivatives and waste products for the formulation
of nutraceuticals***

settore scientifico disciplinare di afferenza: CHIM/08

Dottorando

Tutore

Dott. *Francesco Pagano*

Chiar.mo Prof.

Pietro Campiglia

Co-tutore

Chiar.mo Prof.

Gianluca Sbardella

INDEX

CHAPTER I:

Phytochemicals and health: the effect of polyphenols in the inflammation process	- 1 -
1. Introduction	- 2 -
2. Nutraceutical:	- 2 -
2.1 <i>Definition</i>	- 2 -
2.2 <i>Nutraceuticals marketing</i>	- 3 -
3. Polyphenols	- 5 -
4. High Performance Liquid Chromatography (HPLC):	- 8 -
4.1 <i>Definition</i>	- 8 -
4.2 <i>Fundamental principles</i>	- 9 -
4.3 <i>Chromatographic parameters</i>	- 12 -
4.3.1 <i>Retention</i>	- 12 -
4.3.2 <i>Separation</i>	- 14 -
4.3.3 <i>Column efficiency</i>	- 14 -
5. Optimization of an HPLC separation	- 18 -
5.1 <i>Stationary phase particle size</i>	- 18 -
5.2 <i>Columns with reduced dimensions</i>	- 19 -
6. Mass spectrometric detectors	- 21 -
6.1 <i>Definition</i>	- 21 -
6.2 <i>Atmospheric-pressure chemical ionization</i>	- 22 -
6.3 <i>Electrospray ionization</i>	- 23 -
7. Inflammation	- 25 -
7.1 <i>Definition</i>	- 25 -
7.2 <i>Mediators of the inflammatory process</i>	- 27 -
7.2.1 <i>Nitric oxide synthase (iNOS):</i>	- 28 -
7.2.2 <i>Cyclooxygenase</i>	- 30 -

7.2.3 Reactive Oxygen Species (ROS)	- 31 -
8. Aim of research	- 32 -
9. References	- 33 -

CHAPTER II:

Development of fast analytical methods for the characterization of flavonoids in Citrus bergamia juice: An UHPLC-IT-TOF approach ..	- 38 -
Abstract	- 39 -
Keywords	- 39 -
1. Introduction	- 39 -
2. Materials and methods	- 42 -
2.1 Reagents and standards	- 42 -
2.2 Sample preparation.....	- 42 -
2.3 Instrumentation	- 42 -
2.4 UHPLC conditions.....	- 43 -
2.5 ESI-IT-TOF-MS parameters	- 43 -
2.6 Scavenging of 1, 1 diphenyl-2-picrylhydrazyl (DPPH) radicals	- 44 -
3. Results and discussion	- 45 -
3.1 Optimization of chromatographic parameters	- 45 -
3.2 Quantitative analysis of lyophilized juices	- 49 -
3.3 ESI-IT-TOF-MS elucidation of flavonoid profiles.....	- 50 -
3.4 Antioxidant activity.....	- 53 -
4. Conclusions	- 56 -
5. References	- 56 -

CHAPTER III:

UHPLC profiling and effects on LPS-stimulated J774A.1 macrophages of flavonoids from Citrus bergamia juice industry, an underestimated waste product with high anti-inflammatory potential	- 62 -
Abstract	- 63 -
Keywords	- 63 -
1. Introduction	- 63 -
2. Materials and methods	- 65 -
2.1 <i>Reagents and standards</i>	- 65 -
2.2 <i>Sample preparation</i>	- 65 -
2.3 <i>Instrumentation and UHPLC–MS/MS conditions</i>	- 65 -
2.4 <i>Cell culture</i>	- 66 -
2.5 <i>Antiproliferative activity</i>	- 66 -
2.6 <i>Measurement of intracellular reactive oxygen species (ROS)</i>	- 67 -
2.7 <i>Nitrite determination and Western blot analysis for iNOS, COX-2 and HO-1 expression</i>	- 67 -
2.8 <i>Data analysis</i>	- 68 -
3. Results and discussion	- 68 -
3.1 <i>UHPLC–MS/MS quantitative and qualitative analysis of juice</i>	- 68 -
3.2 <i>Effect of bergamot juice on LPS-stimulated macrophages</i>	- 73 -
4. Conclusions	- 79 -
5. References	- 79 -

CHAPTER IV:

Flavonoids from *Citrus sinensis* extract: anti-inflammatory and

hypoglycemic evaluation	- 84 -
Abstract	- 85 -
Keywords	- 85 -
1. Introduction	- 85 -
2. Materials and methods	- 87 -
2.1 <i>Reagents and standards</i>	- 87 -
2.2 <i>Sample preparation</i>	- 88 -
2.3 <i>Instrumentation</i>	- 88 -
2.4 <i>UHPLC-PDA Conditions</i>	- 89 -
2.5 <i>UHPLC-ESI-IT-TOF Conditions</i>	- 89 -
2.6 <i>Cells and Reagents for cell culture</i>	- 90 -
2.7 <i>Antiproliferative assay</i>	- 90 -
2.8 <i>Nitrite Determination and Western Blot Analysis for iNOS, COX-2 and HO-1 Expression</i>	- 91 -
2.9 <i>TNF-α Determination</i>	- 92 -
2.10 <i>Immunofluorescence Analysis with Confocal Microscopy</i>	- 93 -
2.11 <i>Measurement of Intracellular ROS</i>	- 93 -
2.12 <i>Glucose uptake</i>	- 94 -
2.13 <i>Lipid peroxidation assay</i>	- 94 -
2.14 <i>Digestion in vitro</i>	- 95 -
2.15 <i>Statistical Analysis</i>	- 96 -
3. Results and discussions	- 96 -
3.1 <i>Identification of Flavonoids and Polymethoxyflavones</i>	- 96 -
3.2 <i>Quantitative Analysis of <i>Citrus sinensis</i> extract</i>	- 97 -
3.3 <i><i>Citrus sinensis</i> extract reduces LPS-induced NO, iNOS, COX-2 and TNF-α in J774A.1 macrophages</i>	- 99 -

3.4 <i>Citrus sinensis</i> extract inhibits p65 NF- κ B nuclear translocation in LPS-treated macrophages.....	102 -
3.5 Antioxidant activity of <i>Citrus sinensis</i> juice extract	104 -
3.6. <i>Citrus sinensis</i> juice extract induces the cytoprotective enzyme HO-1 in LPS-treated J774A.1 macrophages	105 -
3.7 <i>Citrus sinensis</i> induced antiproliferative effect of HepG2 cell lines ..	106 -
4. Discussion	107 -
4.1 Simulated digestion of the extract of <i>Citrus sinensis</i>	111 -
5. Conclusions	116 -
6. References	116 -

CHAPTER V:

Detailed elucidation of Annurca (<i>M. pumila</i> Miller cv Annurca) apple polyphenols by a combination of RP-UHPLC and HILIC coupled to IT-TOF mass spectrometry	122 -
Abstract	123 -
Keywords	123 -
1. Introduction	123 -
2. Materials and methods	126 -
2.1 <i>Chemicals</i>	126 -
2.2 <i>Fruit collection and sample preparation</i>	126 -
2.3 <i>Instrumentation</i>	127 -
2.4 <i>RP-UHPLC and HILIC-PDA-ESI-IT-TOF conditions</i>	127 -
3. Results and discussion	129 -
3.1 <i>RP-UHPLC-DAD-ESI-IT-TOF profiling of polyphenolic extract</i>	129 -
3.1.1 <i>Hydroxycinnamic acids</i>	130 -
3.1.2 <i>Dihydrochalcones</i>	138 -
3.1.3 <i>Anthocyanins</i>	138 -

3.1.4 Flavonols	- 139 -
3.1.5 Flavanones.....	- 142 -
3.1.6 Flavan-3-ols.....	- 142 -
3.1.7 Other compounds.....	- 143 -
3.1.8 Procyanidins	- 143 -
3.1.9 HILIC-DAD-ESI-IT-TOF profiling of Annurca procyanidins.....	- 144 -
4. Conclusions	- 148 -
5. References	- 149 -

CHAPTER VI:

Vitis vinifera (cv. Aglianico): healthy properties and polyphenolic profile of berry skin, wine and grape juices	- 155 -
Abstract	- 156 -
Keywords	- 156 -
1. Introduction	- 157 -
2. Materials and methods	- 159 -
2.1 Reagents and standards	- 159 -
2.2 Experimental vineyard, plant material, grapes and grape juice	- 160 -
2.3 Lyophilization	- 161 -
2.4 Total Phenolic Content	- 161 -
2.5 Total Flavonol Content	- 161 -
2.6 Total Monomeric Anthocyanin	- 162 -
2.7 Flavonol and anthocyanin extractions from berry skin and wine of Aglianico grapes	- 162 -
2.8 Identification and quantification of flavonols and anthocyanins	- 163 -
2.9 Determination of cis- and trans-resveratrol	- 164 -
2.10 Total antioxidant capacity	- 165 -
2.11 Metal determination.....	- 165 -

<i>2.12 Cell Culture and Viability Test</i>	- 166 -
<i>2.13 Preparation of Cell Extract</i>	- 167 -
<i>2.14 Measurement of Intracellular ROS Accumulation</i>	- 167 -
<i>2.15 Measurement of Cellular Superoxide Dismutase (SOD)</i>	- 168 -
<i>2.16 Measurement of Caspase-3 Activity</i>	- 168 -
<i>2.17 Statistics</i>	- 168 -
3. Results and discussion	- 169 -
<i>3.1 Flavonols and anthocyanins</i>	- 169 -
<i>3.2 Resveratrol and total antioxidant capacity</i>	- 178 -
<i>3.3 Polyphenolic composition and antioxidant capacity</i>	-178 -
<i>3.4 Effects of grape juice after lyophilization on Cardiomyocytes</i>	- 181 -
<i>3.5 Metals</i>	- 186 -
4. References	- 188 -

CHAPTER I

Phytochemicals and health: the effect of polyphenols in the inflammation process

1. Introduction

As the population lives longer, since the standard of living has improved, age and life-style related diseases, such as cardiovascular, neurodegenerative, and cancer pathologies, arise more frequently. Many studies have underlined that a correct and well-balanced diet is one of the best strategies to reduce the possible onset of chronic pathologies and improve or maintain the health status. From ancient times, it is widely accepted that an intake of fruits and vegetables has a direct impact on health. These effects are related to the high content of phytochemicals, that exert many biological activities. These substances, which are usually secondary metabolites in plants and fruits possess a drug-like effect, even if have less potency, but also less side effects. If these molecules are regularly assumed, in daily diet, can show a long term prevention. Driven by these observations the consumers demand for “healthy” foods is increasing. In this regard in the last years there was the appearance on the market of many products containing bioactive phytochemicals derived from plants or fruits, these products are sold in pharmaceutical form (such as tablets, pills, capsules) and incorporate phytochemical extracts. These products cannot be classified as food or drugs, but as a new entity called “Nutraceuticals”, which comprises the terms nutrition and pharmaceutical.

2. Nutraceutical

2.1 Definition

The neologism "nutraceutical" was born from the union of "nutrition" and "pharmaceutical" coined for the first time by Dr. Stephen De Felice in 1989, in order to identify the study of those foods or parts of them that have a beneficial

effect on health human^[1,2]. Such foods are mainly used to associate the nutritional components, such as high digestibility and hypoallergenic, and some healing properties of natural active ingredients extracted from plants of recognized effectiveness. The study of these combined characteristics - nutritional and pharmaceutical - specific foods that, through their properties, stand behind the demarcation line among "food" and "drug". In this way, food can be divided into two distinct categories: the real Nutraceuticals and Functional Foods^[3]. The first refer to specific substances in foods with known medicinal properties; the latter, however, denote foods in the proper sense that exert beneficial properties for the human body through their introduction in the diet. The Nutraceuticals are not to be confused with nutritional supplements, because they identify with biological substances, usually concentrated, with therapeutic and protective characteristics; while functional foods, associated with nutritional factors, the pharmaceutical properties of natural active ingredients, which promote the food matrix enriching it by means of molecules capable of prevent possible diseases. In fact, it is not possible to make a very definite division between the two categories, so that often the terms can be used in a broader sense including nutraceutical foods or functional beverages and dietary supplements^[4,5].

2.2 Nutraceuticals marketing

The market in recent years saw the rapid spread of more and more foods enriched with beneficial molecules, such as milk and yogurt with added coenzyme Q10, Sterols, Omega 3 and vitamins, but also drinks, fruit juices, biscuits and breakfast cereals. Among the most important nutraceuticals, in addition to vitamins, minerals, caffeine, protein, were carnitine, lycopene, the essential polyunsaturated fatty acids, the anthocyanins and resveratrol. What is known is that nutraceuticals are used to improve the health, delay the aging process, prevent chronic disease and

increase life expectancy. For these reasons, these substances are used for the prevention of chronic diseases of aging and the maintenance of the typical functions of youth (beauty, energy, wellbeing) and could have a huge potential in terms of impact on public health. Therefore, the nutraceutical food can be considered a real therapeutic process "ongoing", used throughout life, with no risk of toxicity conceptually inherent to the use of "drugs". Since, then, the power supply is a real daily need for each individual, the use of diet and nutraceutical food, as a means of prevention and "wellness", or maybe anti-aging strategy, could have a decisive impact not only on health but also on the global market. In addition to the proposal of nutraceuticals is in rapid evolution and their application in the world, growing at 20% per year. The nutraceuticals represent a market that, despite the period of global crisis, registered a continuous growth, offering significant investment opportunities for both the pharmaceutical industry and for the food. (Figure 1).

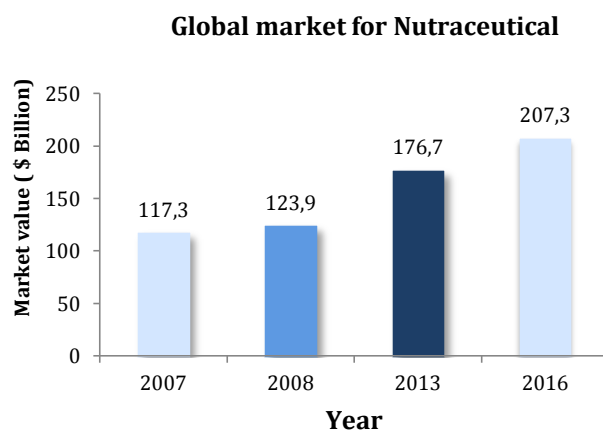
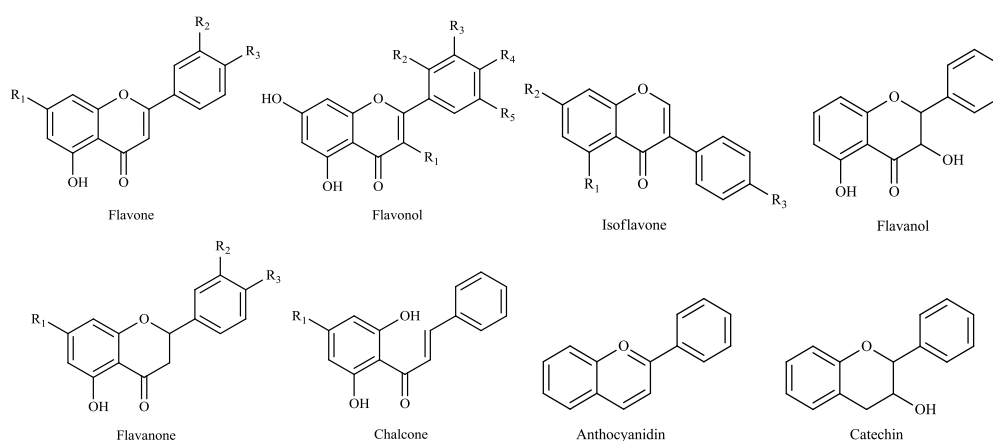


Figure 1: *Trend of nutraceutical market*

3. Polyphenols

Among bioactive phytochemicals contained in these formulations, polyphenols are the most interesting molecules. Polyphenolic compounds originate from one of the main classes of secondary metabolites in plants derived from phenylalanine and, to a lesser extent in some plants, also from tyrosine^[6]. Chemically, phenolics can be defined as substances possessing an aromatic ring bearing one or more hydroxyl groups, including their functional derivatives. Plants and foods contain a large variety of phenolic derivatives including simple phenols, phenylpropanoids, benzoic acid derivatives, flavonoids, stilbenes, tannins, lignans and lignins. In the last ten years flavonoids have gained attention, due to the extensive scientific literature concerning about their biological activity. Flavonoids are a large group of structurally related compounds with a chromane-type skeleton, with a phenyl substituent in the C2 or C3 position. The main flavonoid subclasses are depicted in Figure 2.



Flavanone		R₁	R₂	R₃	MW
1	Hesperetin	OH	OH	OCH ₃	302
2	Hesperidin	7-O-Rha-glu	OH	OCH ₃	610
3	Naringin	7-O-Rha-glu	H	OH	580
4	Naringenin	OH	H	OH	272
5	Eriocitrin	7-O-Rha-glu	OH	OH	596
6	Eriodyctiol	OH	OH	OH	288
7	Isosakuramentin	OH	H	OCH ₃	286

Flavone		R₁	R₂	R₃	MW
8	Chrysoeriol	OH	OCH ₃	OH	300
9	Chrysin	OH	H	H	254
10	Apigenin	OH	H	OH	270
11	Luteolin	OH	OH	OH	286
12	Acacetin	OH	H	OCH ₃	284
13	Genkwanin	OCH ₃	H	OH	284

Flavonol		R₁	R₂	R₃	R₄	R₅	MW
14	Rutin	3-O-Rha-glu	H	OH	OH	H	610
15	Kaempferol	OH	H	H	OH	H	286
16	Quercetin	OH	H	OH	OH	H	302
17	Morin	OH	OH	H	OH	H	302
18	Isorhamnetin	OH	H	OCH ₃	OH	H	316
19	Myricetin	OH	H	OH	OH	OH	318
20	Fisetin	OH	H	H	OH	OH	286

Isoflavone		R₁	R₂	R₃	MW
21	Biochanin A	OH	OH	OCH ₃	284
22	Sissotrin	OH	7-O-glu	OCH ₃	446
23	Genistein	OH	OH	OH	270
24	Genistin	OH	7-O-glu	OH	432
25	Formomonetin	H	OH	OCH ₃	268
26	Omonin	H	7-O-glu	OCH ₃	430
27	Daidzein	H	OH	OH	254
28	Daidzin	H	7-O-glu	OH	416

Figure 2: Structures and molecular weights of the main flavonoid subclasses

Flavonoids are often hydroxylated in positions 3, 5, 7, 3', 4' and/or 5'. Frequently, one or more of these hydroxyl groups are methylated, acetylated, prenylated or sulphated. In plants, flavonoids are often present as O- or C glycosides; O bonding in flavonoids occurs far more frequently than C bonding. The O-glycosides have

sugar substituents bound to a hydroxyl group of the aglycone, usually located at position 3 or 7, whereas the C-glycosides have sugar groups bound to a carbon of the aglycone, usually 6-C or 8-C. The most common carbohydrates are rhamnose, glucose, galactose and arabinose. Flavonoid-diglycosides are also frequently found. Two very common disaccharides contain glucose and rhamnose, 1→6 linked in neohesperidose and 1→2 linked in rutinose. The sugars are often further substituted by acyl residues such as malonate and acetate. Flavonoids are referred to as glycosides when they contain one or more sugar groups (or glucosides in case of a glucose moiety), and as aglycones when no sugar group is present. Given the above structural variety, it will come as no surprise that there is an extremely large number of flavonoids. Typical quotations include “>4000 known flavonoids comprising 12 subclasses”^[7], “more than 3000 flavones and more than 700 known isoflavones exist in plants”^[8] and “almost 6500 different flavonoids are known”^[9]. Flavonoids are one of the largest groups of secondary metabolites, and they play an important role in plants as defence and signalling compounds in reproduction, pathogenesis and symbiosis^[10,11]. Plant flavonoids are involved in response mechanisms against stress, as caused by elevated UV-B radiation^[12-15] infection by microorganisms^[16] or herbivore attack^[17]. Flavonoids are one of the largest groups of secondary metabolites, and they play an important role in plants as defence and signalling compounds in reproduction, pathogenesis and symbiosis^[10,11]. Plant flavonoids are involved in response mechanisms against stress, as caused by elevated UV-B radiation^[12-15], infection by microorganisms^[16] or herbivore attack^[17]. Since the major part of nutraceuticals on the market are based on polyphenols such as anthocyanins, proanthocyanidins, flavonols, stilbenes, hydroxycinnamates, coumarins, ellagic acid (EA) and ellagitannins (ETs), etc. a great attention is focused on their natural sources. In this regard the food industry is not only interested in phytochemicals derived from plants, but also from by-

products of food industry. The processing of plant foods results in the production of by-products that are rich sources of bioactive compounds, including phenolic compounds^[16]. The citrus industry produces large quantities of peels and seed residue, which may account for up to 50 % of the total fruit weight^[19]. Citrus industry by-products, if utilised optimally could be major sources of phenolic compounds as the peels, in particular, have been found to contain higher amounts of total phenolics compared to the edible portions. Gorinstein et al. (2001) found that the total phenolics content in peels of lemons, oranges, and grapefruit were 15% higher than those in the peeled fruits^[20]. The healthy properties of polyphenols are related to the chemical structure, for this reason the isolation, identification and quantitation of the polyphenolic compounds in natural sources has gained a lot of attention during the last years. Among analytical techniques for the analysis and characterization of polyphenols, the most widespread methods are based on high performance liquid chromatography (HPLC) coupled to mass spectrometry (MS).

4. High Performance Liquid Chromatography (HPLC)

4.1 Definition

Liquid Chromatography (LC) is the oldest chromatographic method and one of the most widely used analytical technique. In liquid chromatography, separation is based on the selective distribution of analytes between a liquid mobile phase and a stationary phase. By using LC, it is possible to analyse an extensive range of compounds with various molecular weights, from hundreds to hundreds of thousands. It can be used in several applicational fields such as the pharmaceutical, clinical, biochemistry, food, drugs, several chemical industries and environmental. This method can be applied to trace analyses with detection limits in the ppb range and to preparative analyses when large quantities of compounds are analysed. The

inventors of modern liquid chromatography, Martin and Synge^[21], were aware that, in theory, the stationary phase requires very small particles and hence a high pressure is essential for forcing the mobile phase through the column. As a result, HPLC is sometimes referred to as high-pressure liquid chromatography. Otherwise the term high-performance liquid chromatography (HPLC) is used, but there is still not a general agreement on that term. High Performance Liquid Chromatography as compared with the classical liquid chromatographic techniques is characterized by:

- small diameter (2-5 mm), reusable stainless steel columns;
- column packings with very small (3, 5 and 10 μm) particles and the continual development of new substances to be used as stationary phases;
- relatively high inlet pressures and controlled flow of the mobile phase;
- precise sample introduction without the need for large samples;
- special continuous flow detectors capable of handling small flow rates and detecting very small amounts;
- automated standardized instruments;
- rapid analysis;
- high resolution.

4.2 Fundamental principles

A number of distinct separation modes are employed in liquid chromatography. It can be carried out in various systems depending on the physical form of stationary phase. Two common approaches are used to bring the mobile phase and stationary phase into contact: planar and column chromatography. In the first one, the stationary phase coats a flat glass, metal, or plastic plate and is placed in a developing chamber. A reservoir containing the mobile phase is placed in contact

with the stationary phase, and the mobile phase moves by capillary action. In the second one, the stationary phase is placed in a narrow column through which the mobile phase moves under the influence of gravity or pressure. The stationary phase is either a solid or a thin, liquid film coating on a solid particulate packing material or the column's walls. There are many mechanisms by which the solutes can be separated in LC. Some more common ones are illustrated in Figure 3. In adsorption chromatography (Figure 3a), solutes are separated on the bases of their ability to adsorb to a solid stationary phase. In partition chromatography (Figure 3b), a thin liquid film coating a solid support serves as the stationary phase. Separation is based on the difference in the equilibrium partitioning of solutes between the liquid stationary phase and the mobile phase. In ion-exchange chromatography (Figure 3c), stationary phases consisting of a solid support with covalently attached anionic (e.g., $-\text{SO}_3^-$) or cationic (e.g., $-\text{N}(\text{CH}_3)_3^+$) functional groups are used. Ionic solutes are attached to the stationary phase by electrostatic forces. Ion-pair chromatography represents an alternative to the ion-exchange chromatography. An organic ionic substance is added to the mobile phase and forms an ion pair with a sample component of opposite charge. In size-exclusion (or gel-permeation) chromatography (Figure 3d), porous gels are used as stationary phases, and the separation is due to differences in the size of the solutes. Large solutes are unable to penetrate into the porous stationary phase and pass quickly through the column; smaller solutes enter into the porous stationary phase, increasing the time spent on the column.

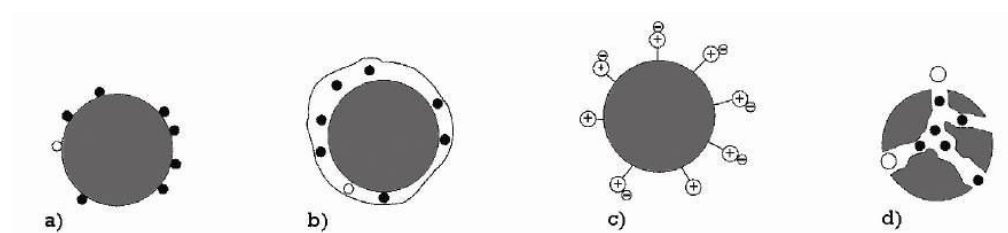


Figure 3: Schematics showing the basis of separation in (a) adsorption chromatography, (b) partition chromatography, (c) ion-exchange chromatography, (d) size exclusion chromatography. For the separations the solute represented by the solid circle (•) is the more strongly retained.

Today, most of HPLC separations are performed by liquid-solid chromatography (LSC), using a relatively non-polar hydrophobic sorbent as stationary phase and a polar mobile phase, referred to as reversed-phase LC (RPLC). A non-polar chemically modified (usually with octyl (C8) or octadecyl (C18) groups) silica gel is the most widespread stationary phase and aqueous organic solvents are commonly used. A solute molecule binds to an immobilized hydrophobic molecule in a polar solvent. This partitioning occurs as a result of the solute molecule tending to have hydrophobic patches at its surface, and binding via those patches to the matrix. An organic modifier is used to dissociate the bound molecule at a point at which the hydrophobic interaction between the exposed patches and the immobilized matrix is less favourable than the interaction between the bound molecule and the solvent. The molecule releases from the matrix and elutes. Reversed phase LC permits to separate components with different functionalities, of a polar and non-polar nature and has gained great popularity which is based on its exceptional range of applications, versatility and simplicity of operation. In terms of dimensions, HPLC columns with 2-5 mm (most often 4.6 mm) internal diameter (I.D.) are mostly used for analytical purposes. Wider columns are generally used for preparative work. On the other hand, the use of columns with

reduced I.D. has been one of the mainstreams of HPLC developments in recent years. Table 1 reports the classification of analytical HPLC columns according to their internal diameter^[22].

Table 1. Classification of HPLC columns according to the internal diameter

Column designation	Typical I.D. (mm)
Conventional HPLC	3-5
Narrow-bore HPLC	2
Micro LC	0.5-1
Capillary LC	0.1-0.5
Nano LC	0.01-0.1
Open tubular LC	0.005-0.05

Analytical HPLC columns are packed generally with micro particulate stationary phases (particle size 10 µm or less, most commonly 5 µm). If micro particulate stationary phases of 10 µm or less are used, the column length is 5, 10, 15 or 25 cm.

4.3 Chromatographic parameters

4.3.1 Retention

The goal of chromatography is to separate a sample into a series of chromatographic peaks, each representing a single component. The most important chromatographic parameters are described as follows. Retention volume V_R for a specific component, is defined as

$$V_R = t_R \cdot F$$

[Eq. 1.1]

where t_R is the retention time of the component and F is the mobile phase flow rate. The ratio of the amount of the compound in the stationary and mobile phase is defined as distribution coefficient K and can be calculated by:

$$K_D = \frac{C_s}{C_m}$$

[Eq. 1.2]

where C_s and C_m are the analyte concentrations in the stationary and mobile phase, respectively. The retention factor (formerly termed as capacity factor k'), k , is used. This can be calculated by

$$k = \frac{t_R - t_0}{t_0} = K_D \cdot \frac{V_S}{V_M} = \frac{n_S}{n_M} = \frac{V_R}{V_m} - 1$$

[Eq. 1.3]

where t_0 is the void time, n_S and n_M are the number of moles of the compound in the stationary and mobile phase, respectively and V_S and V_M are the volumes of the stationary and mobile phase in the column, respectively. From the retention time of an unretained component (void time) t_{R0} and the column length L the average linear velocity u of the mobile phase can be calculated:

$$u = \frac{L}{t_{R0}}$$

[Eq. 1.4]

Typical linear velocities in LC are in the range of 2-10 mm/s. The flow-rate F , which can easily be measured in LC, through a column with internal diameter d_c is given by:

$$F = \frac{1}{4} \pi d_c^2 \epsilon_u u$$

[Eq. 1.5]

4.3.2 Separation

Separation factor α (known also as relative retention) is a factor that is a measure of the selectivity of the chromatographic system. The separation factor for two components is calculated by:

$$\alpha = \frac{k_2}{k_1} = \frac{t_{R2} - t_0}{t_{R1} - t_0}$$

[Eq. 1.6]

where k_1 and k_2 are the retention factors and t_{R1} and t_{R2} are the retention times of the two components. Resolution (R) is a quantitative measure of the degree of separation between two chromatographic peaks, A and B, and is defined as

$$R = \frac{t_{R2} - t_{R1}}{0.5(w_2 + w_1)} = \frac{2\Delta t_R}{w_2 + w_1}$$

[Eq. 1.7]

where w_1 and w_2 are the peak widths of the two compounds at the baseline. The degree of separation between two chromatographic peaks improves with an increase in R . Thus, resolution is a quantitative measure of the effectiveness of a separation process.

4.3.3 Column efficiency

To obtain optimal separations, sharp, symmetrical chromatographic peaks must be obtained; hence band broadening must be limited. It is also convenient to measure the efficiency of the column, which is defined by the number of theoretical plates, N , which is calculated by:

$$N = 16 \left(\frac{t_R}{w} \right)^2 = 5.54 \left(\frac{t_R}{w_{1/2}} \right)^2 = 2\pi \left(\frac{h_P t_R}{A} \right)^2$$

[Eq. 1.8]

where $w_{1/2}$ is the peak width at half-height, h_p peak height and A peak area. The equation 1.8 yields correct results only if the peak has a Gaussian shape. Approximate values for asymmetric peaks can be calculated by the following equation^[23]:

$$N = 41.7 \frac{(t_R / w_{0.1})}{T + 1.25}$$

[Eq. 1.9]

where $w_{0.1}$ is the peak width at 10% of the peak height and T is the tailing factor (or peak asymmetry):

$$T = \frac{b_{0.1}}{a_{0.1}}$$

[Eq. 1.10]

where $a_{0.1}$ and $b_{0.1}$ are the sections (distances from the peak front to the maximum and from the maximum to peak end, respectively) of the peak width at 10% of the peak height. The number of theoretical plates depends on column length L: the longer the column, the higher the number of the plates. Therefore, another term has also been introduced relating the plate number to column length. This is the plate height H (HETP = height equivalent to a theoretical plate), which can be calculated:

$$H = \frac{L}{N}$$

[Eq. 1.11]

The width of a chromatographic peak is affected by a series of parameters, which are present in the van Deemter equation:

$$H = A + \frac{B}{u} + Cu = 1 \left[\left(\frac{1}{C_e d_p} \right) + \left(\frac{D_m}{C_m d_p^2 u} \right) \right] + \frac{C_d D_m}{u} + \frac{C_{sm} d_p^2 u}{D_m}$$

[Eq. 1.12]

where A accounts for multiple paths (H_p), B/u for longitudinal diffusion (H_d), and C_u for solute mass transfer in the stationary and mobile phases (H_s and H_m), being the experimental factors contributing to the broadening of a solute's chromatographic band; d_p is the particle size, D_m diffusion coefficient of a solute in the mobile phase. Factor A (Eddy diffusion) accounts for the fact that the solute molecules, while passing through the column, take random paths between the stationary phase particles. These different paths with different lengths will cause broadening of the solute band. Factor B (longitudinal diffusion) is related to the fact that the concentration of the analyte is lower at the edges of the band with respect to the centre. Analyte diffuses out from the centre to the edges, causing also band broadening. The effect of this factor is decreased when the velocity of the mobile phase is high. The factor C (resistance to mass transfer) depends on the fact that the analyte takes a certain time to equilibrate between the stationary and mobile phase. If the velocity of the mobile phase is high and the analyte has a strong affinity for the stationary phase, then the analyte in the mobile phase will move ahead of the analyte in the stationary phase and the band is broadened. The higher the velocity of the mobile phase, the worse the broadening becomes. Figure 4 represents the plot of the height of a theoretical plate as a function of mobile-phase velocity, so-called van Deemter curve. The optimum flow rate and the contributions to the terms A, B/u , and C_u are also shown.

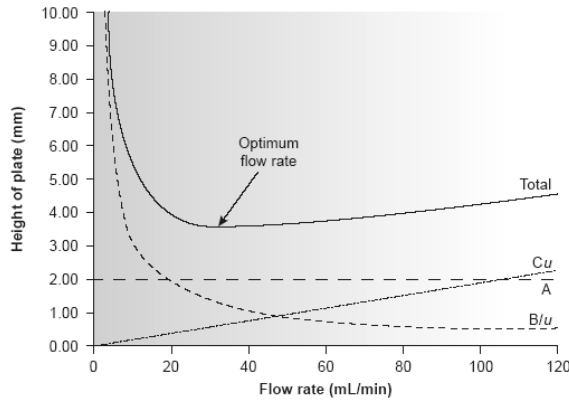


Figure 4: Plot of the height of a theoretical plate as a function of mobilephase velocity (using the van Deemter equation). The contributions to the terms A, B/u, and Cu are also shown.

The resolution R of two peaks is dependent on the separation factor, the column length, the plate height and the capacity ratio:

$$R = \frac{1}{4}(\alpha - 1) \sqrt{\frac{L}{H} \left(\frac{k_1}{1+k} \right)} = \frac{1}{4} \frac{\alpha - 1}{\alpha} \sqrt{\frac{L}{H} \frac{k_2}{1+k}},$$

$$\bar{k} = \frac{k_1 + k_2}{2}$$

[Eq. 1.13]

The efficiency of a separation system is best demonstrated by its peak capacity, n_c , which is the number of solutes that can theoretically be baseline resolved on a given column. An estimate of a column's peak capacity for a retention time window from time t_1 to t_2 is given by:

$$n_c = 1 + \frac{\sqrt{N}}{4R} \ln \left(\frac{t_2}{t_1} \right) = 1 + \frac{\sqrt{N}}{4} \ln(1 + k_{\max}) = 1 + \frac{\sqrt{N}}{4} \ln \frac{V_{\max}}{V_{\min}}$$

[Eq. 1.14]

where V_{\min} and V_{\max} are the smallest and largest volumes of mobile phase in which a solute can be eluted and detected. This estimation is valid for isocratic elution. The peak capacity in gradient elution is generally higher and can be calculated by:

$$n_c \equiv \frac{\sqrt{N}}{4} \left(\frac{t_2}{t_1} - 1 \right) + 1$$

[Eq. 1.15]

5. Optimization of an HPLC separation

Quality of the HPLC analysis depends above all on the nature of the stationary phase, the dimensions of the column and the column packing material. Chromatographic separations are optimized by increasing the number of theoretical plates, the selectivity of the column, or the component's capacity factors.

5.1 Stationary phase particle size

Improvement of column efficiency in terms of the number of theoretical plates realized by increasing column length often yields marginal increases in resolution, with a corresponding increase of analysis time to unacceptable levels. In order to increase the number of theoretical plates without increasing the length of the column, it is necessary to decrease one or more of the terms in equation 1.12. The easiest way to accomplish this is by adjusting the velocity of the mobile phase. At a low mobile-phase velocity, column efficiency is limited by longitudinal diffusion, whereas at higher velocities efficiency is limited by the two mass transfer terms. As shown in Figure 4 (which is interpreted in terms of equation 1.12), the optimum mobile-phase velocity corresponds to a minimum in a plot of H as a function of u. High linear velocity and very flat curves are characteristic of stationary phases consisting of non-porous particles. If the stationary phase is non-porous, the mass-transfer component of band broadening (C-term in Eq. 1.12) disappears or becomes very small, because the diffusion within pores does not occur. The disadvantage is the reduced sample capacity: in order to maintain a certain sample capacity, it is

necessary to use smaller particles (with a diameter of 1-2 μm). The reduction of particle size can lead to better column efficiency on the basis of the smaller contribution of Eddy diffusion and mobile phase mass transfer (A-term) and shorter diffusion paths in the stationary phase pores (C-term) as indicated in Eq. 1.12; hence the small microparticles in column packing are favoured. In order to obtain a higher plate number, it is usually better to use a packing with smaller particles than to lengthen the column: longer column increases the retention volume, thus decreasing the concentration of the peak in the eluate and impairing the detection limit. Smaller particles, instead, reduce the enlargement of the chromatographic band. The disadvantage of the micro particle columns is their relatively high back-pressure which is reversely proportional to the square of the particle diameter.

5.2 Columns with reduced dimensions

Another possibility to improve the separation besides reducing the particle size is to reduce the column internal diameter: as the diameters of HPLC columns are reduced, peaks are eluted in smaller volumes, and there is a greater need to limit the dispersion (band broadening) caused by extra-column components, in order to prevent degradation of resolution. A reduction of the column diameter offers several advantages:

- operation at small volumetric flow-rates; solvent consumption (retention volume V_R) decreases with the square of the column diameter d_c :

$$V_R \sim d_c^2 \quad (\text{because } V_R = (k+1) \frac{\epsilon d_c^2 \pi L}{4})$$

- higher sensibility for concentration sensitive detectors;

- they are essential for trace analyses if the amount of sample is limited. This, as a consequence of better signal height-to-sample mass ratio. The peak maximum concentration c_{max} is proportional to the inverse square of the column diameter d_c :

$$c_{\max} \sim \frac{1}{d_c^2} \quad (\text{because } c_{\max} = \frac{c_i V_i}{V_R} \sqrt{\frac{N}{2\pi}})$$

- the dilution of the sample compounds during the separation process is reduced: the chromatographic dilution D increases proportionally with the square of the column radius

$$D = \frac{c_0}{c_{\max}} = \frac{\varepsilon_t \pi r^2 (1+k) \sqrt{2\pi LH}}{V_{inj}}$$

[Eq. 1.15]

where c_0 is the initial compound concentration in a sample, c_{\max} final compound concentration at the peak maximum, ε_t is the column porosity, r is the column radius, k is the retention factor and V_{inj} is the injected sample volume.

- they offer higher theoretical plate numbers;
- permit to use low eluent flow rates that are required, for example, in LCMS analyses.

The main drawbacks of this technique are the lower sample capacity, which is directly proportional to the quantity of the stationary phase and the loss of detection sensitivity due to the small injection volumes or masses and the need for special, miniaturized, equipment^[24]. However, the decrease of sensitivity deriving from the small injection volumes, can be diminished by sample “focusing” (described following). The number of theoretical plates obtainable by using a single column is about 10 000-25 000 in HPLC. This is due to the high pressure drop associated with small-sized packing materials; under the limitation of operating pressures of 350-400 kg/cm² with current instrumentation (back-pressure is reversely proportional to the square of the particle diameter)^[25]. A compromise between desired column efficiency and the pressure drop is necessary. Outstanding high performances have been achieved recently in ultrahigh pressure LC (UHPLC). With pressures as high as 5000 bar, conventional columns must be replaced with

small I.D. columns, usually of fused silica and with internal diameters of 50 μm or smaller, which could withstand the high pressures. It has been demonstrated that with particle sizes down to 1 μm , very efficient high speed separations can be obtained^[26,27]. Since ultra-high pressures require special pumps, special injectors, and special connectors, such systems are not for routine LC users^[28]. Besides UHPLC, capillary electrochromatography (CEC)^[29] and open tube liquid chromatography^[30] have been used to overcome problems related with high pressure drop. Although CEC has been extensively studied and is known to provide high column efficiency in short times (up to 200,000 plates with 120 s column dead time^[31]), CEC has not been widely used in routine applications due to practical difficulties including frit failure, or bubble formation.

6. Mass spectrometric detectors

6.1 Definition

Mass spectrometry (MS) occupies an important place amongst the various spectrometric techniques for molecular analysis. Moreover, it has the potential to yield information on the relative molecular mass (Mr) and the structure of the analyte. At present, MS is the most sensitive method for molecular analysis^[32]. The principle of MS is the production of ions, which are subsequently separated or filtered according to their mass-to-charge (m/z) ratio and detected. The resulting mass spectrum is a plot of the (relative) abundance of the generated ions as a function of the m/z ratio. A typical mass spectrometer for HPLC consists of three parts: the interface, where the eluate enters the MS and the ions are generated, the mass analyser, and the detector, an electron multiplier which determines the ion beam intensity. The ionization of the analytes can be performed in a number of ways. The available ionization techniques can be classified in four groups: electron

ionization, chemical ionization, desorption ionization and nebulization ionization. Today the most common ionization techniques used in HPLC-MS analyses are those carried out at atmospheric pressure: (atmospheric pressure) electrospray ionization (ESI or APESI) and atmospheric pressure chemical ionization (APCI). In ionization at atmospheric pressure the molecules are at first ionized at atmospheric pressure and then separated mechanically or electrostatically from neutral molecules. APCI is based on chemical ionization by ion-molecule electron-capture reactions carried out in an ion source operated at atmospheric pressure (105 Pa). The ions are generated by corona discharge (3-6 kV). In most cases it yields pseudo-molecular ions $(M+H)^+$, but negative ionization is also possible.

6.2 Atmospheric-pressure chemical ionization

APCI is suitable for small or medium non-polar analytes, but is not suitable for thermally unstable analytes. However, the analytes need some volatility and proton affinity. With aqueous eluents, an additive can be necessary for efficient ionization. With non-aqueous eluents, additives are not necessary, because the reactions with the solvent are possible during ionization. APCI produces a mass-sensitive signal and low detection limits can be achieved due to the high efficiency of the ion molecule reactions under atmospheric pressure conditions, where longer ion lifetimes are achieved (ca. 10 ms in APCI compared to $<10 \mu\text{s}$ in medium pressure chemical ionization)^[32,33] (Figure 5).

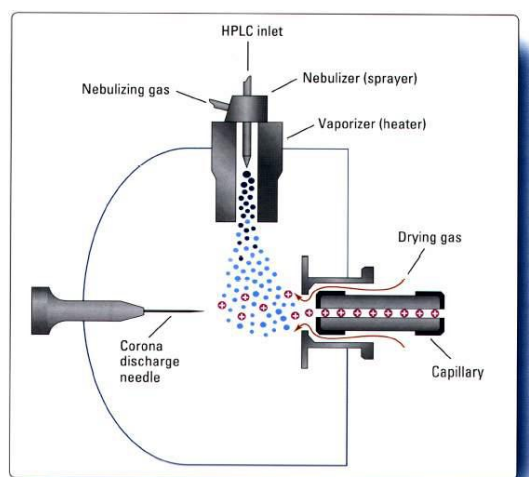
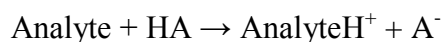


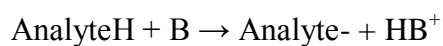
Figure 5 : HPLC-APCI-MS interface.

6.3 Electrospray ionization

In ESI (Figure 6), the ions are generated by ‘coulomb explosion’ (disintegration) of electrically charged droplets. It yields ions with single or multiple charges. In the latter case, spectra with many peaks are obtained, which must not be mixed up with classical spectra showing molecule fragments. ESI is suitable for thermally unstable analytes and macromolecules. It is suitable for small flow rates and therefore useful for micro HPLC. For positive ionization a pH of ca. 5 is suitable, additives are formic and acetic acid, sometimes together with ammonium acetate:



For negative ionization a pH of ca. 9 is suitable and the additives are ammonia, triethylamine and diethylamine, sometimes together with ammonium acetate:



ESI produces a concentration-sensitive signal and is not dependent on the flow. After the production of ions, these are analysed according to their m/z ratio in the mass analyser, i.e. the ions are separated according to their m/z ratio in either time

or space, which can be achieved in number of ways. It must be emphasized that all mass analysers perform a separation of ions according to their m/z ratio. This means that a singly-charged molecule with molecular mass of 400 will give a peak at m/z 400, while a molecule carrying 40 charges and a molecular mass of 16,000 will also give a peak at m/z 400. Five types of mass analysers are currently available: (magnetic) sector, quadrupole mass filter, quadrupole ion trap, time-of-flight and Fourier-transform ion-cyclotron resonance instruments.

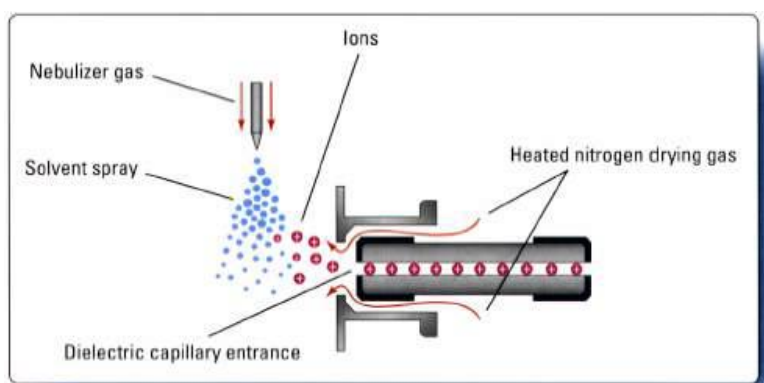


Figure 6: *HPLC-ESI-MS interface.*

7. Inflammation

7.1 Definition

Polyphenolic molecules are responsible for many biological activities including anti-inflammatory. Inflammation is a defense response that is triggered by different conditions, such as an infection or tissue damage^[34]. The site in which the event begins, inflammatory cells exposed to insult produce a number of cytokines and chemokines that act on local vascular endothelium, causing dilatation of blood vessels, leakage and recruitment of neutrophils and monocytes from blood into tissue^[33]. Briefly, the initial recognition of an infection or a tissue damage occur, among other cells, by resident macrophages, which in response to the stimulus produce a variety inflammation mediators, including chemokines (eg. MCP 1), cytokines (eg. TNF- α and IL-1 β), vasoactive amines, prostaglandins^[36].

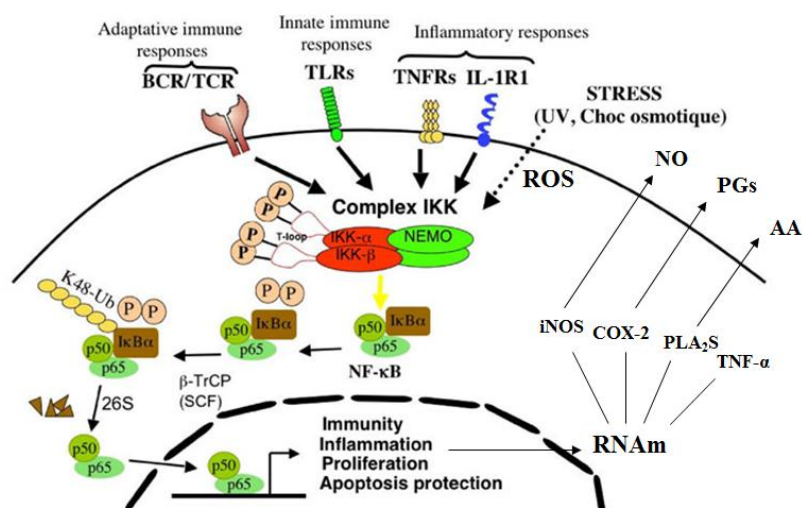


Figure 7 : Production of the main inflammatory mediators following the stimulation by pathogens

In response to these factors the local inflammatory exudate begins to form: plasma proteins and leukocytes (neutrophils and monocytes), leave the circle and access to the tissue at the infection site. Once in the damaged tissue, monocytes and neutrophils are activated, (through direct contact with the pathogen or through the action of cytokines secreted by the cells resident in the fabric) in an attempt to eliminate the invading agent, release toxic factors (reactive oxygen and nitrogen species, proteases, elastase, collagenase) (Figure 7). These factors, not discriminating between microbial targets and host tissues, causing tissue damage as a side effect of defense. It follows that, despite being an essential event for the defense and the integrity of the organism from external attacks, the inflammatory response requires tight control of its activation. During the development and resolution of inflammation^[37] are particularly important mononuclear phagocytes (both circulating monocytes, less mature cells that enter into the inflamed tissue in response to chemokines, the resident macrophages in the tissue, mature cells that monitor and control the tissue integrity). The macrophage activation occurs via two main types of programs: the classical inflammatory activation (or M1), stimulated by bacterial molecules (eg. LPS) and inflammatory cytokines (eg. IFN- γ), and the alternative activation (or M2), whose activating stimuli are anti-inflammatory cytokines (eg. IL-4 and IL-10, TGF- β), immune complexes or glucocorticoids. The initial inflammatory response active M1 macrophages polarization, which become able to eliminate invading microorganisms and promote the inflammatory response, while during the resolution phase of inflammation, macrophages are re-polarization in direction M2, losing responsiveness to inflammatory stimuli and assuming the ability to eliminate damaged cells and tissues, and promote angiogenesis and tissue remodeling. Failure regulation of inflammatory processes is the basis of chronic inflammatory and autoimmune diseases, such as rheumatoid arthritis, multiple sclerosis and systemic lupus^[38].

7.2 Mediators of the inflammatory process

During the inflammatory process important chemical mediators are produced of plasma-derived and that coordinate cellular inflammation, with amplification or adjustment effect. The mediators of the inflammatory process can be either plasma-derived that cells:

- The plasma-derived mediators are produced by the liver are silent form and are activated by factor XII and the complement system.
- The mediators of cellular origin, however, are divided into two subgroups, those preformed and those synthesized de novo.

The preformed mediators are accumulated in secretory granules, are released after appropriate stimuli and are: histamine, serotonin, lysosomal enzymes. The histamine causes, in the immediate phase, the dilation of the arterioles and the increase of the permeability of venules.

The mediators synthesized de novo are:

- Prostaglandins, synthesized by the enzyme cyclo-oxygenase (COX) that converts the substrate (arachidonic acid) into prostaglandin, which in turn, through PGH₂ generates Prostacyclin, substance-acting vasodilator and platelet aggregation inhibition.
- Thromboxane A₂, such as prostaglandins, is synthesized by action of COX, is vasoconstrictor and promoter of platelet aggregation.
- Leukotrienes, synthesized by the action of lipoxygenase, damage vasoconstriction, increased permeability and chemotaxis. Leukotrienes, prostaglandins and thromboxane are all arachidonic acid derivatives.
- Platelet-activating factors (PAF) have pro-inflammatory actions, such as increased vascular permeability, vasodilation, platelet activation and chemotaxis.

- Reactive oxygen species (ROS): O₂ free radicals are released by white blood cells into the extracellular environment after exposure to chemotactic agents, immune complexes or during phagocytosis. Their release can cause damage to the host.
- Nitrogen monoxide (NO): soluble gas produced by endothelial cells, macrophages and neurons, have short half-life and local action; causes vasodilation.
- Cytokines: proteins produced by different cell types that modulate the function of other cells, are involved in immunity and inflammation, including interleukin (IL) and chemokines.

7.2.1 Nitric oxide synthase (iNOS)

Inflammation is classified on a temporal basis in acute and chronic inflammation. The first manifestation of acute inflammation is vasodilation, which involves the pre-capillary arterioles in the immediate proximity of the injured part. The start and maintenance of vasodilatation are due to the rapid release of mediators such as histamine (vasoactive amine) or prostaglandins and subsequently mediators lenses as IFN- γ , TNF- α , IL-1 β , LPS and PAF (Figure 8).

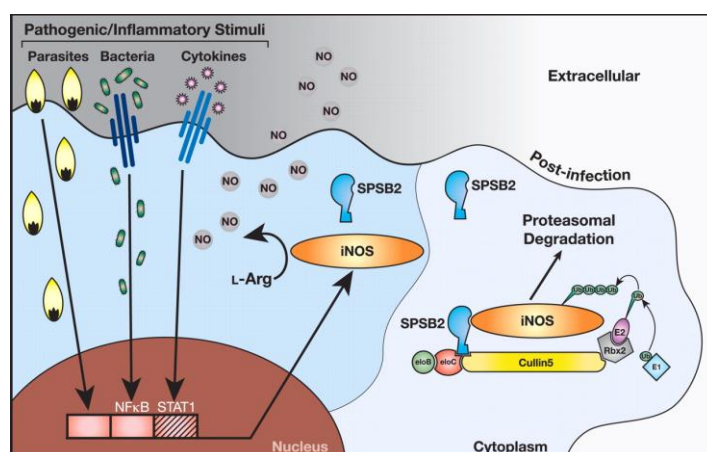


Figure 8: *iNOS* activation during inflammatory process

The mediators stimulate the expression of an enzyme, inducible nitric oxide synthase (iNOS) in vascular endothelial level, while histamine, through an increase in intracellular calcium, causes the rapid activation of the constitutive NO synthase^[39,40]. Both isoforms, constitutive and inducible enzyme, are responsible for the synthesis of nitric oxide, a potent vasodilator, produced by the oxidation of L-arginine, is a mediator of the inflammatory process which participates triggering a nonspecific immune response. Contributes to tissue damage either directly for production of peroxynitrite (ONOO⁻), and indirectly, through the amplification of the inflammatory response^[41]. Agents such as LPS increased the release of NO and activate the expression of iNOS enzymes. In the modulation of the inflammatory response, there are important interactions between the iNOS pathway enzyme and another enzyme triggered by LPS and involved in macrophage response, the isoform COX-2 enzyme whose expression is also influenced by the same NO^[42].

7.2.2 Cyclooxygenase

Of particular importance is the system of cyclooxygenase, responsible for the synthesis of several inflammatory mediators, including prostaglandins and thromboxane whose effects are amplified cascade. It consists of two isoforms, COX-1 and COX-2 (Figure 9).

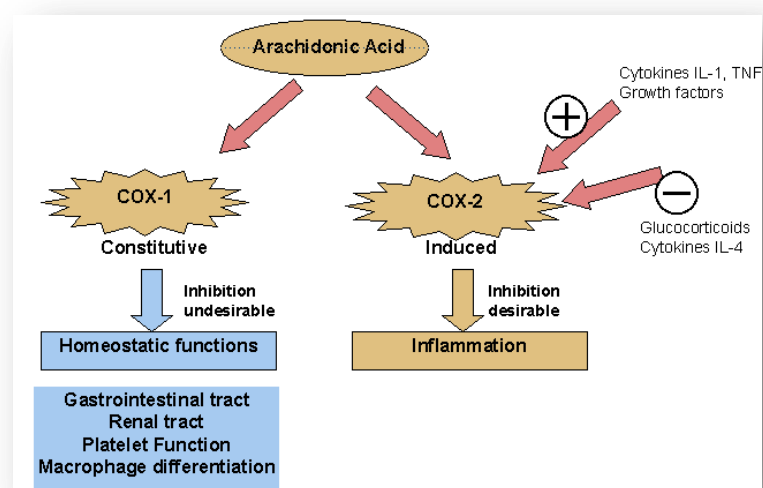


Figure 9: isoforms of cyclooxygenase

The COX-1 isoform type is constitutive, usually expressed in various tissues, plays physiological and homeostatic functions, is not induced by cytokines^[43]. The COX-2 isoform of type inducible, is expressed at the site of inflammation only when it is induced by stimuli such as TNF, IL-1 and PAF, and physio-pathological role. The expression of these mediators of inflammation contributes to the maintenance and increase of the vascular caliber that promote, determines a slowing of the flow, which promotes leukocyte rolling, slows down the possible spread of pathogens and facilitates the adhesion and migration leukocyte.

7.2.3 Reactive Oxygen Species (ROS)

The expression of ROS species, similar to that of the nitrogen monoxide NO, is induced at the site of inflammation as a defense mechanism, however, the levels of ROS (Figure 10), if not properly regulated, can lead to deleterious effects such as tissue damage or dysfunction of organs, as responsible for the formation of radical species that can promote oxidative stress^[44].

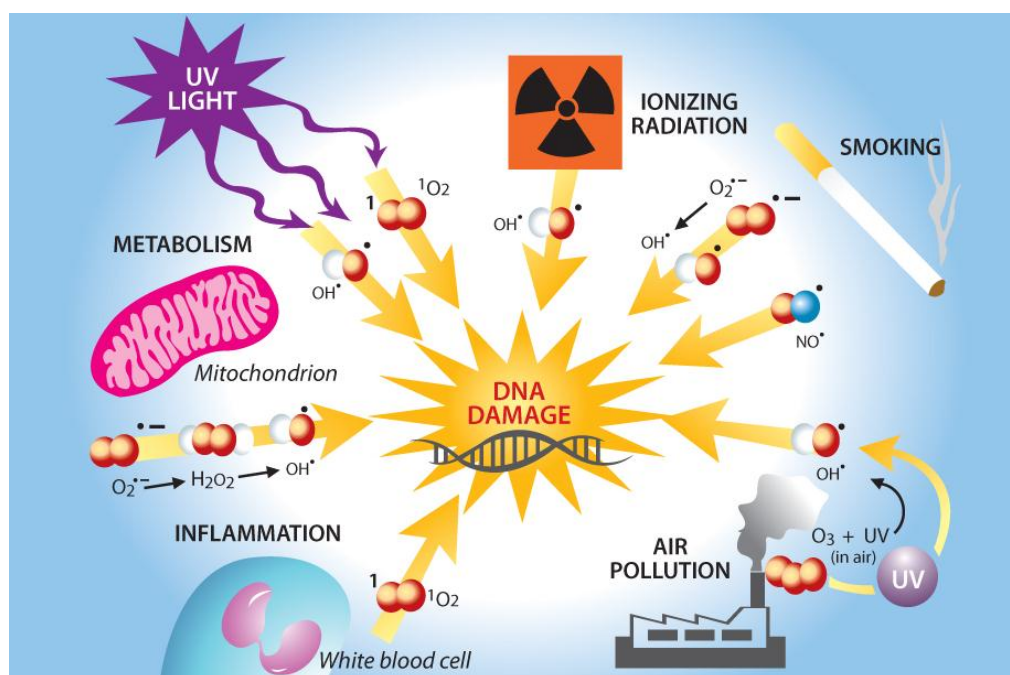


Figure 10: Factors related to the production of ROS

In addition, cells such as macrophages, to protect against oxidative damage and promote inflammatory activity of up-regulation of some defense mechanisms such as the expression of heme oxygenase-OH-1, limiting enzyme in heme^[44]degradation. These enzyme species are normally expressed in various tissues, but is highly inducible by various stimuli such as LPS^[45]. Although in

principle the inflammation is an essential response to eliminate pathogens, it is considered a double edged sword when the initial reaction is not limited, as over-activation of the anti-inflammatory mechanisms, in which the macrophages play a primary role, can cause tissue damage that may be due to the release of lysosomal contents. The causes are various, including: premature degranulation, phagocytosis and exocytosis or is hampered by persistent activation too, all converge in the release of lysosomal enzymes, reactive oxygen species and products of arachidonic acid metabolism. In this case, the anti-inflammatory compounds are therapeutically useful.

8. Aim of research

Owing to the great variety of polyphenolic compounds in natural matrices and their rising importance as biomolecules able to prevent several diseases, we focused on the development of powerful analytical methods capable of identify and quantify a large number of compounds present in several product as Citrus derivatives and fruits. The application of ultra high performance liquid chromatography coupled to accurate mass spectrometry was highlighted, showing the superior efficiency with respect to conventional separation techniques. Moreover the antioxidant and anti-inflammatory properties of these extract were evaluated by in vitro assays, with a special attention to the effects of these molecules against the inflammatory response and the release of pro-inflammatory mediators.

9. References

- [1] Ekta K. Nutraceutical - Definition and Introduction, *Journal of Pharmaceutical Sciences*, **2003**, 5 (3).
- [2] Brower V. Nutraceuticals: poised for a healthy slice of the healthcare market? *Nature Biotechnology*, **1998**;16:728-731.
- [3] Cevallos-Casals, B. A., & Cisneros-Zevallos, L. Stoichiometric and Kinetic Studies of Antioxidants from Andean Purple Corn and Red-Fleshed Sweetpotato, *Journal of Agricultural and Food Chemistry*, **2003**, 51, 3313–3319.
- [4] Lachance, P. A. Nutraceuticals, for real, *Food Technology*, **2002**, 56, 20–20.
- [5] Lachance, P. A., Nakat, Z., & Jeong, W. S. Antioxidants: an integrative approach, *Nutrition*, **2001**, 17, 835–838.
- [6] van Sumere, C.F.. Phenols and phenolic acids, in *Methods in Plant Biochemistry, Plant Phenolics*. Harborne, J.B., Ed., Academic Press, London, **1989**, Volume 1, 29–74.
- [7] D. Strack, V. Wray, in: J.B. Harborne (Ed.), *The Flavonoids*, Chapman & Hall, London, UK, **1994**.
- [8] B. Klejdus, D. Vitamvasova, V. Kuban. Identification of isoflavone conjugates in red clover (*Trifolium - 33 - ereal - 33 - e*) by liquid chromatography-mass spectrometry after two-dimensional solid-phase extraction, *Analitica Chimica Acta*, **2001**, 81, 450.
- [9] J.P. Rauha, H. Vuorela, R. Kostianen. Effect of eluent on the ionization efficiency of flavonoids by ion spray, atmospheric pressure chemical ionization, and atmospheric pressure photoionization mass spectrometry, *Journal of Mass Spectrometry*, **2001**, 36, 1269-1280.
- [10] C.A. Maxwell, D.A. Philips. Concurrent Synthesis and Release of nod-Gene-Inducing Flavonoids from Alfalfa Roots, *Plant Physiology*, **1990**, 93, 1552.

- [11] W. Barz, R. Welle, in: H.A. Stafford (Ed.), *Flavonoid Metabolism*, CRC Press, Boca Raton, FL, USA, **1990**, p. 139.
- [12] D. Strack, in: H.-W. Heldt (Ed.), *Plant Biochemistry*, Academic Press, New York, NY, USA, **1997**, p. 387.
- [13] R.S. Rosenberg Zand, D.J.A. Jenkins, E.P. Diamandis. Flavonoids and steroid hormone-dependent cancers, *Journal Chromatography B*, **2002**, 777, 219.
- [14] L.C. Olsson, M. Veit, G. Weissenbock, J.F. Bornman. Differential flavonoid response to enhanced uv-b radiation in brassica napus, *Phytochemistry*, **1998**, 49, 1021.
- [15] S. Reuber, J.F. Bornman, G. Weissenbock. Phenylpropanoid compounds in primary leaf tissues of rye (*Secale -34- ereal*) – light regulation of their biosynthesis and the possible role in UV-B protection, *Plant Physiology*, **1996**, 97, 160.
- [16] E.M. Middleton, A.H. Teramura. The Role of Flavonol Glycosides and Carotenoids in Protecting Soybean from Ultraviolet-B Damage., *Plant Physiology*, **1993**, 103, 741.
- [17] C.-Y. Wang, H.-Y. Huang, K.-L. Kuo, Y.-Z. Hsieh. Analysis of Puerariae radix and its medicinal preparations by capillary electrophoresis., *Journal Chromatography A*, **1998**, 802, 225.
- [18] Schieber, A., Stintzing, F. C., & Carle, R.. By-products of plant food processing as a source of functional compounds – recent developments. *Trends in Food Science and Technology*, **2001**, 12, 401–413.
- [19] Bocco, A., Cuvelier, M.-E., Richard, H., & Berset, C.. Antioxidant activity and phenolic composition of citrus peel and seed extracts, *Food Chemistry*, **1998**, 46, 2123–2129.
- [20] Gorinstein, S., Martin-Belloso, O., Park, Y.-S., Haruenkit, R., Lojek, A., Ciz, M., et al. Comparison of some biochemical characteristics of different citrus fruits, *Food Chemistry*, **2001**, 74, 309.

- [21] Martin, A. J. P., Synge, R. L. M. A. New form of chromatogram employing two liquid phases, *Biochemical Journal*, **1941**, 35, 1358.
- [22] Saito, Y., Jinno, K., Greibrokk, T. Capillary columns in liquid chromatography: between conventional columns and microchips., *Journal of Separation Science*, **2004**, 27, 1379.
- [23] Foley, J. P., Dorsey, J. G. Equations for calculation of chromatographic figures of merit for ideal and skewed peaks, *Analytical Chemistry*, **1983**, 55, 730.
- [24] Vissers, J. P. C. Recent developments in microcolumn liquid chromatography, *Journal Chromatography A*, **1999**, 856, 117.
- [25] Tanaka, N., Kobayashi, H., Ishizuka, N., Minakuchi, H., Nakanishi, K., Hosoya, K., Ikegami, T. Monolithic silica columns for high-efficiency chromatographic separations, *Journal Chromatography A*, **2002**, 965, 35.
- [26] MacNair, J. E., Lewis, K. C., Jorgenson, J. Ultrahigh-pressure reversed-phase liquid chromatography in packed capillary columns., *Analytical Chemistry*, **1997**, 69, 983.
- [27] Lippert, J. A., Xin, B., Wu, N., Lee, M. L. Fast ultrahigh-pressure liquid chromatography: On-column UV and time-of-flight mass spectrometric detection, *Journal Microbiology separation*, **1999**, 11, 631.
- [28] Saito, Y., Jinno, K., Greibrokk, T. Capillary columns in liquid chromatography: between conventional columns and microchips, *Journal Separation Science*, **2004**, 27, 1379.
- [29] Dittmann, M. M., Rozing, G. P. Capillary electrochromatography: a high efficiency micro-separation technique, *Journal Chromatography A*, **1996**, 744, 63.
- [30] Tock, P. P. H., Boshoven, C., Poppe, H., Kraak, J. C. Performance of porous silica layers in open-tubular columns for liquid chromatography, *Journal Chromatography A*, **1989**, 477, 95.

- [31] Dadoo, R., Zare, R. N., Yan, C., Anex, D. S. Advances in Capillary Electrochromatography: Rapid and High-Efficiency Separations of PAHs, *Analytical Chemistry*, **1998**, 70, , 4787.
- [32] Niessen, W. M. A., Liquid Chromatography-Mass Spectrometry. Marcel Dekker, Inc., New York, Basel, **1999**, P. 31.
- [33] Meyer, V. R., Practical High-Performance Liquid Chromatography. John Wiley and Sons, West Sussex, **2004**.
- [34] Fujiwara, N., Kobayashi, K. Macrophages in inflammation, *Current Drug Targets*, **2005** ;4(3), 281-6.
- [35] Baeuerle, P.A. IkappaB-NF-kappaB structures: at the interface of inflammation control, *Cell*, **1998**, 95, 729-731.
- [36] Popolo, A., Autore, G., Pinto, A., & Marzocco, S. Oxidative stress in patients with cardiovascular disease and chronic renal failure, *Free Radical Research*, **2013**, 47(5), 346–356.
- [37] Pepys MB1, Hirschfield GM, Tennent GA, Gallimore JR, Kahan MC, Bellotti V, Hawkins PN, Myers RM, Smith MD, Polara A, Cobb AJ, Ley SV, Aquilina JA, Robinson CV, Sharif I, Gray GA, Sabin CA, Jenvey MC, Kolstoe SE, Thompson D, Wood SP. Targeting C-reactive protein for the treatment of cardiovascular disease, *Nature*, **2006**, 440,1217-1221.
- [38] Willerson JT, Ridker PM. Inflammation as a cardiovascular risk factor. *Circulation* ,**2004**, 109, 2-10.
- [39] Moncada, S., Palmer, R.M.J. & Higgs, E. Nitric oxide: physiology, pathophysiology and pharmacology, *Pharmacological Reviews*, **1991**, 43, 109–142.
- [40] Moncada, S. & Higgs, A. The arginine NO pathway, *The New England Journal of Medicine*, **1993**, 329,2002–2012.
- [41] Dugo, L., Marzocco, S., Mazzon, E., Di Paola, R., Genovese, T., Caputi, A.P. & Cuzzocrea S. Effects of GW274150, a novel and selective inhibitor of iNOS

activity, in acute lung inflammation, *British Journal of Pharmacology*, **2004**, 141, 979–987.

[42] Ahmad, N., Chen, L.C., Gordon, M.A., Laskin, J.D. & Laskin D.L. Regulation of cyclooxygenase-2 by nitric oxide in activated hepatic macrophages during acute endotoxemia, *Journal of Leukocyte Biology*, **2002**, 71(6), 1005-1011.

[43] Calder, P.D., Albers, R., Antoine, J.M., Blum, S., Bourdet-Sicard, R., Ferns, G. A., Folkerts, G., Friedmann, P.S., Frost, G.S., Guarner, F., Løvik, M., Macfarlane, S., Meyer, P.D., M'Rabet, L., Serafini, M., van Eden, W., van Loo, J., Vas Dias, W. & Vidry, S. Inflammatory disease processes and interactions with nutrition, *British Journal of Nutrition*, **2009**, 101, 1-45.

[44] Wu, M.L., Ho, Y.C., Lin, C.Y. & Yet, S.F. Heme oxygenase-1 in inflammation and cardiovascular Disease, *American Journal of Cardiovascular Disease*, **2011**, 1(2),150-158.

[45] Ryter, S.W., Alam, J. & Choi, A.M. Heme oxygenase-1/carbon monoxide: from basic science to therapeutic applications, *Physiological Reviews*, **2006**, 86, 583-650.

CHAPTER II

**Development of fast analytical methods for the characterization
of flavonoids in Citrus bergamia juice:
An UHPLC-IT-TOF approach**

Abstract: In order to reduce the analysis time, during PhD with the aim to thoroughly characterize the flavonoids in Citrus bergamia juice a fast UHPLC IT-TOF method was carried out for the analysis of flavonoids in Citrus bergamia juice. With respect to the typical methods for the analysis of these matrices, based on conventional HPLC techniques, a ten fold faster separation was attained. The use of a core shell particle column ensured high resolution, within the fast analysis time of only 5 minutes. Unambiguous determination of flavonoid identity was obtained by the employment of a hybrid IT-TOF mass spectrometer with high mass accuracy (average error 1.69 ppm). The system showed good retention time and peak area repeatability, with maximum RSD% values of 0.36 and 3.86, respectively, as well as good linearity ($R^2 \geq 0.99$). Our results show that UHPLC can be a useful tool for ultra fast quali/quantitative analysis of flavonoid compounds in Citrus fruit juices.

Keywords : Bergamot, Flavonoids, Core-Shell, Mass accuracy.

1. Introduction

Flavonoids (or bioflavonoids) are natural chemical compounds, common in higher plants and particularly known and appreciated for their health properties^[1,2] especially for the large number of beneficial effects on human health, including antioxidant, cardioprotective, anticancer, hypolipidemic potential^[3-5]. The class of flavonoids is quite wide know more than 5000 compounds and their therapeutic effect depends largely on the plant complex (all the chemicals contained in drugs or in food)^[1] Flavonoids are a large group of structurally related compounds with a chromane-type skeleton and a phenyl substituent in the C2 or C3 position. Flavonoids are referred as glycosides when they contain one or more sugar groups (or glucosides in case of a glucose moiety), and as aglycones when no sugar group

is present. In plants, flavonoids are often present as O- or C-glycosides; O- bonding occurs far more frequently than C bonding^[6]. The O-glycosides have sugar substituents bound to a hydroxyl group of the aglycone, usually located at position 3 or 7, whereas the C-glycosides have sugar groups bound to a carbon of the aglycone, usually on C6 or C8. The most common sugars are rhamnose, glucose, galactose and arabinose. Citrus plants are of great interest since their fruits and juices contain large amounts of flavonoids and are consumed in large quantities. Regarding the main flavonoid classes in Citrus juices, flavanones predominate, with flavones being present in smaller amounts. Among compounds found in citrus species, naringin, neohesperidin (neohesperidosides), narirutin, and hesperidin (rutosides) are commonly present in major quantity^[7]. During my PhD we focused the attention on bergamot juice (*Citrus bergamia*). Between Citrus fruits, *Citrus bergamia* shows a large content in flavonoids, even if it is not commonly consumed for its bitter taste. In this matrix the analysis of flavonoids can be a challenging task, since it contains compounds present in a wide concentration range and with different polarities. Among the various analytical methods, high performance liquid chromatography (HPLC) occupies a leading position for the analysis of flavonoids, especially when coupled to tandem mass spectrometry (MS-MS). Until recently in the past years the flavonoids of bergamot juice were analyzed by C18 columns packed with conventional particles, with binary gradient of water and an organic modifier (acetonitrile or methanol)^[8-10] furthermore, a higher sensitivity can be obtained by using columns with reduced internal diameter^[11]. In agreement with what indicated by previous authors for the analysis of phenolic compounds, all these approaches are generally characterized by analysis time of approximately 50 minutes^[12], and the detection is usually performed by both UV and MS or MS/MS on low resolution instruments such as ion trap or single quadrupole. On this matrix, high mass accuracy measurements as well as multiple MS_n experiments appear to be limited in the literature, the

employment of hybrid mass spectrometers, such as IT-TOF instruments, capable of high mass accuracy, in both full scan and MS_n stages, which are very informative for structure characterization especially for glycosidate compounds, has not been investigated yet, even if the potentialities of IT-TOF instrumentation for structure elucidation and accurate mass measurements of flavonoids^[13,14] and anthocyanins^[15,16] has been demonstrated previously.

Analysis time is a crucial factor in HPLC techniques since it directly affects the number of samples analyzed per unit of time. The development of ultra-high pressure liquid chromatography (UHPLC) has opened up new possibilities in the analysis of complex matrices, such as foods and biological samples. Commercial UHPLC systems and sub-2 μm totally and partially porous packing materials have led to significant improvement in the resolution, speed and efficiency of separation with respect to conventional HPLC systems. The employment of ultra-high pressure conditions makes it possible to achieve 5- to 10-fold faster separations than what obtained with conventional HPLC systems, while maintaining or increasing resolution^[17,18]. During my PhD, we developed a fast UHPLC IT-TOF method for the fast characterization of flavonoids from bergamot (*Citrus bergamia*) juice based on the use of sub 2-μm core-shell particles columns. The main advantages over conventional methods include very short analysis time, good separation, and unambiguous determination of flavonoid identity.

2. Materials and methods

2.1 Reagents and standards

Ultra pure water (H₂O) was obtained by a Milli-Q system (Millipore, Milan, Italy), acetonitrile (ACN) LC-MS grade and formic acid (HCOOH) were purchased by Sigma Aldrich (Milan, Italy). For the separation of flavonoids a Kinetex C18 100 x 2.1 mm, 1.7 µm column (Phenomenex) was employed. Flavonoid standards caffeic acid, hesperidin, neohesperidin, eriocitrin, quercetin 3-*O* di-glucoside were purchased from Sigma Aldrich (Milan, Italy).

2.2 Sample preparation

In order to remove fibers, juice was centrifuged at 6000 rpm/min for 15 minutes, then lyophilized for 24 hours. From 80 mL of juice, 1.1 g of dry extract was obtained. Sample was stored at 5°C, then solubilized in methanol to a concentration of 1 mg/mL, subjected to ultrasonication and filtered prior to injection on 0.20 µm nylon membrane (Millipore).

2.3 Instrumentation

UHPLC analyses were performed on a Shimadzu Nexera UHPLC system, consisting of a CBM-20A controller, two LC-30AD dual-plunger parallel-flow pumps, a DGU-20 A5 degasser, an SPD-M20A photo diode array detector (equipped with a 2.5 µL detector flow cell volume), a CTO-20A column oven, a SIL-30AC autosampler. The UHPLC system was coupled online to an LCMS-IT-TOF mass spectrometer through an ESI source (Shimadzu, Kyoto, Japan).

data elaboration was performed by the LCMSsolution® software (Version 3.50.346, Shimadzu). The extracolumn volume (ECV) was calculated by injecting toluene, and was estimated in 17 μ L.

2.4 UHPLC conditions

The optimal mobile phase consisted of 0.1% HCOOH/H₂O v/v (A) and 0.1% HCOOH/ACN v/v (B). Analysis was performed in gradient elution as follows: 0-1.50 min, 0-20% B; 1.50-4.00 min, 20-25% B; 4-6.00 min, 25-30% B; 6-6.10, 30-60% B. Flow rate was 0.7 mL/min. Column oven temperature was set to 45°C. Injection volume was 1 μ L of juice extract, in a concentration of 1 mg mL⁻¹. The following PDA parameters were applied: sampling rate, 40 Hz; detector time constant, 0.160 s; cell temperature, 40 °C. Data acquisition was set in the range 190-400 nm and chromatograms were monitored at 280 and 330 nm at the maximum absorbance of the compounds of interest.

2.5 ESI-IT-TOF-MS parameters

UHPLC was coupled on-line to a hybrid IT-TOF-MS instrument, and the flow rate from LC was split 50:50 before the ESI source by means of a stainless steel Tee union (1/16 in., 0.15 mm bore, Valco HX, Texas, USA). The resolution, sensitivity, and mass number calibration of the IT and the TOF analyzer were tuned using a standard sample solution of sodium trifluoroacetate. After the calibrant had flowed, cleaning of the tube and ESI probe was made by flowing CAN (0.2 mL/min, 20 min). MS detection was operated in negative ionization mode with the following parameters: detector voltage, 1.53 kV; CDL (curve desolvation line) temperature, 200 °C; block heater temperature, 200 °C; nebulizing gas flow (N₂), 1.5 L/min, drying gas pressure, 100 kPa. Full-scan MS data were acquired in the range of

150–1000 m/z, ion accumulation time, 40 ms; IT, repeat = 3. MS/MS experiments were conducted in data-dependent acquisition, precursor ions were acquired in the range 150–900 m/z; peak width, 3 Da; ion accumulation time, 45 ms; CID energy, 50%; repeat = 1; execution trigger base peak intensity (BPC) at 95% stop level. Manual acquisition was performed for peaks 3, 8, 9, 10, 11, and 12 by applying the same parameters (exceptions: ion accumulation time, 60 ms; ion exclusion time, 2.5 s).

2.6 Scavenging of 1, 1 diphenyl-2-picrylhydrazyl (DPPH) radicals

0.1 mM solution of DPPH in methanol was prepared and 1.0 mL of this solution was added to 3.0 mL of extract solution in methanol at different concentration (1–16 µg/mL). Thirty minutes later, the absorbance was measured at 517 nm. A blank was prepared without adding extract. Ascorbic acid at various concentrations (1 to 16 µg/mL) was used as standard. Lower the absorbance of the reaction mixture indicates higher free radical scavenging activity. The capability to scavenge the DPPH radical was calculated using the following equation:

$$DPPH \text{ scavenged } (\%) = \frac{A_{control} - A_{test}}{A_{control}} \times 100$$

Where A control is the absorbance of the control reaction and A test is the absorbance in the presence of the sample of the extracts. The antioxidant activity was expressed as IC₅₀ and compared with standard. The IC₅₀ value was defined as the concentration (in µg/ml) of extracts that inhibits the formation of DPPH radicals by 50^[19].

3. Results and discussion

The bergamot juice despite being considered a waste product, is rich in polyphenolic molecules with different biological activities. The objective of this work was to develop a method for the rapid analysis of flavonoids present in Citrus bergamia juice by UHPLC IT-TOF. Compared to the conventional HPLC methods for the analysis of these matrices, a drastic reduction of analysis time was obtained, leading to the separation and identification of 17 compounds in less than 5 minutes with good resolution.

3.1 Optimization of chromatographic parameters

Chromatographic methods for the characterization of polyphenolic molecules of bergamot juice,^[8-10] usually consists of employing C18 columns packed with conventional particles and analysis times of 40–50 min^[20,21]. Although the benefits derived from the use of UHPLC conditions have been highlighted for the analysis of flavonoids^[22,23], in beverages and mixtures of various Citrus extracts^[24,25], to the best of our knowledge, they have never been applied on this matrix so far. In this work, a 100 × 2.1 mm column packed with 1.7 μm core-shell particles was employed. The advantages of columns packed with these particles lie in the reduction of both the longitudinal diffusion (B term) and the eddy dispersion (A term), as well as a very low mass transfer resistance (C term) providing high efficiency and resolution also at high flow rates^[26-28]. Polyphenolic molecules, such as flavonols and flavanones O-glycosides, present in the juice of bergamot, are difficult to characterize with classical analytical methods. In this regard, high-resolution analysis and separation to the baseline are critical essential. For the separation, a gradient program starting with 100% concentration of the weaker solvent (water) was applied, providing a good peak shape especially for the first

eluting peaks. Then, a slow gradient ramp was set in order to elute compounds with very similar behavior. As it can be appreciated from the chromatogram in Figure 1, in the final part of the gradient program a fast ramp up to 60% of the stronger solvent (ACN) was run, to ensure the elution of all the compounds within the fast analysis time of only 5 min. In order to shorten retention times and reduce system backpressure, different column temperatures were investigated, ranging from 35 to 55 °C. Finally, a temperature of 45 °C was selected, which was the best compromise between backpressure (maximum value of 680 bar, significantly below column and system limits) and resolution.

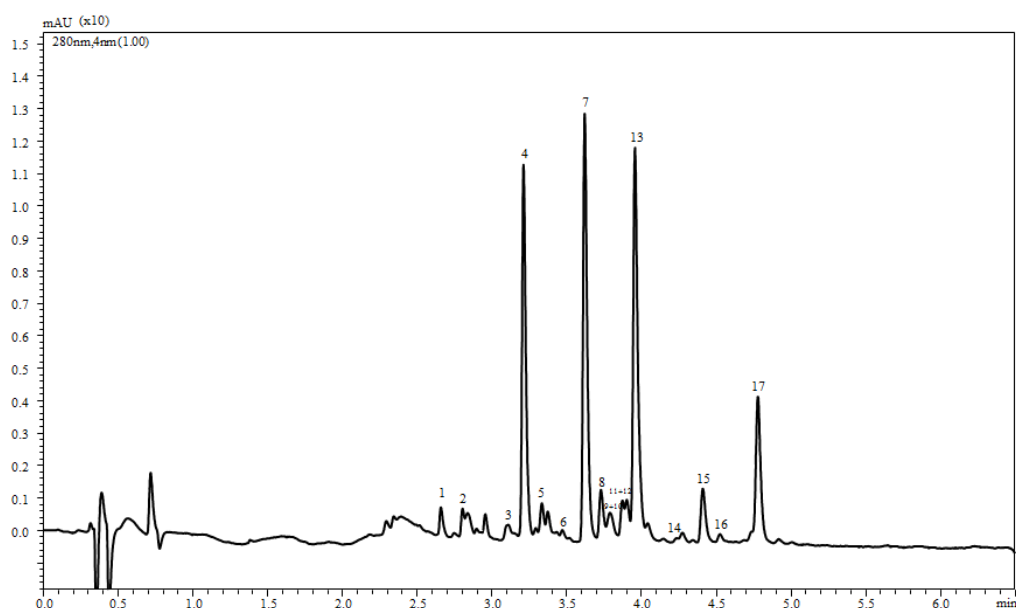


Figure 1. UHPLC–PDA chromatogram of *Citrus bergamia* juice. Column: Kinetex C18 100 × 2.1 mm, 1.7 μm. Flow 0.7 μL/min, Oven 45 °C, injection volume 1 μL of juice extract, detection: PDA, λ: 280 nm.

Moreover, with respect to a conventional analysis performed with a 4.6 mm column^[9,10], solvent consumption was decreased from 45 to 4.5 mL, as well as injection volume from 20 to 1µL. In order to evaluate the performance of the gradient separation, the peak capacity was calculated using the method defined by Neue^[29] [Eq. (1)]:

$$P_c = 1 + \frac{t_g}{(1/n) \sum_1^n w}$$

in which t_g is the time of the gradient run, n is the number of peaks selected for the calculation, and w is the average peak width. The presence of closely related peaks in the chromatogram hinders reliable calculation of the peak width over the spanning time scale^[30]. For this reason, a mixture of four compounds (caffeic acid, eriocitrin, hesperidin, and naringin), providing a clear representation of the entire sample mixture due to their elution profile over the separation window, was analyzed under the same experimental conditions, and used for the estimation of the peak capacity. A value of 41 was attained. Triplicate analyses were run on the system and the repeatability of the retention times and areas was calculated (Table 1). Retention time repeatability with maximum RSD% values of 0.36% and peak area values with RSD% below 3.9% further demonstrated the precision of the system employed.

Table 1: Repeatability and quantitative data calculated for the 17 flavonoids identified.

Peak	tr		Area		Regression Curve	R2	Quantity mg g ⁻¹	RSD %	LOD mg g ⁻¹	LOQ mg g ⁻¹
	Mean	RSD %	Mean	RSD %						
1	2.61	0.22	11926.5	2.12	$y = 1.27^{-06}x - 1.83^{-03}$	0.9980	13.38	± 0.77	0.834	1.232
2	2.74	0.36	9446	1.41	$y = 1.27^{-06}x - 1.83^{-03}$	0.9980	11.33	± 1.75	0.812	1.131
3	3.05	0.33	10915	3.86	$y = 1.27^{-06}x - 6.30^{-04}$	0.9951	13.26	± 0.54	0.850	0.989
4	3.17	0.18	168060	0.37	$y = 1.02^{-06}x - 4.54^{-03}$	0.9993	166.62	± 0.63	0.801	0.942
5	3.29	0.18	10647	2.40	$y = 2.19^{-06}x + 1.81^{-03}$	0.9984	25.58	± 0.37	1.017	1.045
6	3.43	0.17	10710	0.07	$y = 1.27^{-06}x - 1.83^{-03}$	0.9980	11.74	± 0.01	0.809	1.492
7	3.59	0.16	183269	0.49	$y = 1.02^{-06}x - 4.54^{-03}$	0.9993	286.97	± 1.41	0.811	0.925
8	3.71	0.16	12312	2.21	$y = 1.57^{-06}x - 9.20^{-04}$	0.9968	20.82	± 2.96	1.007	1.201
9	3.76	0.15	23118	2.03	$y = 1.40^{-06}x - 4.57^{-03}$	0.9959	29.89	± 5.92	0.805	1.324
10	3.81	0.15	2986	1.71	$y = 9.12^{-07}x + 3.15^{-03}$	0.9991	2.04	± 0.73	0.811	1.912
11	3.85	0.15	164504.5	3.05	$y = 1.57^{-06}x - 9.20^{-04}$	0.9968	62.27	± 10.95	0.831	0.987
12	3.88	0.30	25731	3.46	$y = 1.57^{-06}x - 9.20^{-04}$	0.9968	12.77	± 2.25	1.030	1.091
13	3.92	0.26	19271.5	3.51	$y = 1.03^{-06}x - 4.39^{-03}$	0.9967	166.51	± 6.90	1.024	1.720
14	4.25	0.24	13274	2.41	$y = 1.03^{-06}x - 4.39^{-03}$	0.9959	13.03	± 1.00	0.804	2.174
15	4.40	0.26	30914	0.75	$y = 1.03^{-06}x - 4.39^{-03}$	0.9967	27.50	± 0.24	0.827	1.150
16	4.52	0.13	3579	2.73	$y = 1.27^{-06}x - 1.83^{-03}$	0.9980	2.09	± 0.33	0.875	1.904
17	4.78	0.21	110805.5	2.24	$y = 1.03^{-06}x - 4.39^{-03}$	0.9967	98.60	± 7.23	0.810	1.264

3.2 Quantitative analysis of lyophilized juices

For the quantification of flavonoids, seven compounds were selected as external standards: neoeriocitrin, diosmetin 6,8-di-C-glucoside, rhoifolin, neohesperidin, eriocitrin, quercetin 3 β -diglucoside. Stock solutions (1 mg/mL) were prepared in methanol, for naringin, neohesperidin, and neoeriocitrin, calibration curves were obtained in a concentration range of 50–300 μ g/mL, while for other compounds, calibration curves were obtained in the range of 0.5–100 μ g/mL, with seven concentration levels, triplicate injections of each level were run. Peak areas, relative to the wavelength of maximum absorbance, of each standard were plotted against the corresponding concentrations (μ g/mL). The amount of the compounds in the sample was expressed as milligram per grams of lyophilized juice extract (Table 1). Linear regression was used to generate calibration curves, and the R² values were ≥ 0.995 , showing good linearity. The instrumental intraday repeatability and the recovery were calculated for six replicate injections at three concentration levels. Concerning intraday repeatability, RSD% values less than 6% were obtained, while recovery values ranged from 83.3 to 103.4% (except for isoquercetin 68.2%), demonstrating satisfactory precision and accuracy. As can be seen from Table 1, the flavanones neoeriocitrin, naringin, and neohesperidin are the compounds in the highest amount in the juice, in good agreement with several observations reported in the literature^[8-10] with slight differences due to production processes. Also abundant were the flavones neodiosmin, rhoifolin, and poncirin, while C-glucosidic compounds are present in a minor quantity. Particularly interesting was the presence in a relevant quantity of the two compounds melitidin and brutieridin, since they show important biological activities.

3.3 ESI-IT-TOF-MS elucidation of flavonoid profiles

The identification of flavonoid compounds in the juice was carried out on the basis of diode array detection spectra, MS molecular ions, and MS/MS fragmentation patterns. The data obtained were compared with those in the literature. Molecular formulae were calculated by the Formula Predictor software (Shimadzu), setting a low tolerance (deviation from mass accuracy max: 5 ppm, MS/MS fragmentation data, nitrogen rule) so that most of the identified compounds were in position 1 in the list of the possible candidates. The results are shown in Table 2 in order of peak elution. Compounds 1 and 2 showed a typical fragmentation pattern of C-glucosides^[10,31] along with the presence of two fragments at $[M-H-120]^-$ (base peak) and $[M-H-90]^-$, suggesting the loss of two hexose moieties. These compounds were identified as lucenin-2 and lucenin-2,4'-methylether. The diode array detection spectra of 4, 7, and 13 showed the flavanone nature of the aglycone. Both compounds 4 and 7 revealed a fragment at m/z 459 resulting from the loss of $[M-H-136]^-$ and $[M-H-120]^-$, respectively, as a consequence of retrocyclization^[32] and were identified as neoeriocitrin and naringin. Compound 13 showed a fragment at $[M-H-326]^-$ due to the loss of a sugar moiety, and was identified as neohesperidin. These three compounds were the most abundant in the sample, as mentioned above. Compound 5 showed two fragments at m/z 447 and 285, due to the loss of one or both sugar residues, and was positively identified as poncirin.

Table 2: UHPLC-PDA-ESI-IT-TOF elucidation of flavonoids in bergamot juice.

Peak	Molecular Formula	[M-H] ⁻ observed	[M-H] ⁻ calculated	Error [ppm]	MS ² m/z	Polyphenol sub-class	Compound
1	C27H30O15	593.1496	593.1506	1.68	<u>503</u> ,473,383,353	Flavone C-glucoside	Apigenin 6,8 di C-glucoside
2	C28H32O16	623.1618	623.1621	0.48	<u>503</u> ,384	Flavone C-glucoside	Diosmetin 6,8 di C-glucoside
3	C27H32O15	595.1647	595.1662	2.52	<u>287</u>	Flavanone O-glycoside	Eriodictyol 7-O-rutinoside
4	C27H32O15	595.1654	595.1662	1.34	<u>459</u> ,357,235	Flavanone O-glycoside	Eriodictyol 7-O-neohesperidoside
5	C28H34O14	593.1517	593.1512	2.19	<u>285</u> ,447	Flavone O-glycoside	5,7-dihydroxy-4' methoxyflavone 7-O-rutinoside
6	C22H22O11	461.1106	461.1089	-3.69	<u>341</u> ,371	Flavone C-glucoside	Diosmetin 8-C-glucoside
7	C27H32O14	579.1711	579.1713	0.34	<u>313</u> ,271,459	Flavanone O-glycoside	Naringenin 7-O-neohesperidoside
8	C27H30O14	577.1566	577.1557	-1.56	<u>269</u> ,311	Flavone O-glycoside	Apigenin 7-O-neohesperidoside
9	C28H34O15	609.1831	609.1819	-1.97	<u>301</u> ,459	Flavanon O-glycoside	Hesperetin-7-O-rutinoside
10	C21H20O12	463.1260	463.1246	-3.02	<u>301</u>	Flavonol O-glucoside	Quercetin-3-β-glucopyranoside
11	C28H32O15	607.1674	607.1662	-1.97	<u>284</u> ,299,341,443	Flavone O-glycoside	Diosmetin 7-O-neohesperidoside
12	C33H40O19	739.2050	739.2032	-2.43	<u>593</u>	Flavone O-glycoside	Apigenin 7-O-neohesperidoside-4'-glucoside
13	C28H34O15	609.1810	609.1819	1.48	<u>301</u> ,343,447,489	Flavanon O-glycoside	Hesperetin-7-O-neohesperidoside
14	C27H32O14	579.1711	579.1719	1.38	<u>271</u> ,459,313	Flavanon O-glycoside	Naringenin-7-O-rutinoside
15	C33H40O18	723.2138	723.2142	0.55	<u>579</u> ,271,677	Flavanone O-glycoside	Naringenin 7-[2''-α-rhamnosyl-6''-[3'''-hydroxy-3'''-methylglutaryl]-β-glucoside]
16	C35H70O14	713.47	-	-	<u>677</u> ,451,225	Unknown C-glycoside	-
17	C34H42O19	753.2238	753.2241	0.39	<u>609</u> ,301,651	Flavanone O-glycoside	Hesperetin 7-[2''-α-rhamnosyl-6''-[3'''-hydroxy-3'''-methylglutaryl]-β-glucoside]

Compound 6 also belongs to the C-glucosides; the fragment observed at m/z 341 $[M-H-120]^-$ is the product of the loss of the phenyl moiety in position 1, and was therefore identified as orientin-4'-methyl ether. Finally, for closely eluting peaks, such as compounds 3, 8, 9, 10, 11, and 12, the acquisition was switched from automatic to manual mode, in order to correctly select precursors and obtain pure MS/MS spectra. In this way, all compounds listed above were successfully identified. Compound 14 showed several fragments, particularly, at m/z 271 and 459, corresponding to the loss of the disaccharide moiety and rearrangement of the aglycone, and was confirmed as narirutin. Figure 2 illustrates the structures and MS/MS spectra of compounds 15 and 17. They were assigned as melitidin and brutieridin; their fragmentation patterns showed ions at m/z 579 and 609, respectively, resulting from the loss of a 3-hydroxy-3-methylglutaril residue. These compounds are particularly interesting due to their statin-like structures^[33] and their hypolipidemic activity^[34]. Finally, compound 16 was tentatively identified as a C-glucoside compound^[35], MS_n and NMR spectroscopic experiments are underway to confirm the structure.

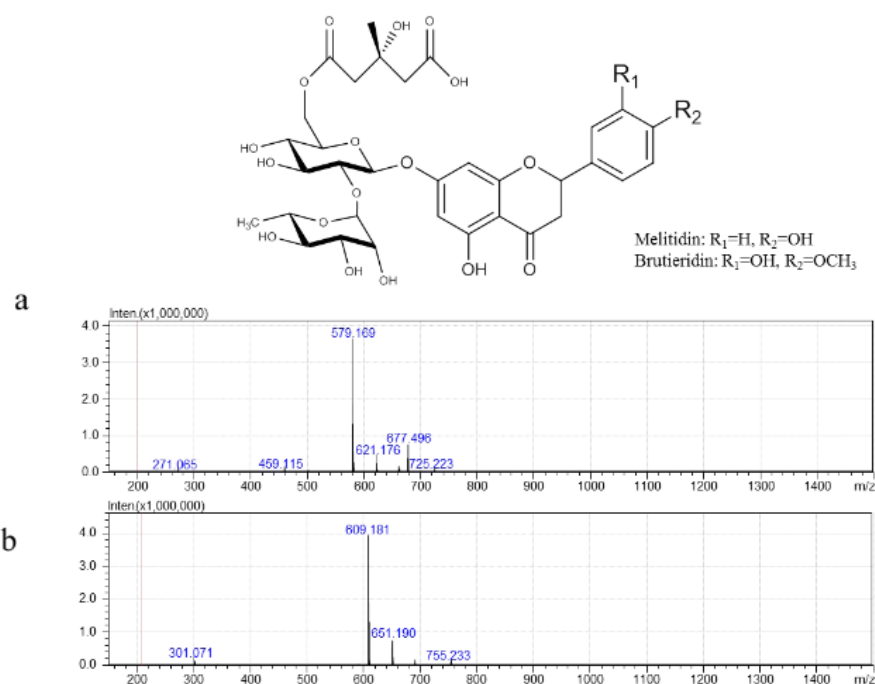


Figure 2. Structure and MS/MS spectra for Melitidin (A)

($C_{33}H_{40}O_{18}$, error 0.55 ppm) and Brutieridin (B) ($C_{34}H_{42}O_{19}$, error 0.39 ppm)

3.4 Antioxidant activity

The scavenging activity of the juice of bergamot was assessed using the spectrophotometric assay DPPH (2,2-diphenyl-1-picrylhydrazyl), a commercial radical oxidant that in solution gives a characteristic color purple. The DPPH in the presence of antioxidants, is reduced to DPPH-H with consequent modification of the color, in fact, undergoes a color change from purple to yellow. The degree of discoloration is directly proportional to the antioxidant potential of the test sample. The antioxidant activity of the flavonoids of bergamot juice was expressed in terms of IC₅₀ and compared with the standard (Figure 3).

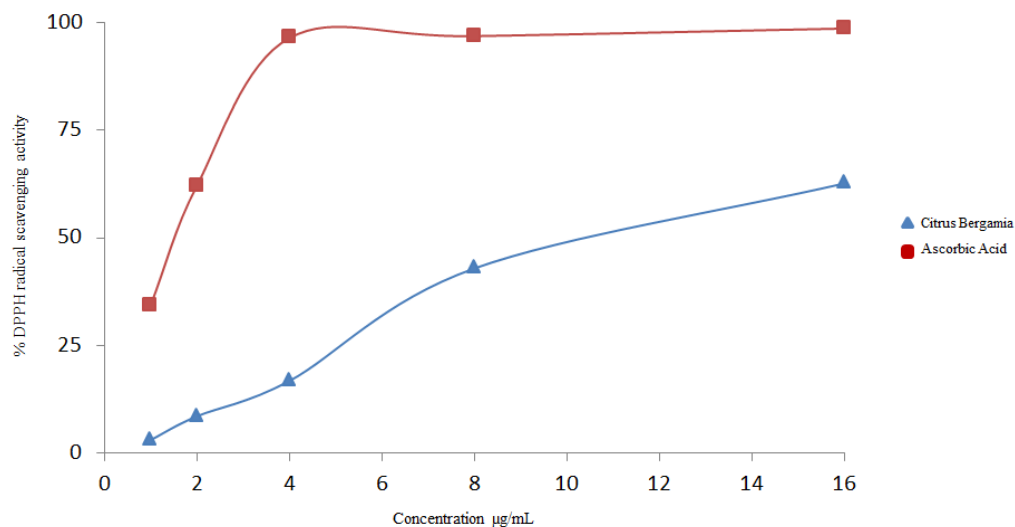


Figure 3: Antioxidant activity of flavonoids bergamot juice measured by the DPPH assay: (▲) Flavonoids Bergamot (■) Ascorbic Acid

In Figure 3 were compared the antioxidant capacity of the raw extract of flavonoids and ascorbic acid. Were used samples of the crude extract of bergamot juice at different concentrations, from 1 to 16 mg / mL.

The same procedure was performed with the ascorbic acid used as a positive control. With increasing concentration of the sample, the methanolic solution of DPPH, initially purple in color, has undergone continuous modifications, until the attainment of a yellow color which highlighted the overcoming of the steady-state where the radicals present had been completely neutralized (Figure 4).



Figure 4: Colorimetric change of radical DPPH

The results shown in Figure 3 have indicated that the activity of the flavonoids of the juice of bergamot, despite being lower than the standard used for the analysis, however, exerts a modest anti-radical action. IC₅₀ values of flavonoids and ascorbic acid were respectively 10.3 µg / mL and 1.5 µg / mL (Table 3)^[36] The results of this assay gave a further confirmation of the antioxidant juice bergamot.

Table 3: Antioxidant activity of flavonoids bergamot juice

Tested Material	Concentration (µg / mL)	% DPPH Radical Scavenging	IC ₅₀ (µg / mL)
Ascorbic Acid	1	34.36	1.5 (µg / mL)
	2	62.11	
	4	96.47	
	8	96.91	
	16	98.68	
Citrus bergamia	1	3.00	10.30 (µg / mL)
	2	8.50	
	4	16.73	
	8	42.91	
	16	62.66	

4. Conclusions

In this work, a UHPLC–IT-TOF-MS method for the fast analysis of flavonoids in bergamot juice was developed. A core–shell column was employed to obtain the separation of 17 compounds in less than 5 min, a tenfold reduction with respect to a conventional HPLC separation. Unambiguous determination of the flavonoid identities as well as high mass accuracy were attained. This method shows the potential of UHPLC as a tool for the rapid and accurate characterization of flavonoids that can be applied to other Citrus juices for qualitative/quantitative purposes, or to analyze large batches of samples.

5. References

- [1] Maxwell, C.A, Philips, D.A. Concurrent synthesis and release of *nod* gene expression in *Rhizobium trifolii*, *Plant Physiology*, **1990**, 93, 1552-1558.
- [2] Olsson, L. C., Veet, M., Weissenback, G., Barnman, J. F. Differential flavonoid response to enhanced uv-b radiation in brassica napus, *Phytochemistry*, **1998**, 49, 1021–1028.
- [3] Tanaka, T., Makika, H., Kawabata, K., Mori, H., Kakumoto, M., Satoh, K., Hara, A., Sumida, T., Tanaka, T., Ogawa, H. Chemoprevention of azoxymethaneinduced rat colon carcinogenesis by naturally occurring flavonoids, diosmin and hesperidin, *Carcinogenesis*, **1997**, 18, 957–965.
- [4] Tenore G.C., Manfra M., Stiuso P., Coppola L., Russo M., Ritieni A. and Campiglia P. “Polyphenolic pattern and in vitro cardioprotective properties of typical red wines from vineyards cultivated in Scafati (Salerno, Italy)”, *Food Chemistry*, **2013**, 140, 803-809.

- [5] Prouillet, C., Maziere, J.-C., Maziere, C., Wattel, A., Brazier, M., Kamel, S. Stimulatory effect of naturally occurring flavonoids quercetin and kaempferol on alkaline phosphate activity in MG-63 human osteoblasts through ERK and estrogen receptor pathway, *Biochemical Pharmacology*, **2004**, 67, 1307– 1313.
- [6] Rice Evans, C.A., Miller, N.J., Paganga, G. Free Radical Structure-antioxidant activity relationships of flavonoids and phenolic acids, *Free Radical Biology & Medicine*, **1996**, 20, 933-956.
- [7] Tripoli, E., La Guardia, M., Giammanco, S., Di Majo, D., Giammanco, M. Citrus flavonoids: Molecular structure, biological activity and nutritional properties: A review, *Food Chemistry*, **2007**, 104, 466–479.
- [8] Gardana, C., Nalin, F., Simonetti, P. Evaluation of flavonoids and furanocoumarins from *Citrus bergamia* (Bergamot) juice and identification of new compounds, *Molecules*, **2008**, 13, 2220-2228.
- [9] Pernice, R., Borriello, G., Ferracane, R., Borrelli, R.C., Cennamo, F., Ritieni, A. Bergamot: a source of natural antioxidants for functional fruit juices, *Food Chemistry*, **2009**, 112, 545-550.
- [10] Gattuso, G., Caristi, C., Gargiulli, C., Bellocco, E., Toascano, G., Leuzzi, U. Flavonoid glycosides in bergamot juice (*Citrus bergamia* Risso), *Food Chemistry*, **2006**, 54, 3929-3935.
- [11] Dugo, P., Lo Presti, M., Ohman, M., Fazio, A., Dugo, G., Mondello, L. Determination of flavonoids in citrus juices by micro-HPLC-ESI-MS, *Journal Separation Science*, **2005**, 28, 1149-1156.
- [12] Molnar-Perl, I., Fuzfai, Z. Chromatographic, capillary electrophoretic and capillary electrochromatographic techniques in the analysis of flavonoids, *Journal Chromatography A*, **2005**, 1073, 201-227.
- [13] Dugo, P., Donato, P., Cacciola, F, Germano, M. P., Rapisarda, A. Mondello, L. Characterization of the polyphenolic fraction of *Morus alba* leaves extracts by

HPLC coupled to a hybrid IT-TOF MS system, *Journal Separation Science*, **2009**, 32, 3627–3634.

[14] Wu, X., Ding, W., Zhong, J., Wan, J., , Xie, Z. Simultaneous qualitative and quantitative determination of phenolic compounds in *Aloe barbadensis* Mill by liquid chromatography–mass spectrometry-ion trap-time-of-flight and high performance liquid chromatography-diode array detector, *Journal of Pharmaceutical and Biomedical Analysis*, **2013**, 80, 94– 106.

[15] Barnes, J. S., Nguyen, H. P., Shen, S., Schug, K. A. General Method for Extraction of Blueberry Anthocyanins and Identification Using High Performance Liquid Chromatography-Electrospray Ionization-Ion Trap-Time of Flight Mass Spectrometry, *Journal Chromatography A*, **2009**, 1216, 4728–4735.

[16] Barnes, J. S., Schug, K. A. Structural characterization of cyanidin-3, 5-diglucoside and pelargonidin-3, 5-diglucoside anthocyanins: Multi-dimensional fragmentation pathways using high performance liquid chromatography-electrospray ionization-ion trap-time of flight mass spectrometry, *International Journal of Mass Spectrometry and Ion Processes*, **2011**, 308, 71– 80.

[17] Kalili, K.M., Cabooter, D., Desmet, G., de Villiers, A. Kinetic optimisation of the reversed phase liquid chromatographic separation of proanthocyanidins on sub-2µm and superficially porous phases, *Journal Chromatography A*, **2012**, 1236, 63-76.

[18] Kalili, K.M., de Villiers, A. Recent developments in the HPLC separation of phenolic compounds, *Journal Separation Science*, **2011**, 34, 854-876.

[19] Gamal-Eldeen, A. M., Kawashty, S. A., Ibrahim, L. F., Shabana, M. M., El-Negoumy, S. I. Evaluation of antioxidant, anti-inflammatory, and antinociceptive properties of aerial parts of *Vicia sativa* and its flavonoids, *Journal of Natural Remedies*, **2004**, 4, 81-9620.

[20] Mencherini, T., Campone, L., Piccinelli, A., Garcia Mesa, M., Sanchez, D.M., Aquino, R.P., Rastrelli, L. HPLC-PDA-MS and NMR characterization of a

hydroalcoholic extract of *Citrus aurantium* L. var. amara peel with antiedematogenic activity, *Journal of Agricultural and Food Chemistry*, **2013**, 61, 1686-1693.

[21] Mata Bilbao, M.d.L., Andres-Lacueva, C., Jauregui, O., Lamuela-Raventos, R.M. Determination of flavonoids in a Citrus fruit extract by LC–DAD and LC–MS, *Food Chemistry*, **2007**, 101, 1742-1747.

[22] Motilva, M.J., Serra, A., Macia, A. Analysis of food polyphenols by ultra high-performance liquid chromatography coupled to mass spectrometry: an overview, *Journal Chromatography A*, **2013**, 1292, 66-82.

[23] Guillarme, D., Casetta, C., Bicchi, C., Veuthey, J.L. High throughput qualitative analysis of polyphenols in tea samples by ultra-high pressure liquid chromatography coupled to UV and mass spectrometry detectors, *Journal Chromatography A*, **2010**, 1217, 6882-6890.

[24] Di Donna L., Taverna, D., Mazzotti, F., Benabdelkamel, H., Attya, M., Napoli, A. and Sindona, G. Comprehensive assay of flavanones in citrus juices and beverages by UHPLC–ESI-MS/MS and derivatization chemistry, *Food Chemistry*, **2013**, 141, 2328–2333.

[25] Medina-Rem, A. , Tulipani, S., Rotches-Ribalta, M., Mata-Bilbao, M. D.L., Andres-Lacueva, C., and Lamuela-Raventos, R. M. A fast method coupling ultrahigh performance liquid chromatography with diode array detection for flavonoid quantification in citrus fruit extracts, *Journal of Agricultural and Food Chemistry*, **2011**, 59, 6353–6359.

[26] Guiochon, G., Gritti, F. Shell particles, trials, tribulations and triumphs, *Journal Chromatography A*, **2011**, 1218, 1915-1938.

[27] Gritti, F., Guiochon, G. Performance of columns packed with the new shell Kinetex-C18 particles in gradient elution chromatography, *Journal Chromatography A*, **2010**, 1217, 1604-1615.

- [28] Fekete, S., Olah, E., Fekete, J. Fast liquid chromatography: The domination of core-shell and very fine particles, *Journal Chromatography A*, **2012**, 1228, 57-71.
- [29] Neue, U.D. Theory of peak capacity in gradient elution, *Journal Chromatography A*, **2005**, 1079, 153-161.
- [30] Donato, P., Cacciola, F., Sommella, E., Fanali, C., Dugo, L., Dacha, M., Campiglia, P., Novellino, E., Dugo, P., Mondello, L. Online Comprehensive RPLC × RPLC with Mass Spectrometry Detection for the Analysis of Proteome Samples, *Analytical Chemistry*, **2011**, 83, 2485–2491.
- [31] Ferreres, F., Silva, B.M., Andrade, P.B., Seabra, R.M., Ferreira, M.A. Approach to the study of C-glycosyl flavones by Ion Trap HPLC-PAD-ESI/MS/MS: application to seeds of quince (*Cydonia oblonga*), *Phytochemical Analysis*, **2003**, 14, 352-359.
- [32] Rijke, E., Out, P., Niessen, W.M.A., Ariese, F., Gooijer, Brinkman, U.A.Th. Analytical separation and detection methods for flavonoids, *Journal Chromatography A*, **2006**, 1112, 31.
- [33] Di Donna, L., Gallucci, G., Malaj, N., Romano, E., Tagarelli, E., Sindona, G. Recycling of industrial essential oil waste: Brutieridin and Melitidin, two anticholesterolaemic active principles from bergamot albedo, *Food Chemistry*, **2009**, 125, 438-441.
- [34] Mollace, V., Sacco, I., Janda, I., Malara, C., Ventrice, D., Colica, C., Visalli, V., Muscoli, S., Ragusa, S., Muscoli, C., Rotiroti, D., Romeo, F. Hypolipemic and hypoglycaemic activity of bergamot polyphenols: from animal models to human studies, *Fitoterapia*, **2011**, 82, 309-316.
- [35] Simirgiotis, M. J., Schmeda-Hirschmann, G., Bórquez, J., Kennelly, E. J. The *Passiflora tripartita* (Banana Passion) Fruit: A Source of Bioactive Flavonoid C-Glycosides Isolated by HSCCC and Characterized by HPLC–DAD–ESI/MS/MS, *Molecules*, **2013**, 18, 1672-1692.

^[36] Nahak, G., Sahu, R.K. Phytochemical Evaluation and Antioxidant activity of Piper cubeba and Piper nigrum, *Journal of Applied Pharmaceutical Science*, **2011**, 01 (08),153-157.

CHAPTER III

**UHPLC profiling and effects on LPS-stimulated J774A.1
macrophages of flavonoids from Citrus bergamia juice industry, an
underestimated waste product with high anti-inflammatory
potential**

Abstract: Despite its high content of flavonoids, Citrus bergamot juice, is considered a waste product of the essential oil industry. In the present contribution, the potential of industrial bergamot juice against inflammation process is highlighted. This product differs from bergamot juice crude because it is subjected to continuous thermal stress. After a fast and accurate characterization, by a novel UHPLC-IT-TOF platform, we evaluated the in vitro effect of bergamot juice against inflammatory response induced by Escherichia coli lipopolysaccharide (LPS) in J774A.1 murine macrophages. Polyphenolic compounds present in bergamot juice reduced reactive oxygen species (ROS) release and other important pro-inflammatory mediators, such as nitric oxide (NO), inducible nitric oxide synthase (iNOS) and cyclooxygenase-2 (COX-2) protein expression. Moreover, the cytoprotective haem-oxygenase-1 (HO-1) enzyme expression in LPS-stimulated J774A.1 macrophages was enhanced. Our results demonstrated that industrial bergamot juice acts as antioxidant and anti-inflammatory agent in LPS-treated J774A.1 macrophages.

Keywords: Bergamot, Flavonoids, UHPLC, LPS, Inflammation.

1. Introduction

Among Citrus plants, Citrus bergamia is widely used in the cosmetic and essential oil industry, but its juice, characterized by a bitter taste, is considered a waste in the production process, although several studies^[1-3] have highlighted the large quantity of flavonoids contained in this fruit. Many studies have recently focused in the attention on the potential health effects of flavonoids from different natural sources, such as anticancer, and anti-inflammatory properties^[4], as well as the ability to reduce oxidative stress^[5-10]. In this regard, macrophages play a major role

in host defense during inflammatory and immune response; however, excessive activation of these cells may cause extensive damage to tissues. In response to lipopolysaccharide (LPS), a component of gram-negative bacterial cell walls, macrophages produce and release inflammatory mediators, including cytokines, pro-inflammatory enzymes, as inducible nitric oxide synthase (iNOS) and cyclooxygenase-2 (COX-2), and highly reactive species, as nitric oxide (NO) and reactive oxygen species (ROS). Despite ROS has many physiological usefulness and protective role in human health their levels, if not properly regulated, could also lead to a number of deleterious effects^[11]. The qualitative and quantitative characterization of the major biomolecules present in the industrial bergamot juice is usually carried out by standard HPLC–MS^[12] techniques, employing C18 columns packed with conventional particles^[7,9,10]. All these approaches are generally characterized by long analysis times of approximately 50 min, in agreement with the literature, for the analysis of phenolic compound^[13]. Ultra-high pressure liquid chromatography (UHPLC) has opened up new possibilities in the analysis of complex matrices, such as foods and biological samples, achieving 5- to 10-fold faster separations than what obtained with conventional HPLC systems, while maintaining or increasing resolution^[14]. During my PhD, after a fast and accurate characterization of flavonoids through a novel UHPLC–MS-IT-TOF platform, we evaluated the anti-inflammatory potential of industrial bergamot juice on NO, iNOS, COX-2, ROS and heme oxygenase-1 (HO-1) expression in J774A.1 murine macrophages stimulated with LPS.

2. Materials and methods

2.1 Reagents and standards

Ultra pure water (H₂O) was obtained by a Milli-Q system (Millipore, Milan, Italy), acetonitrile (ACN) LC–MS grade and formic acid (HCOOH) were purchased by Sigma–Aldrich (Milan, Italy). For the separation a Kinetex C18 150 × 4.6 mm, 2.6µm and a 150 × 2.1mm columns were employed (Phenomenex, Bologna, Italy).

2.2 Sample preparation

The industrial bergamot juice was subjected to centrifugation in order to remove the fibers. The centrifuge was set at 6000 rpm/min for 20 minutes, then lyophilized for 24 hours. From 80 mL of juice, 1.2 g of dry extract was obtained. Sample was stored at 5°C, then solubilized in methanol to a concentration of 1 mg/mL, subjected to ultrasonication and filtered prior to injection on 0.45 µm nylon membrane (Millipore).

2.3 Instrumentation and UHPLC–MS/MS conditions

UHPLC analyses were performed on a Shimadzu Nexera UHPLC system, The UHPLC system was coupled online to an LCMS–IT-TOF mass spectrometer through an ESI source (Shimadzu, Kyoto, Japan). The optimal mobile phase consisted of 0.1% (v/v) HCOOH/H₂O (A) and 0.1% (v/v) HCOOH/ACN (B). Analysis was performed in gradient elution as follows: 0.01– 2.00 min, 10–15% B, 2–10 min, 15–20% B, 10–15min, 20–35% B, 15–16 35–50% B. Flow rate was 1.8 mL/min. Column oven temperature was set to 40 °C. Injection volume was 2 µL of

juice chromatograms were monitored at 280 and 330 nm at the maximum absorbance of the compounds of interest. MS detection was operated in negative ionization mode (ESI), for LC–MS/MS analysis a 2.1 mm I.D column was used with the same parameters, except a flow rate of 0.5 mL/min.

2.4 Cell culture

Unless stated otherwise, all reagents and compounds were purchased from Sigma Chemicals Company (Sigma, Milan, Italy). J774A.1 murine monocyte/macrophage cell line (American Type Culture Collection, Rockville, MD, USA), was grown in adhesion on Petri dishes and maintained with Dulbecco's modified Eagle's medium (DMEM) supplemented with 10% foetal calf serum (FCS), 25 mM HEPES, 2 mM glutamine, 100 µ/mL penicillin and 100 mg/mL streptomycin at 37 °C in a 5% CO₂ atmosphere.

2.5 Antiproliferative activity

Cells (3.5×10^4 /well) were plated on 96-well plates and allowed to adhere for 2 h. Thereafter, the medium was replaced with of fresh medium and of serial dilutions of Citrus bergamia juice (500–10 µg/mL) was added. Cells were incubated for 24, 48 and 72 h. Cell viability was assessed through MTT assay as previously reported^[15]. Macrophages viability, in response to treatment with Citrus bergamia juice, was calculated as: % dead cells = $100 \times [(OD \text{ treated}/OD \text{ control})]$.

2.6 Measurement of intracellular reactive oxygen species (ROS)

ROS formation was evaluated through the probe 2',7'-dichlorofluorescein- diacetate (H₂DCF-DA) as previously reported^[16]. Briefly, J774A.1 cells were plated at a density of 3.0×10^4 cells/well into 24-well plates and allowed to grow for 24 h. The medium was then replaced with fresh medium and cells were incubated *Citrus bergamia* juice (250–10 µg/mL) for 1 h and then co-exposed to lipopolysaccharide from *Escherichia coli* (LPS; 1 µg/mL) for 24 h. Cells fluorescence was evaluated using a fluorescence-activated cell sorting (FACS-scan; Becton Dickinson) and elaborated with Cell Quest software. Data are then expressed as mean fluorescence intensity.

2.7 Nitrite determination and Western blot analysis for iNOS, COX-2 and HO-1 expression

Macrophages J774A.1 were seeded in P60 plates (1.8×10^6 /P60) and allowed to adhere for 2 h. Thereafter, the medium was replaced with fresh medium and cells were pretreated with juice (250–10 µg/mL) for 1 h and then co-exposed to LPS (1 µg/mL) for further 24 h. NO generation was measured as nitrite (NO₂⁻; 1 µM), index of NO released by cells, in the culture medium, as previously reported^[17,18]. iNOS, COX-2 and HO-1 expression was assessed by Western blot as previously reported^[16]. Briefly after NO₂⁻ determination cell pellet was lysed and protein concentration was estimated by the Bio-Rad protein assay using bovine serum albumin as standard. Equal amounts of protein (50 µg) were dissolved in Laemmli's sample buffer, boiled, and run on a SDS polyacrylamide gel electrophoresis minigel and then transferred into 0.45 µm hybond polyvinylidene difluoride membrane. Membranes were probed with mouse monoclonal anti-iNOS,

anti-COX-2 (BD Laboratories), anti HO-1 or anti-tubulin antibody (Santa Cruz Biotechnologies, Santa Cruz, CA, USA). Blots were then incubated with horseradish peroxidase conjugated goat anti-mouse immunoglobulin (Ig)G (1:5.000) And then immunoreactive bands were visualized using electrochemiluminescence assay (ECL) detection system according to the manufacturer's instructions and exposed to Kodak X-Omat film. The protein bands of iNOS, COX-2, HO-1 and tubulin on XOmat films were quantified by scanning densitometry (Imaging Densitometer GS-700 BIO-RAD, Hercules, CA, USA). Data are normalized with tubulin expression, used as reference protein, and expressed as arbitrary densitometric units as previously reported^[19].

2.8 Data analysis

Data are reported as mean \pm standard error mean (s.e.m.) values of independent experiments, which were done at least three times, each time with three or more independent observations. Statistical analysis was performed by analysis of variance test, and multiple comparisons were made by Bonferroni's test. A P-value less than 0.05 was considered significant.

3. Results and discussion

3.1 UHPLC–MS/MS quantitative and qualitative analysis of juice

The classic methods reported for the analysis of flavonoids in Citrus bergamia juice^[7,9,10] and in other species of citrus^[20] usually consists in employing C18 columns packed with conventional particles and analysis time of 40– 50 min. The benefits deriving from the use of UHPLC conditions have been highlighted for the

analysis of flavonoids^[21] in other matrices, but, to best of our knowledge, never on industrial bergamot juice. In this work, column packed with 2.6 μm core-shell particles was employed. As can be seen from Figure 1, despite a considerable reduction of analysis time with respect to conventional methods present in literature^[7,9,10], high resolution and baseline separation of compounds were obtained. The quantitative analysis was performed using the external standard method. For this reason were calculated different calibration curves using the following standard: neoeriocitrin, diosmetin 6,8 di C-glucoside, rhoifolin, neohesperidin, eriocitrin, quercetin 3-b di glucoside. Stock solution (1 mg mL⁻¹) were prepared in methanol, for naringin, neohesperidin, and neoeriocitrin calibration curves were obtained in a concentration range of 50–300 mg mL⁻¹, while for other compounds in the range of 0.5–100 mg mL⁻¹, with seven concentration levels, triplicate injection of each level were run.

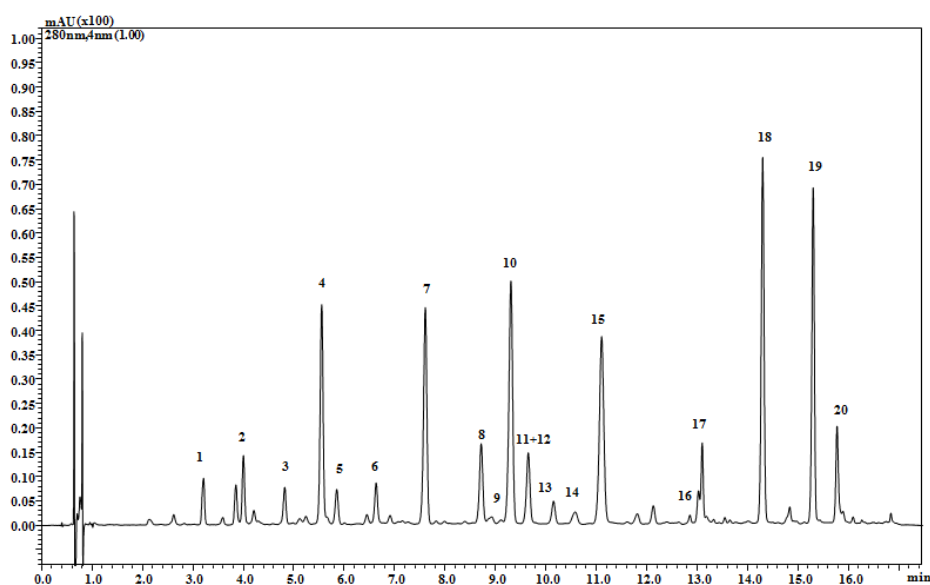


Fig.1 : UHPLC–PDA chromatogram of industrial bergamot juice

The flavanones neoeriocitrin, naringin and neohesperidin, whose inflammatory activity has been highlighted^[22], are the compounds in the highest amount in the

juice, in good agreement with several observations reported in literature, also abundant were the flavone compounds Neodiosmin, Rhoifolin, while C-glucosidic compounds are present in minor quantity (Table 1). Particularly interesting was the presence in significant quantity of the two compounds Melitidin and Brutieridin, since they show a hypolipidemic activity, due to their statin-like structure^[23]. The qualitative/quantitative difference of Citrus bergamia juice compared to industrial juice crude, is represented exclusively by the presence of three compounds 7, 11 and 13. The formation of such molecules is attributed to thermal stress to which the juice is subjected during the machining process. In order to confirm the identity of the individual molecules, UV absorbance, MS molecular ions and MSMS fragmentation patterns were used. Results are shown in Table 2 in order of peak elution. UHPLC conditions allowed to halve analysis time, which is a crucial factor to analyze large batch of samples, furthermore obtaining high separation efficiency and low solvent consumption. Moreover high mass accuracy in both full scan and MS/MS stage led to an unambiguous identification of flavonoids.

Table 1: Repeatability and quantitative data calculated for the 17 compounds identified.

Peak	tr		Area		Regression Curve	R2	Quantity mg g ⁻¹	RSD %	LOD mg g ⁻¹	LOQ mg g ⁻¹
	Mean	RSD %	Mean	RSD %						
1	3.23	0.37	10012	3.03	y = 667134.5971x + 971.6246	0.9984	9.04	± 0.30	0.867	1.113
2	4.52	2.91	8961.5	6.14	y = 667134.5971x + 971.6246	0.9984	12.80	± 0.59	0.819	1.047
3	4.83	0.32	7210.5	1.23	y = 901211.9240x + 2243.8768	0.9992	<LOQ	± 0.49	0.811	n.d
4	5.94	0.38	54944	4.31	y = 901211.9240x + 2243.8768	0.9992	39.14	± 0.52	0.765	0.981
5	7.51	0.27	7562.5	1.19	y = 562603.1127x + 468.2642	0.9990	<LOQ	-	0.890	n.d
6	7.63	0.38	12578.5	3.32	y = 667134.5971x + 971.6246	0.9984	<LOQ	-	0.892	n.d
7	8.33	0.31	59727.5	1.96	y = 678612x - 401.21	0.9998	53.50	± 0.29	0.841	0.957
8	9.71	0.27	1532.5	2.06	y = 901211.9240x + 2243.8768	0.9992	1.81	± 1.56	1.002	1.697
9	9.35	0.28	7339	2.46	y = 562603.1127x + 468.2642	0.9990	10.56	± 0.49	0.815	1.271
10	10.14	0.27	2849.5	5.24	y = 901211.9240x + 2243.8768	0.9992	59.99	± 0.77	0.801	0.997
11	10.19	0.20	2849.5	2.67	y = 579042.9939x - 1819.9253	0.9984	<LOQ	-	0.887	n.d
12	10.55	0.27	4820.5	3.62	y = 562603.1127x + 468.2642	0.9990	2.32	± 0.07	0.999	1.142
13	10.64	0.27	1532.5	2.06	y = 901211.9240x + 2243.8768	0.9992	2.86	± 0.22	1.002	1.697
14	11.39	0.21	97504.5	1.95	y = 934280.4687x + 1841.4291	0.9947	<LOQ	± 0.89	0.897	1.999
15	11.51	1.04	81670.5	4.88	y = 667134.5971x + 971.6246	0.9984	2.57	± 0.42	0.837	1.955
16	12.14	0.23	5492	1.41	y = 678612x - 401.21	0.9998	6.29	± 0.91	0.800	1.059
17	13.16	0.09	9167	3.08	y = 678612x - 401.21	0.9998	19.86	± 0.56	0.806	1.198
18	14.87	0.08	87119.5	0.48	y = 678612x - 401.21	0.9998	56.74	± 0.37	0.789	1.651
19	15.62	0.06	87119.5	0.44	y = 901211.9240x + 2243.8768	0.9992	29.56	± 0.27	0.987	1.987
20	15.88	0.06	25726.5	2.30	y = 678612x - 401.21	0.9992	14.03	± 0.52	0.953	1.424

Table 2: UHPLC–PDA-ESI-IT–TOF elucidation of flavonoids in industrial *Citrus bergamia* juice.

Peak	Molecular Formula	[M-H] ⁻ observed	[M-H] ⁻ calculated	Error [ppm]	MS ² m/z	Polyphenol sub-class	Compound
1	C ₂₇ H ₃₀ O ₁₅	593.1496	593.1506	1.68	503,473,383,353	Flavone C-glycoside	Apigenin 6,8 di C-glucoside
2	C ₂₈ H ₃₂ O ₁₆	623.1618	623.1621	0.48	503,384	Flavone C-glycoside	Diosmetin 6,8 di C-glucoside
3	C ₂₇ H ₃₂ O ₁₅	595.1647	595.1662	2.52	287	Flavanone O-glycoside	Eriodictyol 7-O-rutinoside
4	C ₂₇ H ₃₂ O ₁₅	595.1654	595.1662	1.34	459,357,235	Flavanone O-glycoside	Eriodictyol 7-O-neohesperidoside
5	C ₂₈ H ₃₄ O ₁₄	593.1517	593.1512	2.19	285,447	Flavone O-glycoside	5,7-dihydroxy-4' methoxyflavone 7-O-rutinoside
6	C ₂₂ H ₂₂ O ₁₁	461.1106	461.1089	-3.69	341,371	Flavone C-glycoside	Diosmetin 8-C-glucoside
7	C ₂₇ H ₃₂ O ₁₄	579.1711	579.1713	0.34	313,271,459	Flavanone O-glycoside	Naringenin 7-O-neohesperidoside
8	C ₂₈ H ₃₄ O ₁₅	609.1831	609.1819	-1.97	301,459	Flavanon O-glycoside	Hesperetin-7-O-rutinoside
9	C ₂₇ H ₃₀ O ₁₄	577.1566	577.1557	-1.56	269,311	Flavone O-glycoside	Apigenin 7-O-neohesperidoside
10	C ₂₁ H ₂₀ O ₁₂	463.1260	463.1246	-3.02	301	Flavanol O-glucoside	Quercetin-3-β-glucopyranoside
11	C ₂₈ H ₃₄ O ₁₅	609.1810	609.1819	1.48	301,343,447,489	Flavanon O-glycoside	Hesperetin-7-O-neohesperidoside
12	C ₃₃ H ₄₀ O ₁₉	739.2050	739.2032	-2.43	593	Flavone O-glycoside	Apigenin 7-O-neohesperidoside-4'-glucoside
13	C ₂₈ H ₃₂ O ₁₅	607.1674	607.1662	-1.97	284,299,341,443	Flavone O-glycoside	Diosmetin 7-O-neohesperidoside
14	C ₂₇ H ₃₂ O ₁₄	579.1711	579.1719	1.38	271,459,313	Flavanon O-glycoside	Naringenin-7-O-rutinoside
15	C ₃₅ H ₇₀ O ₁₄	713.47	-	-	677,451,225	Unknown C-glycoside	-
16	C ₃₃ H ₄₀ O ₁₈	723.2138	723.2142	0.55	579,271,677	Flavanone O-glycoside	Naringenin 7-[2''-α-rhamnosyl-6''-[3'''-hydroxy-3''''-methylglutaryl]-β-glucoside]
17	C ₃₄ H ₄₂ O ₁₉	753.2238	753.2241	0.39	609,301,651	Flavanone O-glycoside	Hesperetin 7-[2''-α-rhamnosyl-6''-[3'''-hydroxy-3''''-methylglutaryl]-β-glucoside]
18	C ₁₅ H ₁₂ O ₅	271.0593	271.0879	0.14	227	Flavanon	
19	C ₁₆ H ₁₄ O ₆	301.0704	301.0790	0.29	268,227	Flavanon	
20	C ₁₆ H ₁₂ O ₆	299.0546	299.0587	1.15	284,256	Flavanon	

3.2 Effect of industrial bergamot juice on LPS-stimulated macrophages

Inflammation is a pathological condition that can be triggered by several factors, including lipopolysaccharides. LPS is an important structural component of the outer membrane of Gram negative bacteria and is known to modulate macrophage response during sepsis. LPS induces an inflammatory response that culminates in the release of pro-inflammatory mediators, such as NO, iNOS, COX-2, ROS and HO-1. NO is produced from the oxidation of L-arginine by NOS that occurs in two major classes: constitutive, and inducible. The iNOS may be expressed in different cell types (e.g. macrophages, smooth muscle cells, epithelia) by various pro-inflammatory agents such as LPS. NO can be considered an immune modulator owing to its complex activity during host cellular defence^[19]. When macrophages are activated by the endotoxin from the bacterial wall components LPS, or by IFN- γ , iNOS is significantly expressed, and massive amounts of NO are produced to exert a nonspecific immune response. Induced NO, in addition to being a final common mediator of inflammation, is essential for the up-regulation of the inflammatory response. Furthermore, NO contributes to tissue damage, both directly via the formation of peroxynitrite, and indirectly through the amplification of the inflammatory response. In our experiment, LPS induced in J774A.1 macrophages a marked increase in NO release associated to an increase in iNOS expression. Industrial Citrus bergamia juice at concentrations of 250–50 $\mu\text{g/mL}$ significantly reduced NO release ($P < 0.01$ vs. LPS alone; Figure 3), while higher concentrations (250–150 $\mu\text{g/mL}$) were necessary to obtain a still appreciable reduction in iNOS expression ($P < 0.05$ vs. LPS alone; Figure 4).

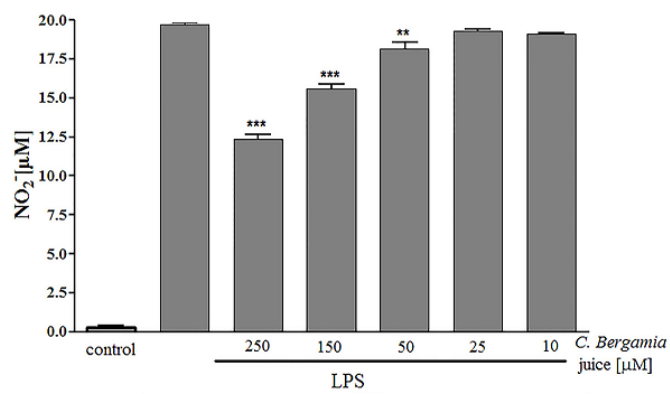


Figure 3: Effect of industrial *Citrus bergamia* juice (250–10 µg/mL) on NO release, evaluated as NO₂⁻ (µM), by macrophages J774A.1 stimulated with LPS. Values are expressed as mean ± s.e.m of NO₂⁻ (µM), of at least three independent experiments with three replicates each.

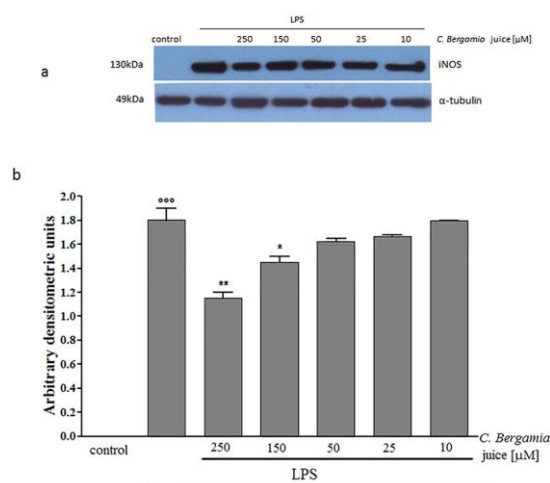


Figure 4: Representative Western blot of inducible nitric oxide synthase (iNOS) expression (a). Densitometric analysis of the concentration dependent effect of industrial *Citrus bergamia* juice (250–10 µg/mL) on LPS-induced iNOS expression in J774A.1 macrophages (b). Values, mean ± s.e.m., are expressed as arbitrary densitometric units at least 3 independent experiments with three replicates each.

An interaction between NOS and COX pathway represents an important mechanism for the modulation of the inflammatory response^[24]. COX-2 is a well known pro-inflammatory enzyme triggered by agents as LPS, it is involved in macrophage response and its expression is also influenced by NO^[25]. Thus, we evaluated the effect of industrial Citrus bergamia juice on COX-2 expression. Our data showed that, similarly to NO and iNOS, also COX-2 protein expression resulted significantly inhibited by industrial juice (250–150 $\mu\text{g}/\text{mL}$, $P < 0.01$ vs. LPS alone; (Fig. 5) further contributing to the reduction of LPS induced inflammation in J774A.1 macrophages.

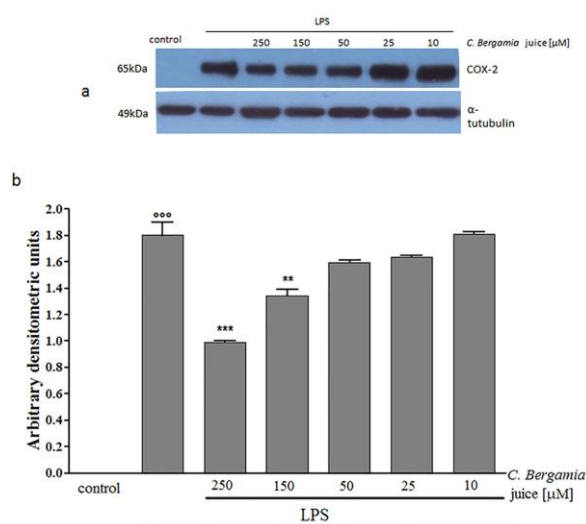


Figure 5: Representative Western blot of cyclooxygenase-2 (COX-2) expression (a). Densitometric analysis of the concentration dependent effect of industrial Citrus bergamia juice (250–10 $\mu\text{g}/\text{mL}$) on LPS-induced COX-2 expression in J774A.1 macrophages (b). Values, mean \pm s.e.m., are expressed as arbitrary densitometric units at least 3 independent experiments with three replicates each.

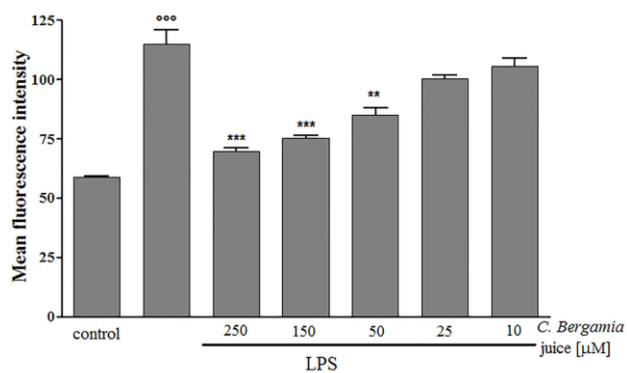


Figure 6: Effect of industrial *Citrus bergamia* juice (250–10 µg/mL) on ROS formation, evaluated by means of the probe 2',7' dichlorofluorescein-diacetate (H2DCF-DA), in LPS-stimulated J774A.1 macrophages. Values, mean \pm s.e.m., are expressed as arbitrary densitometric units at least 3 independent experiments with three replicates each.

Cells, as macrophages, in order to protect themselves against inflammatory and oxidative injury up-regulate some defence mechanisms as HO-1 expression. HO-1, the rate limiting enzyme in heme degradation, catalyzes the oxidation of heme to generate several biologically active molecules carbon monoxide (CO), biliverdin, and ferrous ion^[26]. This enzyme is normally expressed at low levels in most tissues/organs except for spleen; however, it is highly inducible in response to a variety of stimuli, as LPS, to protect cells against oxidative and inflammatory injury. Present in J774A.1 macrophages at low levels in basal condition, HO-1 resulted significantly increased by LPS ($P < 0.001$ vs. control; Figure 7). Bergamot uice (250–50 µg/mL) significantly, and in a concentration related manner, further increased HO-1 enzyme expression in J774A.1 macrophages ($P < 0.05$ vs. LPS alone; Figure 7) resulting in a protective effect for cells in presence of LPS. HO-1 can increase cellular anti-oxidant status by generating antioxidants such as bilirubin^[27], that can inhibit iNOS protein expression and suppress NO

production^[28]. Moreover, carbon monoxide (CO), a major product of HO-1 activity, was shown to inhibit COX-2 protein expression^[29]. CO was also shown to inhibit iNOS enzymatic activity thus decreasing NO production^[30]. Thus, considering the literature in the field, we can also hypothesize the important contribution of OH-1 expression in reducing inflammatory response associated to bergamot juice in LPS-stimulated J774A.1 macrophages. Moreover, MTT assay revealed that bergamot juice at all concentrations (10–500 µg/mL) and incubation times (24, 48 and 72 h) did not affect macrophage proliferation indicating its absence of toxic effects on macrophages and that the observed effects were not due to disruption of normal cellular function.

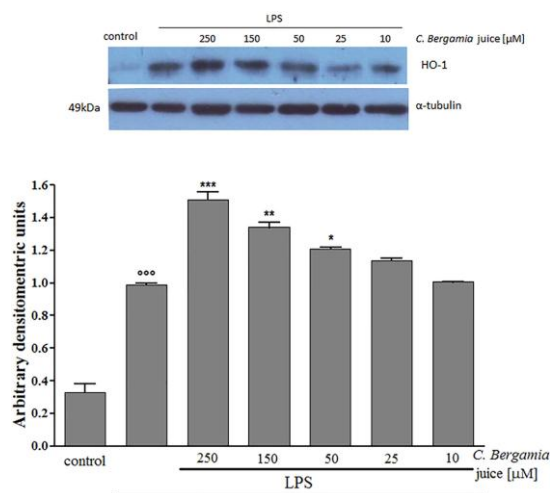


Fig. 7: Representative Western blot of heme-oxygenase (HO-1) enzyme expression (a). Densitometric analysis of the concentration dependent effect of *Citrus bergamia* juice (250–10 µg/mL) on LPS-induced OH-1 expression in J774A.1 macrophages (b). Values, mean ± s.e.m., are expressed as arbitrary densitometric units at least 3 independent experiments with three replicates each.

The capacity of flavonoids of industrial bergamot juice to reduce the release and the expression of several inflammatory mediators, has been previously investigated

in the literature. Our results are in accordance with a previous study regarding the protective effect of a bergamot extract on keratinocytes in inflammatory conditions. In particular, it has been reported that the main flavonoids, such as neoeriocitrin, naringin and neohesperidin, occurring in bergamot extract, were protective against inflammatory injuries in human keratinocytes by reducing pro-inflammatory mediators as NO and iNOS^[31]. Our data provided evidences that Citrus bergamia juice constituents could exert beneficial effects as antioxidants and inhibitors of inflammation process in LPS-stimulated J774A.1 macrophages. This effects could be addressed also to the presence of its flavanone constituents as neohesperidin, neoeriocitin and naringin, as previously reported. The antioxidant and anti-inflammatory effects of naringin and neohesperidin in LPS-induced inflammation have been also studied^[32]. As highlighted in the analytical characterization, the amount of flavonoids in juice is elevated, especially of flavanones compounds. This observation, together with the antioxidant and the anti-inflammatory activity described above, focus the attention on this bio-product, that could be easily turned from a mere waste product to a possible nutraceutical. In this regard, through a spray-drying technique the juice can be converted in microparticulate powder, thus obtaining enhanced solubility and high dissolution rate in biological fluids, as well as major stability of polyphenolic compounds and better organoleptic characteristics (masking the bitter taste of Citrus bergamia juice). This process, currently under evaluation, is particularly suitable for the production of new oral formulations, as tablets, or other preparations for functional foods.

4. Conclusions

Although the recent increasing interest in its health promoting properties^[10], industrial Citrus bergamia juice still remains an underestimated waste product of the essential oil industry. Our results showed that despite this matrix considered a by-product, is rich in polyphenolic molecules able to modulate, with excellent results, the release and the expression of numerous mediators responsible for the inflammatory conditions and oxidative stress process.

5. References

- [1] Gardana, C., Nalin, F., & Simonetti, P. Evaluation of flavonoids and furocoumarins from C.b (Bergamot) juice and identification of new compounds, *Molecules*, **2008**, 13, 2220–2228.
- [2] Gattuso, G., Caristi, C., Gargiulli, C., Bellocco, E., Toascano, G., & Leuzzi, U. Flavonoid glycosides in bergamot juice. (C.b Risso), *Journal of Agricultural and Food Chemistry*, **2006**, 54, 3929–3935.
- [3] Pernice, R., Borriello, G., Ferracane, R., Borrelli, R.C., Cennamo, F., Ritieni, A. Bergamot: a source of natural antioxidants for functional fruit juices, *Food Chemistry*, **2009**, 112, 545-550.
- [4] Albishi, T., John, J. A., Al-Khalifa, A. S., & Shahaidi, F. Antioxidant, anti-inflammatory and DNA scission inhibitory activities of phenolic compounds in selected onion and potato varieties, *Journal of Functional Foods*, **2013**, 5, 930–939.
- [5] Braca, A., Dal Piaz, F., Marzocco, S., Autore, G., Vassallo, A., & De Tommasi, N. Triterpene derivatives as inhibitors of protein involved in the inflammatory

process: Molecules interfering with phospholipase A(2), cyclooxygenase, and lipoxygenase, *Current Drug Targets*, **2011**, 12(3), 302–321.

[6] Calder, P. C., Albers, R., Antoine, J. M., Blum, S., Bourdet-Sicard, R., Ferns, G. A., Folkerts, G., Friedmann, P. S., Frost, G. S., & Guarner, F. Inflammatory disease processes and interactions with nutrition, *British Journal of Nutrition*, **2009**, 101, 1–45.

[7] Chahar, M. K., Sharma, N., Dobhal, M. P., & Joshi, Y. C. Flavonols: A versatile source of anticancer drugs, *Pharmacognosy Reviews*, **2011**, 5, 1–12.

[8] Huang, M., Lu, J. J., Huang, M. Q., Bao, J. L., Chen, X. P., & Wang, Y.T. Terpenoids: Natural products for cancer therapy, *Expert Opinion on Investigational Drugs*, **2012**, 21(12), 1801–1818.

[9] Juliao, Lde. S., Piccinelli, A. L., Marzocco, S., Leitaõ, S. G., Lotti, C. Autore, G., & Rastrelli, L. Phenylethanoid glycosides from *Lantana fucata* with in vitro anti-inflammatory activity, *Journal of Natural Products*, **2009**, 72(8), 1424–1428.

[10] Sannigrahi, S., Mazumder, U. K., Pal, D., Mishra, M. L., & Maity, S. Flavonols of *Enhydra fluctuans* exhibits analgesic and anti-inflammatory activity in different animal models, *Pakistan Journal of Pharmaceutical Sciences*, **2011**, 24, 369–375.

[11] Popolo, A., Autore, G., Pinto, A., & Marzocco, S. Oxidative stress in patients with cardiovascular disease and chronic renal failure, *Free Radical Research*, **2013**, 47(5), 346–356.

[12] Chandrasekara, A., & Shahidi, F. Determination of antioxidant activity in free and hydrolyzed fractions of millet grains and characterization of their phenolic profiles by HPLC–DAD–ESI–MSn, *Journal of Functional Foods*, **2011**, 3(3), 144–158.

- [13] Molnar-Perl, I., & Fuzfai, Z. Chromatographic, capillary electrophoretic and capillary electrochromatographic techniques in the analysis of flavonoids, *Journal of Chromatography A*, **2005**, 1073, 201–227.
- [14] Kalili, K. M., & de Villiers, A. Recent developments in the HPLC separation of phenolic compounds, *Journal of Separation Science*, **2011**, 34, 854–876.
- [15] Cioffi, G., Sanogo, R., Vassallo, A., Dal Piaz, F., Autore, G., Marzocco, S., & De Tommasi, N. Pregnane glycosides from *Leptadenia pyrotechnica*, *Journal of Natural Products*, **2006**, 69(4), 625–635.
- [16] Adesso, S., Popolo, A., Bianco, G., Sorrentino, R., Pinto, A., Autore, G., & Marzocco, S. The uremic toxin indoxyl sulphate enhances macrophage response to LPS, *PLoS One*, **2013**, 8(9), 776–778.
- [17] Bianco, G., Russo, R., Marzocco, S., Velotto, S., Autore, G., & Severino, L. Modulation of macrophage activity by aflatoxins B1 and B2 and their metabolites aflatoxins M1 and M2, *Toxicon*, **2012**, 59(6), 644–650.
- [18] Geronikaki, A. A., & Gavalas, A. M. Antioxidants and inflammatory disease: Synthetic and natural antioxidants with anti-inflammatory activity. *Combinatorial Chemistry & High Throughput Screening*, **2006**, 9, 425–442.
- [19] Moncada, S., & Higgs, A. The L-arginine NO pathway, *The New England Journal of Medicine*, **1993**, 329, 2002–2012.
- [20] Mencherini, T., Campone, L., Piccinelli, A., Garcia Mesa, M., Sanchez, D. M., Aquino, R. P., & Rastrelli, L. HPLC–PDA– MS and NMR characterization of a hydroalcoholic extract of *Citrus aurantium* L. Var. amara Peel with antiedematogenic activity, *Journal of Agricultural and Food Chemistry*, **2013**, 61, 1686–1693.

- [21] Motilva, M. J., Serra, A., & Macia, A. Analysis of food polyphenols by ultra high-performance liquid chromatography coupled to mass spectrometry: An overview, *Journal of Chromatography A*, **2013**, 1292, 66–82.
- [22] Jain, M., & Parmar, H. S. Evaluation of antioxidative and anti-inflammatory potential of hesperidin and naringin on the rat air pouch model of inflammation, *Inflammation Research*, **2011**, 60(5), 483–491.
- [23] Di Donna, L., Gallucci, G., Malaj, N., Romano, E., Tagarelli, E., & Sindona, G. Recycling of industrial essential oil waste: Brutieridin and Melitidin, two anticholesterolaemic active principles from bergamot albedo, *Food Chemistry*, **2009**, 125, 438–441.
- [24] Moncada, S., Palmer, R. M. J., & Higgs, E. Nitric oxide: physiology, pathophysiology and pharmacology, *Pharmacological Reviews*, **1991**, 43, 109–142.
- [25] Meng-Ling, W., Yen-Chun, H., Chen-Yu, L., & Shaw-Fang, Y. Heme oxygenase-1 in inflammation and cardiovascular disease, *American Journal of Cardiovascular Disease*, **2011**, 1(2), 150–158.
- [26] Lin, C. C., Liu, X. M., Peyton, K., Wang, H., Yang, W. C., Lin, S. J., & Durante, W. Far infrared therapy inhibits vascular endothelial inflammation via the induction of heme oxygenase-1, *Arteriosclerosis, Thrombosis, and Vascular Biology*, **2008**, 28(4), 739–745.
- [27] Wang, W. W., Smith, D. L., & Zucker, S. D. Bilirubin inhibits iNOS expression and NO production in response to endotoxin in rats, *Hepatology*, 2004, 40(2), 424–433.
- [28] Suh, G. Y., Jin, Y., Yi, A. K., Wang, X. M., & Choi, A. M. CCAAT/enhancer-binding protein mediates carbon monoxide-induced suppression of cyclooxygenase-2, *American Journal of Respiratory Cell and Molecular Biology*, **2006**, 35(2), 220–226.

- [29] Thorup, C., Jones, C. L., Gross, S. S., Moore, L. C., & Goligorsky, M. S. Carbon monoxide induces vasodilation and nitric oxide release but suppresses endothelial NOS, *American Journal of Physiology*, **1999**, 277, 882–889.
- [30] Graziano, A., Cardile, V., Crasci, L., Caggia, S., Dugo, P., Bonina, F., & Panico, A. Protective effect of an extract from C.b against inflammatory injury in interferon-gamma and histamine exposed human keratinocytes, *Life Sciences*, **2012**, 90, 968–974.
- [31] Limasset, B., Doucen, C. L., Dore, J. C., Ojasoo, T., Damon, M., & Paulet, A. C. Effects of flavonoids on the release of reactive oxygen species by stimulated human neutrophils, *Biochemical Pharmacology*, **1993**, 46, 1257–1271.
- [32] Je-Min, C., Byoung-Seok, Y., Sang-Kyou, L., Jae-Kwan, H., & Ryung, R. Antioxidant properties of neohesperidin dihydrochalcone: Inhibition of hypochlorous acid-induced DNA strand breakage, protein degradation, and cell death, *Biological & Pharmaceutical Bulletin*, **2007**, 30(2), 324–330.

CHAPTER IV

Flavonoids from Citrus sinensis extract: anti-inflammatory and hypoglycemic evaluation

Abstract Citrus plants contain a large amount of flavonoids with beneficial effects on human health. This study reports on a detailed profiling of the major polyphenolic constituents of Citrus sinensis juice extract by UHPLC-MS/MS-IT-TOF. Furthermore the nutraceutical potential of Citrus sinensis extract was evaluated in vitro, on J774A.1 murine macrophages and in human hepatoblastoma cells HepG2. Our results demonstrate that Citrus sinensis extract reduced nitric oxide, Tumor Necrosis Factor- α release and inducible nitric oxide synthase and cyclooxygenase-2 expression in macrophages acting on nuclear transcription factor NF-kB activation. Moreover Citrus sinensis extract reduced reactive oxygen species release and increased heme-oxygenase-1 expression. Citrus sinensis extract significantly inhibited HepG2 cell proliferation and significantly decreased cellular glucose uptake. Our results provide evidence that the polyphenolic constituents of Citrus sinensis extract could have potential nutraceutical properties.

Keywords: Citrus sinensis, Flavonoids, Anti-inflammatory, Antioxidant, Hypoglycemic.

1. Introduction

Plants rich in certain flavonoids have been traditionally used for their anti-inflammatory properties and, recently, attention has been given to isolated flavonoids, including those in Citrus, as potential anti-inflammatory and as natural antioxidant agents. Citrus is one of the largest species among plants; it consists of 40 types of which are distributed in all continents and its fruits, which are consumed mostly fresh, have been used as a herbal medicine or additive or food supplement^[1]. Citrus is believed to possess bioactivities such as anticancer, antimicrobial, antioxidant and anti-inflammatory^[2].

Inflammation is a combined biological process, induced by microbial infection or tissue injury potentially leading to sepsis, multiple organ failure and death. Inflammatory response is essential to eliminate threats but can be deleterious when the initial reaction is not limited. In these cases, anti-inflammatory compounds are therapeutically useful and administered to control the inflammation response. Macrophages have an important role during inflammatory and immune response; however, their excessive activation may cause extensive tissue damage. Macrophages activation by bacterial cell wall components as Lipopolysaccharide (LPS), a component of gram-negative bacteria, promotes the synthesis and release of large amounts of pro-inflammatory mediators as cytokines, nitric oxide (NO), pro-inflammatory enzymes (e.g cyclooxygenase-2; COX-2) and reactive oxygen species (ROS), all mediators involved in the inflammatory onset. NO synthesis during inflammation is mainly due to inducible nitric oxide synthase (iNOS) activity and drugs that inhibits iNOS have been proposed as anti-inflammatory agents^[3]. During inflammatory responses transient activation of the nuclear transcription factor NF-kB constitutes an important step and plays a key role in the regulated expression of several pro-inflammatory mediators including cytokines and pro-inflammatory enzymes^[4]. Because of this pivotal role, NF-kB is a relevant target for the pharmacological action of anti-inflammatory molecules activation in a variety of inflammatory conditions. Certain types of cells, such as macrophages, in order to protect themselves against inflammatory and oxidative injury up-regulates some defence mechanisms as heme oxygenase-1 (HO-1) enzyme expression, also in response to LPS. Although oxidative response regulates many physiological response in human health, as the inflammatory one, if not properly regulated it could also lead to a number of deleterious effects mediating many aspect of inflammatory-induced tissue damage and dysfunctions^[5]. Nowadays, the study of oxygen-containing free radicals in humans and their role has been of growing interest among scientists. The most important and useful source for such

inhibitors, both with anti-inflammatory and anti-oxidant properties, is the area of natural products. Many studies report on the potential health effects of flavonoids from different natural sources, such as anticancer and antiinflammatory properties as well as antioxidants^[6,7]. During my PhD, in order to evaluate the molecular mechanism involved in these observations, after the characterization of the main flavonoid compounds present in Citrus sinensis juice extract, by a fast and accurate UHPLC-ESI-IT-TOF platform and in vitro bioavailability studies, we evaluated the nutraceutical potential of Citrus sinensis juice extract. The anti-inflammatory effect of Citrus sinensis juice extract was evaluated on J774A.1 macrophage stimulated with LPS. In particular we have investigated the effect of Citrus sinensis juice extract on 1) NO production; 2) iNOS and COX-2 expression; 3) TNF- α release; 4) p65 NF- κ B nuclear translocation; 5) ROS production and 6) HO-1 expression. Furthermore we have evaluated the effect of Citrus sinensis juice extract on cell proliferation, glucose uptake, free NO release and lipid peroxidation in hepatoma cell lines HepG2.

2. Materials and methods

2.1 Reagents and standards

Ultra pure water (H₂O) was obtained by a Milli-Q Direct 8 system (Millipore, Milan, Italy), acetonitrile (ACN) LC-MS grade and formic acid (HCOOH) were purchased by Sigma Aldrich (Milan, Italy). For the quantitative and qualitative analysis of flavonoids, two columns were employed respectively: a Kinetex C18 150 \times 4.6 mm (100 Å), length \times internal diameter (L \times I.D.), packed with 2.6 μ m particles, and a Kinetex C18 150 \times 2.1 mm, L \times I.D., 2.6 μ m column (Phenomenex, Bologna, Italy). Both columns were protected with C18 precolumns (Phenomenex). Flavonoids standards (diosmetin 6,8 di C-glucoside, neohesperidin,

eriocitrin, isoquercetin, narirutin, diosmetin, hesperetin) and polymethoxyflavones (tangeretin) were purchased from Sigma Aldrich (Milan, Italy).

2.2 Sample preparation

The flavonoid fraction of *Citrus sinensis* var. Tarocco was provided by the company “Agrumaria Corleone” (Palermo, Italy), which used fruits from plants cultivated in Sicily (Italy). The extract was stored at a temperature of -20 °C until its use. In order to remove fibers, the extract were centrifuged at 12000 rpm/min for 15 minutes, lyophilized for 24 hours and then stored in small aliquots at -20 °C. From 100 mL of juice, 400 mg of dry extract was obtained. For the chemical analysis, sample was solubilized in methanol to a concentration of 1 mg/mL, subjected to ultrasonication and filtered prior to injection on 0.45 µm nylon membrane (Millipore).

2.3 Instrumentation

UHPLC analysis were performed on a Shimadzu Nexera UHPLC system, consisting of a CBM-20A controller, two LC-30AD dual-plunger parallel-flow pumps, a DGU-20 A5R vacuum degasser, an SPD-M20A photo diode array detector (equipped with a 2.5 µL detector flow cell volume), a CTO-20AC column oven, a SIL-30AC autosampler. The UHPLC system was coupled online to an LCMS-IT-TOF mass spectrometer through an ESI source (Shimadzu, Kyoto, Japan). LC-MS data elaboration was performed by the LCMSsolution® software (Version 3.50.346, Shimadzu).

2.4 UHPLC-PDA Conditions

The mobile phases A and B consisted of water (plus 0.1 % v/v HCOOH) and acetonitrile (plus 0.1 % v/v HCOOH). Analysis was performed in gradient elution as follows: 0.01-2.00 min, 10-15% B; 2.00-10.00 min, 15-20% B; 10.00-14.00 min, 20-35% B; 14.00-18.00 min, 35-75% B. Separation was carried out at 40 °C with a flow rate 1.8 mL/min. Injection volume was 2 µL of Citrus sinensis extract. The following PDA parameters were applied: sampling rate, 40 Hz; detector time constant, 0.160 s; cell temperature, 40 °C. The chromatograms were monitored at 280 and 330 nm.

2.5 UHPLC-ESI-IT-TOF Conditions

The optimal mobile phase consisted of 0.1% HCOOH/H₂O v/v (A) and 0.1% HCOOH/ACN v/v (B). Analysis was performed in gradient elution as follows: 0.01-2.50 min, 5-15% B, 2.50-10.00 min, 15-25% B, 10.00-12.00 min, 25-55% B, 12.00-14.50 min, 55-65% B, 14.50-15.00 min, 65-70% B. Flow rate was 0.5 mL/min. The column temperature was set at 40 °C. Injection volume was 2 µL of flavonoids extract. UHPLC system was coupled on-line to a hybrid IT-TOF instrument. MS detection was operated both positive and negative ionization mode with the following parameters: detector voltage, 1.55 kV; CDL (curved desolvation line) temperature, 200 °C; block heater temperature, 200 °C; nebulizing gas flow (N₂), 1.5 L/min, drying gas pressure, 100 kPa. Full scan MS data were acquired in the range of 200-800 m/z (ion accumulation time, 40 ms; IT, (repeat=2). MS/MS experiments were conducted in data dependent acquisition, precursor ions were acquired in the range 150-800 m/z; peak width, 3 Da; ion accumulation time, 60 ms; CID energy, 50%, collision gas 50%, repeat =1; execution trigger (BPC) intensity, at 95% stop level.

2.6 Cells and Reagents for cell culture

Unless stated otherwise, all reagents and compounds were purchased from Sigma Chemicals Company (Sigma, Milan, Italy). J774A.1 murine monocyte macrophage cell line (American Type Culture Collection, Rockville, MD), was grown in adhesion on Petri dishes and maintained with Dulbecco's modified Eagle's medium (DMEM) supplemented with 10% foetal calf serum (FCS), 25 mM HEPES, 2 mM glutamine, 100 u/mL penicillin and 100 mg/mL streptomycin at 37 °C in a 5% CO₂ atmosphere. Human hepatocellular liver carcinoma cells (HepG2) were obtained from American Type Culture Collection. Monolayers of cells were grown in DMEM medium (Dulbecco's Modified Eagle's Medium; Sigma Chemical Co., St. Louis, MO) supplemented with 10% (v/v) fetal bovine serum (FBS), 1% antibiotic/antimycotic solution (Gibco-Invitrogen, MountWaverley, Australia), 0.375% NaHCO₃, and 20 mmol/L HEPES, pH 7.4, and incubated at 37 °C in a humidified atmosphere of 5% CO₂ in air. Assays were performed by incubating the HepG2 cells (72 h) with 0, (control) 0.5 and 1 µg of Citrus Sinensis juice extract.

2.7 Antiproliferative assay

Cells (5×10^4 /well) were seeded on 96-well multiwell and allowed to adhere for 4 h at 37°C in a 5% CO₂ atmosphere. The medium was then replaced with fresh medium and serial dilutions of Citrus sinensis extract (250-10 µg/mL) was added for 24 h. Cell viability was assessed through MTT assay as previously reported^[8]. Briefly, 25 µL of MTT (5 mg/mL) were added to cells and, after 3 h, cells were lysed and the dark blue crystals solubilised with 100 µL of a solution containing 50% (v/v) N,N dimethylformamide, 20% (w/v) SDS with an adjusted pH of 4.5. The optical density (OD) was measured with a microplate spectrophotometer

(Titertek Multiskan MCC/340) equipped with a 620 nm filter. Macrophage cell viability in response to treatment with *Citrus sinensis* juice extract was calculated as: % dead cells = $100 \times [(OD \text{ treated}/OD \text{ control}) \times 100]$.

2.8 Nitrite Determination and Western Blot Analysis for iNOS, COX-2 and HO-1 Expression

Macrophages J774A.1 were seeded in P60 plates (1.8×10^6 /P60) and allowed to adhere for 2 h. Thereafter, the medium was replaced with fresh medium and cells were pretreated with *Citrus sinensis* extract (250-10 $\mu\text{g}/\text{mL}$) for 1 h before and with LPS (1 $\mu\text{g}/\text{mL}$) for further 24 h. NO release was measured as nitrite (NO_2^- , μM), index of NO released by cells, in the culture medium 24 h after LPS stimulation, as previously reported^[9]. Briefly, 100 μL of cell culture medium were mixed with 100 μL of Griess reagent equal volumes of 1% (w/v) sulphanilamide in 5% (v/v) phosphoric acid and 0.1% (w/v) naphthylethylenediamine-HCl and incubated at room temperature for 10 min, and then the absorbance was measured at 550 nm in a microplate reader Titertek (Dasit, Cornaredo, Milan, Italy). The amount of NO_2^- as μM concentration, in the samples was calculated from a sodium nitrite standard curve. iNOS, COX-2 and HO-1 expression was assessed by Western blot, as previously reported^[10]. Briefly after 24 h incubation cells were scraped off, washed with ice-cold PBS, and centrifugated at 5.000 g for 10 min at 4 °C. The cell pellet was lysed in a buffer containing 20 mM Tris hydrogen chloride (HCl; pH 7.5), 1 mM sodium orthovanadate, 1 mM phenylmethylsulfonyl fluoride, 10 $\mu\text{g}/\text{mL}$ leupeptin, 10 mM sodium fluoride, 150 mM sodium chloride, 10 mg/mL trypsin inhibitor, and 1% Tween-20. Bio-Rad protein assay using bovine serum albumin as standard was used to determine protein concentration. Equal amounts of protein (50 μg) were run on a SDS polyacrylamide gel electrophoresis (SDS-PAGE) minigel (8% polyacrylamide) and then transferred for 40 min at 5 mA cm² into

0.45 µm hybrid polyvinylidene difluoride membrane. Membranes were blocked for 40 min in PBS and 5% (w/v) nonfat milk and subsequently probed overnight at 4 °C with mouse monoclonal anti-iNOS, anti-COX-2 antibody (BD Laboratories), anti HO-1 or anti-tubulin (Santa Cruz Biotechnologies) in PBS, 5% w/v non fat milk, and 0.1% Tween-20. Membranes were then incubated with horseradish peroxidase conjugated goat anti-mouse immunoglobulin (Ig)G (1:5.000) for 1 h at room temperature. Immunoreactive bands were visualized using electrochemiluminescence assay (ECL) detection system according to the manufacturer's instructions and exposed to Kodak X-Omat film. The protein bands on XOmat films were quantified by scanning densitometry (Imaging Densitometer GS-700 BIO-RAD U.S.A.). Data are normalized with tubulin expression, used as reference protein, and expressed as arbitrary densitometric units as previously reported^[11].

2.9 TNF-α Determination

TNF-α concentrations in macrophage culture medium stimulated for 20 h with LPS (1 µg/mL) and Citrus sinensis juice extract (250-10 µg/mL) as previously described were assessed by an Enzyme-Linked Immuno Sorbent Assay (ELISA) assay by using a commercial kit, for murine TNF-α, according to manufacturer's instruction (e-Biosciences, CA, USA). Results calculated as pg/mL and expressed as percentage inhibition vs TNF-α released by J774A.1 treated with LPS alone.

2.10 Immunofluorescence Analysis with Confocal Microscopy

For immunofluorescence assay, J774A.1 cells (1×10^6 /well) were seeded in 12 well plate and treated with Citrus sinensis extract at a medium concentration range (150-50 µg/mL) for 1 h and then simultaneously with LPS (1 µg/mL) for 20 min.

Cells then were fixed with paraformaldehyde (4% in PBS) for 15 min and permeabilized for 15 min with saponin (0.1% in PBS). After 1 h of blocking (BSA plus PBS), cells were incubated with anti-phospho p65 antibody (Santa Cruz Biotechnologies) for 2 h at room temperature. The slides were then washed with PBS for three times and fluorescein-conjugated secondary antibody (FITC) were added for 1 h, DAPI was used for counterstaining of nuclei. The coverslips were washed and mounted on microscope slides. A total of 10-z-line scans with a step distance of 0.9 mm were collected and single planes or three-dimensional maximum intensity projections were performed with Zeiss LSM510 laser scanning confocal microscope (Carl Zeiss Microimaging GmbH, Germany). Images were acquired in sequential scan mode by using the same acquisition parameters (laser intensities, gain photomultipliers, pinhole aperture, objective 63X, zoom 2) when comparing experimental and control material. For the production of figures, brightness and contrast of images were adjusted by taking care to leave a light cellular fluorescence background for visual appreciation of the lowest fluorescence intensity features and to help comparison among the different experimental groups.

2.11 Measurement of Intracellular ROS

The formation of ROS was evaluated by means of the probe 2',7'-dichlorofluorescein-diacetate (H₂DCF-DA) as previously reported^[12,13]. In the presence of intracellular ROS, H₂DCF is rapidly oxidized to the highly fluorescent 2',7'-dichlorofluorescein. Briefly, J774A.1 cells were plated at a density of 3.0×10^4 cells/well into 24-well plates. Cells were allowed to grow for 24 h; the medium was then replaced with fresh medium and cells were stimulated with Citrus sinensis extract (250-10 µg/mL) for 1h before and simultaneously to LPS (1 µg/mL). After 24 h cells were then collected, washed twice with PBS and then incubated in PBS

with H₂DCF-DA (10 μM) at 37 °C. After 45 minutes, cells fluorescence was evaluated by a fluorescence-activated cell sorting (FACSscan; Becton Dickinson) and elaborated with Cell Quest software.

2.12 Glucose uptake

The Glucose uptake were performed in the medium of the HepG2 cell after 72h of treatment with 0, 0.5 and 1 μg of *Citrus sinensis* juice extract^[14].

2.13 Lipid peroxidation assay

Lipid peroxidation was evaluated using an analytical quantitative methodology. It relies upon the formation of a coloured adduct produced by the stechiometric reaction of aldehydes with thiobarbituric acid (TBA). The thiobarbituric acid reactive substances (TBARS) assay was performed on membranes extracted from cells, using an ice-cold lysis buffer (50 mM Tris, 150 mM NaCl, 10 mM EDTA, 1% Triton) supplemented with a mixture of protease inhibitors. The chromogen (TBARS) was quantified by spectrophotometry at a wavelength of 532 nm. The amount of TBARS was expressed as mM·μg⁻¹ proteins. All data are the mean ± SD of three experiments^[15].

2.14 Digestion in vitro

In order to assess the bioavailability following oral administration of the extract of *Citrus sinensis*, the following protocol was adopted: *Salivary Phase*: the sample was dissolved in 40 mL of H₂O. Were added 6 mL of artificial saliva containing 3 mg of α-amylase. The whole was placed on the plate at 37 °C under stirring for 3 minutes. At the end of the phase of saliva were collected 10 mL of sample

(digested salivary) which were subsequently subjected to chromatographic analysis. *Gastric phase*: the remaining volume of the sample from step salivary was brought to an acid pH (pH = 2) by the addition of HCl 6 N. At the sample were added 10 mL of 0.1 N HCl in which they were previously dissolved 3 mg of pepsin. The whole was placed on the plate at 37 °C under stirring for 2 h. At the end of the gastric phase were collected 10 mL of sample (digested gastric) which were analyzed by HPLC. *Intestinal phase*: the residual volume of the sample coming from the gastric phase was added a dialysis membrane. The membrane was pre-washed internally and externally with a solution of 0.9% NaCl, and was then filled with 5.5 mL of 0.9% NaCl and with 5.5 mL of 0.5 M NaHCO₃ it was left suspended in the solution of gastric digested for 20 minutes, at 37 °C on plate in agitation. Subsequently, by the addition of a few mL of a solution of 0.5 M NaHCO₃, the solution pH was brought to 6.5 to reproduce the intestinal environment. Are added another 18 mL of 0.1N NaHCO₃ in which were dissolved 20 mg of pancreatin and 125 mg of bile salts. The whole was placed on the plate at 37 °C under stirring for 2h. At the end of the intestinal phase were collected 10 mL of the sample solution from the intestinal phase (digested intestinal) and 10 mL from the dialysis membrane (fraction absorbed by the intestine) which were subsequently subjected to chromatographic analysis^[16].

2.15 Statistical Analysis

Data are reported as mean ± standard error mean (s.e.m.) values of at least three independent experiments, each in triplicate. Statistical analysis was performed by analysis of variance test, and multiple comparisons were made by Bonferroni's test. A P-value less than 0.05 was considered as significant.

3. Results and discussions

3.1 Identification of Flavonoids and Polymethoxyflavones

Identification was carried out on the basis of standard retention time, UV spectra, and comparing MS/MS data with those present in literature^[17]. Peaks 1 and 2 showed a typical fragmentation pattern of C-glucosides along with the presence of two fragments at $[M-H-120]^-$ (base peak) and $[M-H-90]^-$ suggesting the loss of two hexose moieties (Figure 1). DAD spectra showed the flavanone nature of the aglycone of compounds 3 and 4, peak 3 showed a fragment at $[M-H-326]^-$ due to the loss of sugar moiety, and was identified as neohesperidin, peak 4 showed a fragment with mass 287 and was recognized as eriocitrin, peak 5 and 6 were identified as isoquercitrin and narirutin, the latter with fragment at m/z 271 (base peak). Finally the most intense peak 8 was easily identified as hesperidin. Most retained compounds were identified as polymethoxyflavones, in this case positive electrospray ionization was performed. Most intense compounds were peaks 12-14-17, showing fragments at m/z 312, 373 and 343, corresponding to the loss of 61 amu $[M+H-CH_3-CO-H_2O]^+$ and 30 amu $[M+H-2CH_3]^+$ respectively, and were identified as sinensetin and nobiletin and tangeretin.

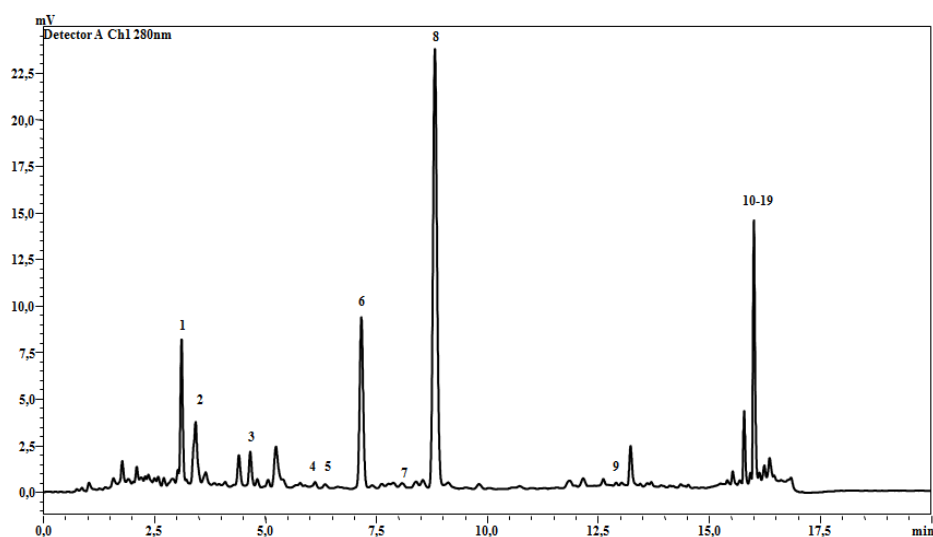


Fig. 1: Chromatographic profile acquired by HPLC-DAD (280 nm) of flavonoids in *Citrus sinensis* extract. Peaks identified are: (1) vicenin-2; (2) lucenin-2 4'-methyl ether; (3) neohesperidin; (4) eriocitrin; (5) isoquercitrin; (6) narirutin; (7) neodiosmin; (8) hesperidin; (9) didymin; (10) isosinensetin; (11) hexamethoxyflavone; (12) sinensetin; (13) hexamethoxyflavone (isomer); (14) nobiletin; (15) tetramethyl-o-isoscutellarein; (16) heptamethoxyflavone; (17) tangeretin; (18) hydroxypentamethoxyflavone; (19) 3-hydroxynobiletin.

3.2 Quantitative Analysis of *Citrus sinensis* extract

For the quantification of flavonoids, eight compounds were selected as external standards: diosmetin 6,8 di C-glucoside, neohesperidin, eriocitrin, isoquercetin, narirutin, diosmetin, hesperetin and tangeretin. Standard solutions (1 mg mL⁻¹) were prepared in methanol, the calibration curves were obtained in a concentration range of 0.5-100 µg mL⁻¹. The amount of the compounds in the sample was expressed as milligram per gram of extract (Table 1).

Table 1: Qualitative and quantitative profile of polyphenols from *Citrus sinensis*.

Peak	[M-H] ⁻	[M-H] ⁺	MS ² m/z	Regression Curve	R ²	<i>Citrus sinensis</i> extract*	Compound
1	593.1518	–	353.0691	$y = 1.2604E^{-06} x - 1.0047E^{-03}$	0.9981	49.11 ± 2.87	vicenin-2
2	623.1628	–	383.0791	$y = 1.2604E^{-06} x - 1.0047E^{-03}$	0.9981	32.77 ± 0.47	lucenin-2 4'-methyl ether
3	609.1478	–	301.0382	$y = 1.0012E^{-06} x - 2.2930E^{-03}$	0.9953	9.75 ± 2.97	neohesperidin
4	595.1692	–	288.9530	$y = 1.2657E^{-06} x - 2.3642 E^{-04}$	0.9962	5.86 ± 0.11	eriocitrin
5	463.0890	–	301.0353	$y = 8.9337E^{-07} x - 1.7211E^{-03}$	0.9983	4.06 ± 0.94	isoquercitrin
6	579.1835	–	271.0636	$y = 1.0043E^{-06} x - 3.2128E^{-04}$	0.9996	55.14 ± 1.97	narirutin
7	607.1317	–	300.0320	$y = 4.7437E^{-07} x + 1.5354E^{-04}$	0.9996	2.72 ± 0.62	neodiosmin
8	609.1738	–	301.0736	$y = 6.4061E^{-07} x - 1.9685E^{-03}$	0.9966	207.65 ± 1.77	hesperidin
9	593.1895	–	285.0763	$y = 6.4061E^{-07} x - 1.9685E^{-03}$	0.9966	3.55 ± 0.15	didymin
10	–	373.1236	343.0805	$y = 4.2086E^{-07} x + 9.9601E^{-04}$	0.9975	3.62 ± 1.25	isosinensetin
11	–	403.1371	373.0918	$y = 4.2086E^{-07} x + 9.9601E^{-04}$	0.9975	2.35 ± 0.97	hexamethoxyflavone
12	–	373.1268	312.0990	$y = 4.2086E^{-07} x + 9.9601E^{-04}$	0.9975	7.64 ± 0.99	sinensetin
13	–	403.1362	373.0923	$y = 4.2086E^{-07} x + 9.9601E^{-04}$	0.9975	2.66 ± 0.78	hexamethoxyflavone isomer
14	–	403.1331	373.0936	$y = 4.2086E^{-07} x + 9.9601E^{-04}$	0.9975	21.22 ± 1.15	nobiletin
15	–	343.1166	282.0876	$y = 4.2086E^{-07} x + 9.9601E^{-04}$	0.9975	2.82 ± 1.37	tetramethyl- <i>o</i> -isoscuteellarein
16	–	433.1472	403.1019	$y = 4.2086E^{-07} x + 9.9601E^{-04}$	0.9975	4.06 ± 1.49	heptamethoxyflavone
17	–	373.1238	343.0809	$y = 4.2086E^{-07} x + 9.9601E^{-04}$	0.9975	5.54 ± 0.79	tangeretin
18	–	389.1215	359.0741	$y = 4.2086E^{-07} x + 9.9601E^{-04}$	0.9975	–	hydroxypentamethoxyflavone
19	–	419.1318	389.0866	$y = 4.2086E^{-07} x + 9.9601E^{-04}$	0.9975	–	3-hydroxynobiletin

3.3 *Citrus sinensis* extract reduces LPS-induced NO, iNOS, COX-2 and TNF- α in J774A.1 macrophages

To assess if *Citrus sinensis* influences NO production, we measured NO₂⁻ release, a stable end-product of NO, in cellular medium of J774A.1 macrophage stimulated with *Citrus sinensis* extract (250-10 μ g/mL) alone or in combination with LPS (1 μ g/ml). LPS induced in macrophages a marked increase in NO release; *Citrus sinensis* extract significantly reduced NO release (250-25 μ g/mL; P<0.01 vs LPS alone; Figure 2 panel A). Interestingly, *Citrus sinensis* extract when added after LPS also inhibited NO release by J774.A1 macrophages indicating its inhibitory effect both on the iNOS enzyme expression and on its activity at the higher concentrations (250-150 μ g/mL; P<0.001 vs LPS alone; Figure 2 panel B). In the same experimental conditions LPS induces also a significant iNOS and COX-2 expression in J774.A1 macrophage. When *Citrus sinensis* extract (250-10 μ g/mL) was added to J774.A1 macrophages, 1h before and simultaneously with LPS, a significant and concentration-dependent reduction in iNOS expression was observed (P<0.05 vs LPS alone; Figure 2 panel C). Moreover, we evaluated the effect of *Citrus sinensis* extract on COX-2 expression. Our data show that, as well as for NO and iNOS, also COX-2 protein expression was significantly inhibited by *Citrus sinensis* juice extract (250-50 μ g/mL; P<0.05 vs LPS alone; Figure 2 panel D).

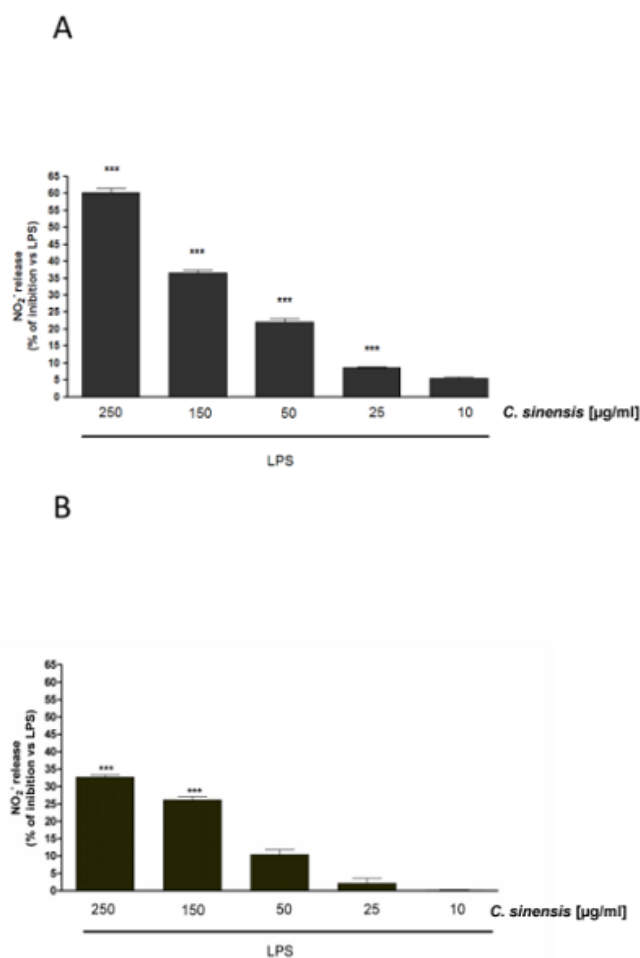


Figure 2: Effect of *Citrus sinensis* extract on NO release, evaluated as NO_2^- (μM), by J774A.1 macrophages stimulated with LPS. (panel A) *Citrus sinensis* extract (250–10 $\mu\text{g/mL}$) was added to J774A.1 macrophages 1 h before and simultaneously with LPS (1 $\mu\text{g/mL}$) challenge for 24 h. (panel B) In order to verify the effect on iNOS activity, *Citrus sinensis* extract (250–10 $\mu\text{g/mL}$) was added to J774A.1 macrophages 24 h after with LPS challenge and then co-exposed together for further 24 h. Values are expressed as % inhibition vs J774A.1 treated with LPS alone, *** denotes $P < 0.001$ versus LPS alone.

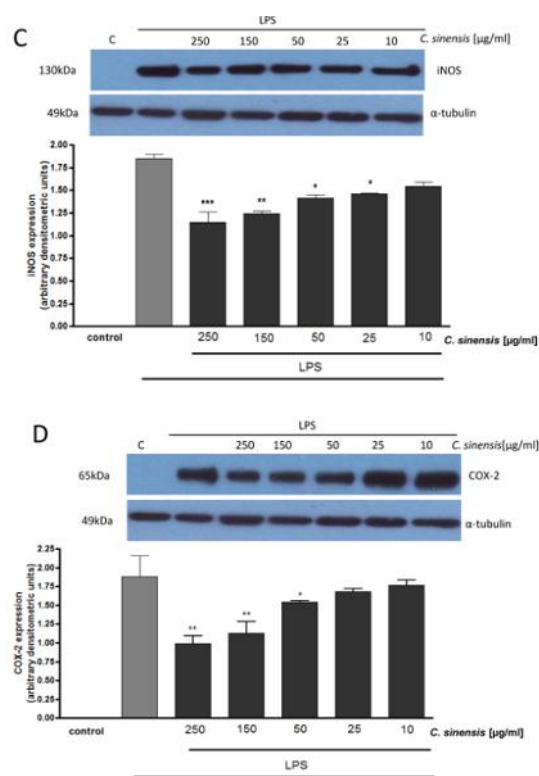


Figure 2: Representative Western blot of iNOS expression (upper panel C) and densitometric analysis of the concentration dependent effect of *Citrus sinensis* extract (250-10 µg/mL) on LPS-induced iNOS expression in J774A.1 macrophages (lower panel C). *Citrus sinensis* extract (250–10 µg/mL) was added to J774A.1 macrophages 1 h before and simultaneously with LPS (1 µg/mL) challenge for 24 h. Representative Western blot of COX-2 expression (upper panel D). Densitometric analysis of the concentration dependent effect of *Citrus sinensis* extract (250–100 µg/mL) on LPS-induced COX-2 expression in J774A.1 macrophages (lower panel D). *Citrus sinensis* extract (250–10 µg/mL) was added to J774A.1 macrophages 1 h before and simultaneously with LPS challenge for 24 h. Values, mean ± s.e.m., are expressed as arbitrary densitometric units, ^{ooo} denotes $P < 0.001$ vs control; ***, ** and * denote $P < 0.001$, $P < 0.01$, $P < 0.05$ respectively versus J774A.1 macrophages treated with LPS alone.

LPS induced a significant induction in TNF- α levels in J774A.1 macrophage. This release was significantly reduced by *Citrus sinensis* extract added to cells 1 h before and simultaneously with LPS ($P < 0.05$ vs LPS alone; Figure 3).

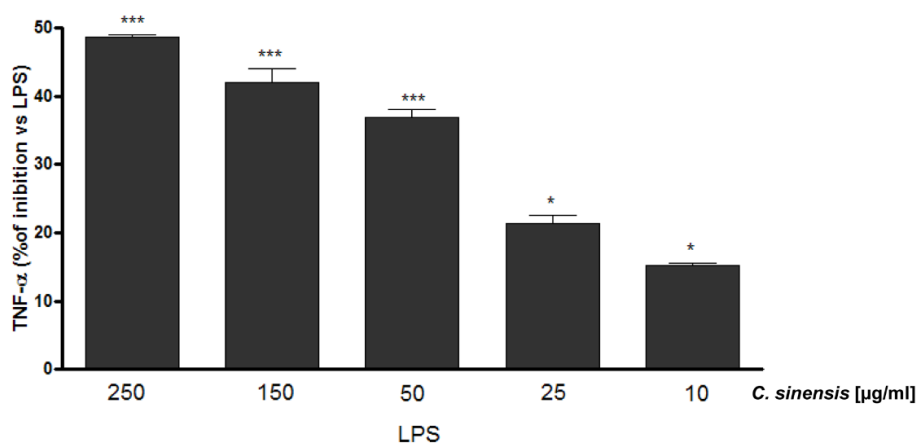


Figure 3. Effect of *Citrus sinensis* juice extract on LPS-induced TNF- α production in J774A.1 macrophages. TNF- α production was measured in the medium of J774A.1 cells treated with *Citrus sinensis* juice extract (250–10 $\mu\text{g/ml}$) and LPS (1 $\mu\text{g/ml}$) for 18 h by means of ELISA. Results are expressed as mean \pm s.e.m., ^{ooo} denotes $P < 0.001$ versus control; ***, ** and * denote $P < 0.001$, $P < 0.01$ and $P < 0.05$ versus LPS alone.

3.4 *Citrus sinensis* extract inhibits p65 NF- κB nuclear translocation in LPS-treated macrophages

Following p65 phosphorylation, the free NF- κB dimers translocate into the nucleus and bind to specific sequences to regulate the downstream genes expression^[18]. So we labelled p65 with a green fluorescence to track the influence of *Citrus sinensis* tested at two medium concentrations of *Citrus sinensis* extract (150-50 $\mu\text{g/ml}$) and

added 1h before LPS (1 $\mu\text{g}/\text{mL}$) on NF- κB translocation. As shown in Figure 4, NF- κB p65 nuclear translocation was increased after 15 minutes by LPS and was reduced by *Citrus sinensis* extract in J774A.1 treated macrophages compared to LPS alone.

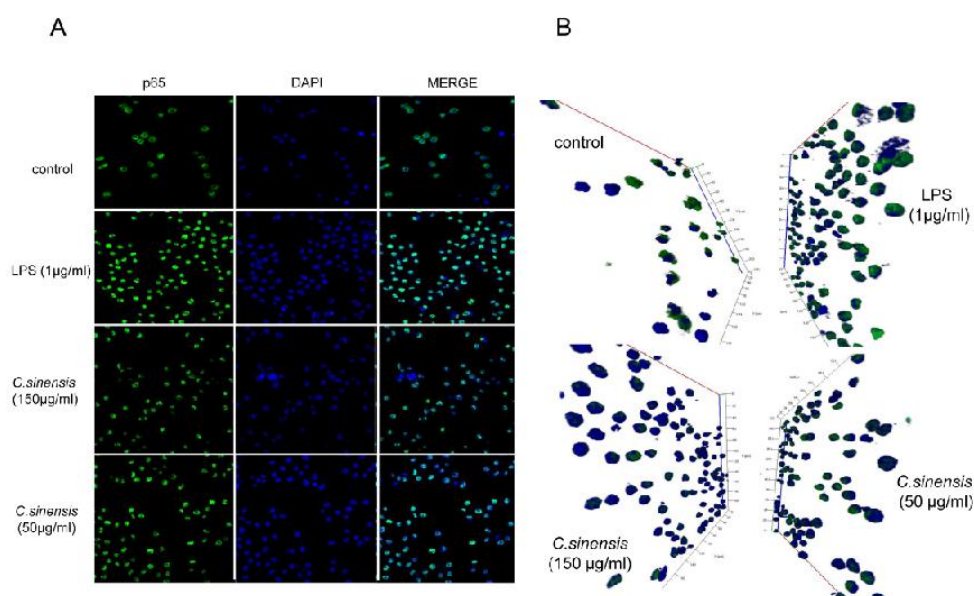


Figure 4: *Effect of Citrus sinensis* extract on LPS-induced p65 nuclear translocation in J774A.1 macrophages. Cells were treated with *Citrus sinensis* extract (150–50 $\mu\text{g}/\text{mL}$) for 1 h and then co-exposed to LPS (1 $\mu\text{g}/\text{mL}$) for 20 min and nuclear translocation of NF- κB p65 subunit was detected using immunofluorescence assay at confocal microscopy. Scale bar, 10 μm . A representative image of three experiments was shown (panel A). Three-dimensional projection of *Citrus sinensis* extract on LPS-induced p65 nuclear translocation. Blue and green fluorescences indicate localization of nucleus (DAPI) and p65 respectively (panel B). Analysis was performed by confocal laser scanning microscopy.

3.5 Antioxidant activity of *Citrus sinensis* juice extract

To verify the effect of *Citrus sinensis* on ROS release in LPS-stimulated macrophages we evaluated intracellular ROS by incubating J774A.1 with *Citrus sinensis* extract (250-10 $\mu\text{g/mL}$), 1h before and simultaneously with LPS. After 24 h LPS induced a significant increase of ROS release. Treatment with *Citrus sinensis* extract (250-10 $\mu\text{g/mL}$), reduced ROS production in macrophages ($P < 0.001$ vs LPS alone; Figure 5 panel A).

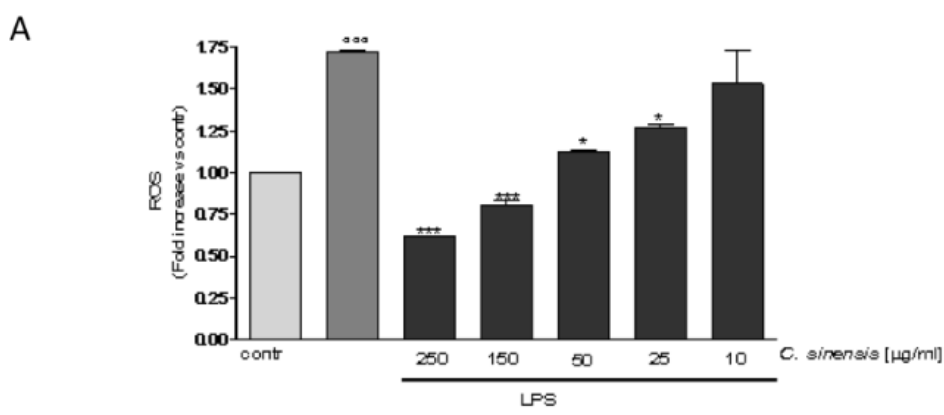


Figure 5: ROS formation was evaluated by means of the probe 2',7' dichlorofluorescein-diacetate ($\text{H}_2\text{DCF-DA}$) in J774A.1 macrophages (panel A). *Citrus sinensis* extract (250–10 $\mu\text{g/mL}$) was added to J774A.1 macrophages 1 h before and simultaneously with LPS (1 $\mu\text{g/mL}$) stimulation for 24 h. Values, mean \pm s.e.m., are expressed as mean fluorescence intensity; $^{\circ\circ\circ}$ denotes $P < 0.001$ vs control; *** denotes $P < 0.001$ respectively versus LPS-treated macrophages.

3.6. *Citrus sinensis* juice extract induces the cytoprotective enzyme HO-1 in LPS-treated J774A.1 macrophages

Considering the beneficial role of OH-1 in controlling various inflammatory mediators, we evaluated whether its expression was influenced by *Citrus sinensis* extract. OH-1 is expressed in J774A.1 macrophages at low levels in basal condition and was increased by LPS. *Citrus sinensis* extract further increased HO-1 enzyme expression in J774A.1 macrophages respect to LPS alone ($P < 0.01$ vs LPS; Figure 5 panel B). Moreover, MTT assay revealed that *Citrus sinensis* extract at all concentrations and time tested (24, 48 and 72 h) did not affect J774A.1 macrophage viability.

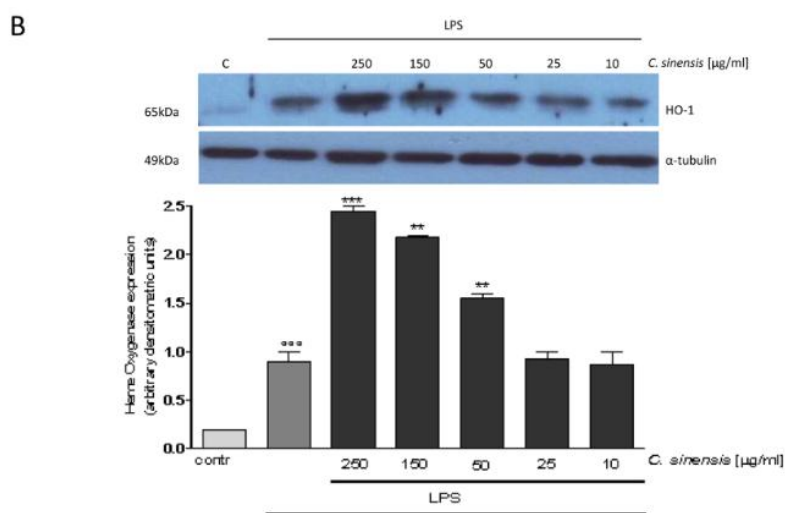


Figure 5: Representative Western blot of HO-1 enzyme expression (upper panel B). Densitometric analysis of the concentration dependent effect of *Citrus sinensis* extract (250–10 µg/mL) on LPS-induced OH-1 expression in J774A1 macrophages (lower panel B). *Citrus sinensis* extract (250–10 µg/mL) was added to J774A.1 macrophages 1 h before and simultaneously with LPS (1 µg/mL) stimulation for 24 h.

3.7 Citrus sinensis induced antiproliferative effect of HepG2 cell lines

The influence of Citrus sinensis juice extract on cell proliferation, oxidative stress and metabolism was evaluated in HepG2 hepatoma cells, a model system frequently used for metabolic study^[19]. All experiments above were of the duration of 72 h. Citrus sinensis juice extract significantly inhibited proliferation of HepG2 cell lines between 0.25-0.5 µg/mL range (Figure 6 panel A) and was not cytotoxic to the cells compared to the control (untreated cells). The antiproliferative activity exhibited by Citrus sinensis juice extract was not due to necrosis, since the amount of lactate dehydrogenase (LDH) released from cells incubated with the juices was not significantly different from that released from the control cells. The ability of Citrus sinensis juice extract to inhibit glucose uptake on HepG2 cell lines was tested. The results indicated that Citrus sinensis juice extract treatment of HepG2 cells caused (Figure 6 panel B) a reduction of glucose uptake when compared with the control. The Citrus sinensis juice extract-treated HepG2 cell saw an almost fivefold increased in NO concentration compared to untreated cells (Figure 6 panel C), without the increase of iNOS expression, this results confirmed the antioxidant capacity of juice. Cells treated with with Citrus sinensis juice extract showed a twofold increase of lipid peroxide level (thiobarbituric acid-reactive substances, TBARS) compared to the untreated cells (Figure 6 panel D).

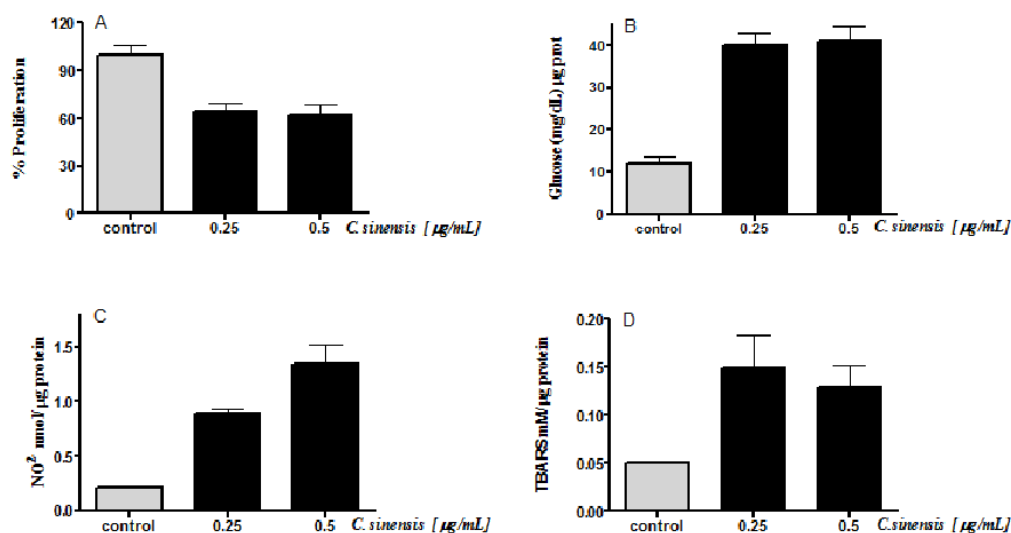


Figure 6. Effect of *Citrus sinensis* extract on HepG2 proliferation, glucose uptake, lipid peroxidation and Nitric Oxide. All evaluation were conducted after 72 h of *Citrus sinensis* extract treatment of HepG2 cells.

4. Discussion

Citrus plants contain a large amount of flavonoids which, in recent years, has gained considerable attention especially for the large number of beneficial effects on human health including its anticancer, cardioprotective and anti-inflammatory properties^[20]. Data showed that the mixture of phenolic compounds in *Citrus sinensis* juice extract has anti-inflammatory and antioxidant effects. In particular, our results provides evidence that *Citrus sinensis* extract reduces (1) NO release; (2) iNOS and COX-2 expression; (3) TNF- α release, (4) NF- κ B nuclear translocation, (5) ROS release and (6) induce the cytoprotective HO-1 enzyme expression. Moreover *Citrus sinensis* extract induced antiproliferative effect of HepG2 cell lines. Macrophages activation by LPS triggers an inflammatory response, releasing pro-inflammatory mediators such as NO, iNOS, COX-2 and

ROS associated to mechanisms aimed to protect cell, as HO-1 enzyme expression. NO is a pleiotropic mediator that acts in a variety of physiological and pathophysiological processes. During inflammation, iNOS is significantly induced, and high amounts of NO are released to induce a non-specific immune response by macrophages. During inflammation NO, in addition to being a ‘final common mediator’ of this process, is essential for inflammatory response up-regulation. In our experiments, LPS induced in J774A.1 macrophages a marked increase both in NO release and in iNOS expression; Citrus sinensis extract significantly reduced NO release and iNOS expression. Interestingly, also when the extract was added after LPS, it inhibited NO release by J774.A1 macrophages indicating its inhibitory effect both on the iNOS enzyme expression and on its activity. An interaction between iNOS and COX pathway modulates inflammatory response. COX-2 is a well known pro-inflammatory enzyme triggered by LPS, it regulates macrophage response during inflammation and its expression was also influenced by NO^[21]. The results show that, as for NO and iNOS, also COX-2 expression was significantly inhibited by Citrus sinensis extract, thus further contributing to the reduction of LPS inflammatory response in J774A.1 macrophages. TNF- α is a cytokine elevated in sepsis and its production is tightly dependent both on NF- κ B activation and ROS levels. Moreover, TNF- α itself induces iNOS expression and large amounts of NO production^[22]. In our experimental model Citrus sinensis juice extract significantly reduced TNF- α release, thus contributing to the reduction of inflammatory response also by pro-inflammatory cytokine release inhibition. LPS is known to activate the pro-inflammatory transcription factor NF- κ B, also regulated via a number of second messengers, including ROS^[23]. NF- κ B regulates immune responses, also with pro-inflammatory enzyme production (e.g. iNOS, COX-2), antigen presentation, pattern recognition and phagocytosis. After p65 NF- κ B subunit phosphorylation, the free NF- κ B dimers translocate into the nucleus and bind to specific sequences to regulate the downstream genes expression^[18]. Our

evidence indicates that in the presence of LPS Citrus sinensis juice inhibits the phosphorylation and p65 subunits nuclear translocation, thus reducing NF- κ B activity in J774A.1 macrophages. These results indicate an activity of Citrus sinensis on the early steps of inflammatory response. As NO, ROS generation in the inflammatory response is induced as a defensive reaction intended to clear infectious stimulus. On the other hand, ROS activation could also have an adverse effect on abnormal inflammatory disease. Treatment with Citrus sinensis reduced ROS production in macrophages, thus indicating its antioxidant effects. In order to protect themselves against inflammatory and oxidative injury, cells such as macrophages, up-regulates some defence mechanisms as HO-1 expression. HO-1 is the rate-limiting enzyme in heme degradation and catalyzes heme oxidation to generate several biologically active molecules (e.g. carbon monoxide (CO), biliverdin, and ferrous ion;^[24] HO-1 generates antioxidants such as bilirubin, which can inhibit iNOS protein induction and suppress NO production, can also contribute to increase the cellular anti-oxidant status^[25]. In addition CO, a major product of HO-1 activity, was shown to inhibit COX-2 expression and iNOS enzymatic activity, thus contributing to the reduction of inflammatory state^[26]. HO-1 is generally low expressed in most tissues/organs. Despite this, HO-1 is highly inducible in response to a variety of stimuli, as LPS, to protect cells against oxidative and inflammatory injury^[24]. Considering the beneficial role of OH-1 in controlling various inflammatory mediators, we evaluated whether its expression was modulated by Citrus sinensis extract. Expressed in J774A.1 macrophages at low levels in basal condition OH-1 resulted increased by LPS and Citrus sinensis extract further increased HO-1 enzyme expression in J774A.1 macrophages. Thus, during LPS-induced inflammation in macrophages Citrus sinensis juice if on the one hand inhibits pro-inflammatory mediators, on the other stimulates a cytoprotective response. Flavonoids have been found to possess beneficial effects on health and have drawn attention because of their safety and increasing evidence

of their antidiabetic effects in animals and humans^[27]. The liver plays a critical role in maintaining blood glucose concentration both through its ability to supply glucose to the circulation via glycogenolysis and gluconeogenesis in the post-absorptive state and to remove glucose from the circulation after meal ingestion^[28]. Malignant cells have been shown to have high levels of glucose transporters associated to an enhanced rate of glycolysis. Glucose depletion decreased NO level and the presence of a NO donor protected against glucose depletion-induced cytotoxicity by modulation of mitochondrial biogenesis and function in hepatoma cells. In our experimental condition we showed that the antioxidant activity of Citrus sinensis juice increases the levels of free NO and protects against cytotoxicity induced by glucose deprivation. Under the glucose depletion condition, cancer cells can obtain energy supply using alternative energy substrates such as fatty acids for β -oxidation. The increase of lipid peroxidation in the Citrus sinensis juice extract-treated cells is probably due to the increase in fatty acid β -oxidation. Among the major Citrus sinensis juice constituents were flavonones as hesperidin, narirutin, vicenin-2 and polymethoxyflavones as nobiletin. Previous studies reported the anti-inflammatory and antioxidant activity of hesperidin and of narirutin in macrophage^[29,30] and also nobiletin has been reported to have anti-inflammatory activity and to suppress gene expression of IL-1, TNF- α in mouse J774A.1 macrophages^[31]. Moreover, nobiletin also suppressed the expression of COX-2, NF- κ B dependent transcription^[32]. The presence of these compounds and their potential additive/synergic pharmacological activity in Citrus sinensis juice highlights its anti-inflammatory, antioxidant and hypoglycaemic potential.

4.1 Simulated digestion of the extract of *Citrus sinensis*

Figures 7-10 show the different chromatographic profiles flavonoid extract juice *Citrus sinensis*, respectively digestion salivary, gastric, intestinal and dialysis. From the simple comparison of the retention times of the four chromatograms, it denotes an identical qualitative profile of polyphenols, emphasizing resistance to hydrolytic processes that the matrix undergoes after oral administration.

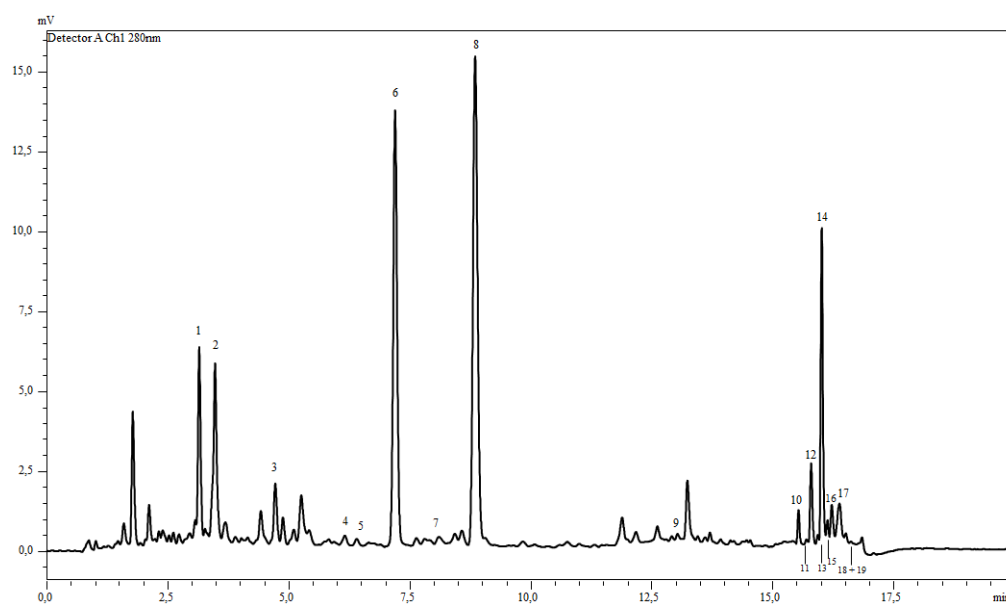


Figure 7: Salivary phase flavonoid extract of *Citrus sinensis*.

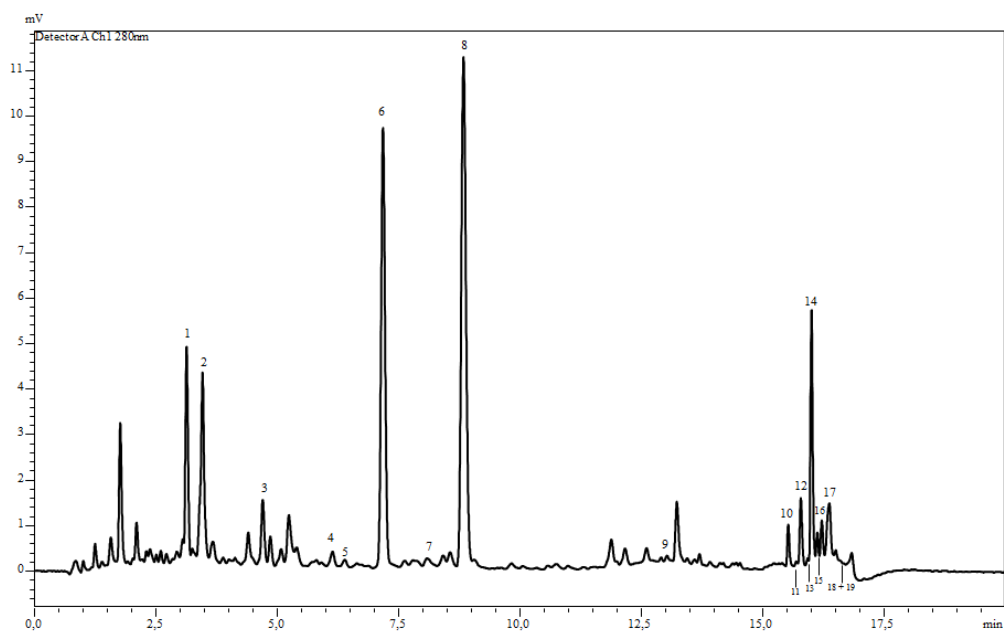


Figure 8: Gastric phase flavonoid extract of *Citrus sinensis*.

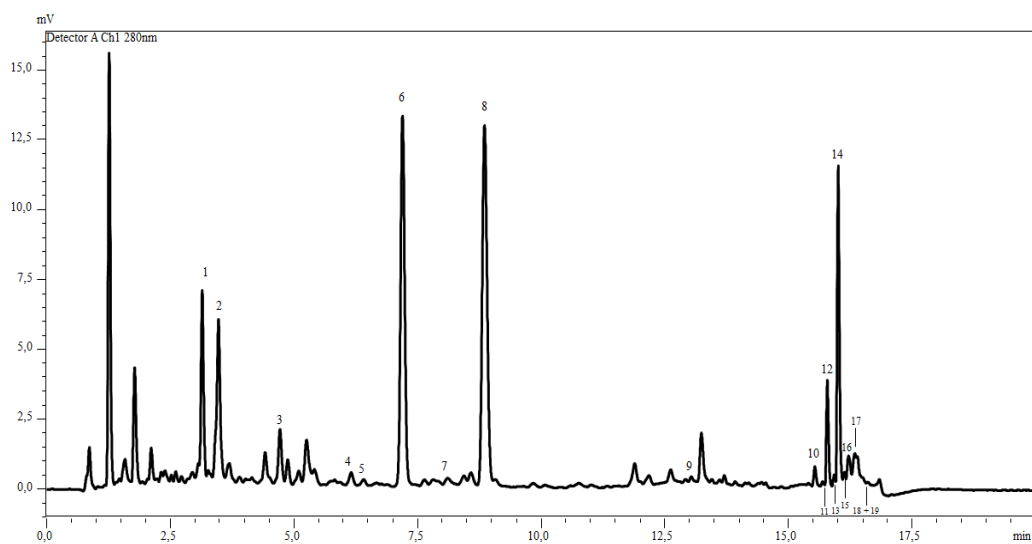


Figure 9: Intestinal phase flavonoid extract of *Citrus sinensis*.

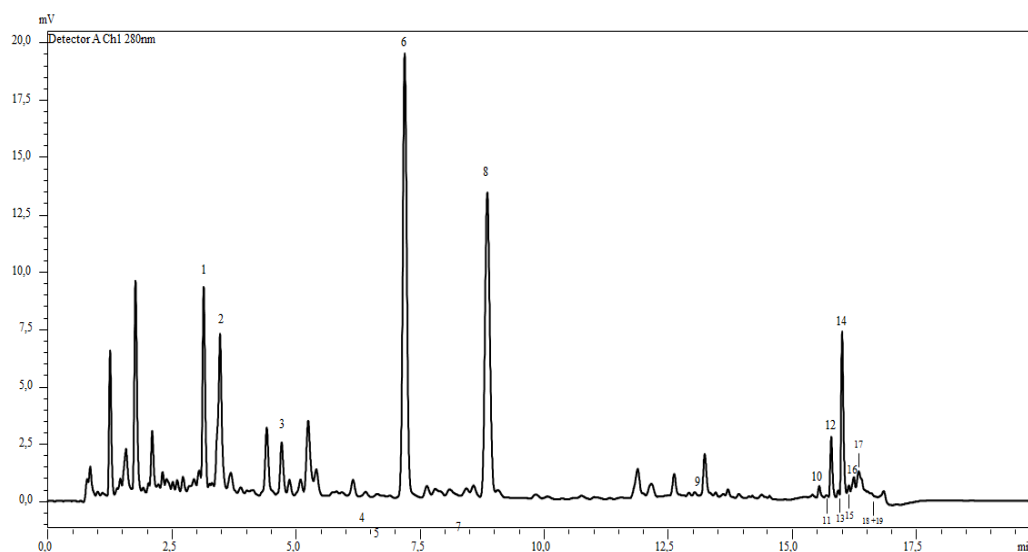


Figure 10: Dialysis phase flavonoid extract of *Citrus sinensis*.

Table 2 shows the concentration of the different analytes identified in the extract of *Citrus sinensis*, in the different steps of the simulated digestion.

Table 2: Quantitative analysis of the extract of *Citrus sinensis* flavonoid following simulated digestion *in vitro*.

Salivary	Gastric	Intestinal	Dialysis	Compound
36.86 ± 0.42	34.38 ± 0.20	8.01 ± 0.13	2.53 ± 0.01	Vicenin-2
26.24 ± 0.80	24.58 ± 0.29	4.65 ± 0.12	1.71 ± 0.02	Lucenin-2 4'-methyl ether
8.31 ± 0.88	7.81 ± 0.04	1.98 ± 0.10	0.95 ± 0.08	Neohesperidin
5.27 ± 0.07	4.98 ± 0.12	1.31 ± 0.12	0.57 ± 0.02	Eriocitrin
4.02 ± 0.45	3.57 ± 0.08	0.76 ± 0.09	0.36 ± 0.01	Isoquercitrin
43.01 ± 0.93	40.25 ± 0.55	13.34 ± 1.62	2.93 ± 0.09	Narirutin
2.26 ± 0.24	2.15 ± 0.05	0.55 ± 0.02	0.26 ± 0.03	Neodiosmin
184.81 ± 2.76	176.51 ± 1.05	30.94 ± 3.49	10.73 ± 0.07	Hesperidin

3.37 ± 0.07	3.12 ± 0.20	0.71 ± 0.13	0.31 ± 0.03	Didymin
2.79 ± 0.21	2.64 ± 0.03	1.81 ± 0.13	1.64 ± 0.02	Isosinensetin
0.96 ± 0.09	–	–	–	Hexamethoxyflavon
6.42 ± 0.60	6.03 ± 0.28	3.96 ± 0.23	3.57 ± 0.04	Sinensetin
–	–	–	–	Hexamethoxyflavon <i>isomer</i>
21.04 ± 0.31	20.12 ± 0.71	11.51 ± 0.72	9.42 ± 0.05	Nobiletin
2.40 ± 0.10	1.98 ± 0.03	–	–	Tetramethyl- <i>o</i> -isoscuteallarein
3.75 ± 0.54	2.24 ± 0.06	0.85 ± 0.04	–	Heptamethoxyflavon
4.26 ± 0.66	2.93 ± 0.01	0.74 ± 0.04	–	Tangeretin
–	–	–	–	Hydroxypentamethoxyflavon
–	–	–	–	3-hydroxynobiletin

The data shows a gradual decrease in the concentration of flavonoids present in the extract of sweet orange. On average, the concentrations of flavonoids extract of *Citrus sinensis* during digestion salivary^[33] were found to be between 75.1% and 99.2% compared to the extract as received, indicating good stability of the analytes to the biochemical conditions of oral cavity (Table 2). The oral mucosa can promote the bioavailability of a wide range of both polar and hydrophobic compounds, allowing to quickly reach the blood circulation by-passing the gastrointestinal system. Also, since most of the nutrients are gastro-sensitive and are poorly absorbed in the intestinal tract, salivary extraction and absorption through the epithelium of the oral mucosa would allow to target bioactive compounds to specific tissues and organs without being degraded by digestion gastrointestinal or be excreted in the feces. The gastric phase^[34] (Table 2) revealed a good stability of the flavonoids at the acidic pH of the stomach. The flavonoid glycoside were quite resistant to acid hydrolysis and thus are able to reach the gut in intact form without generating the corresponding aglyconic molecules^[35]. The experimental results obtained have confirmed that the degradation of flavonoids

occurs especially in the intestine^[36]. On average, there was a loss of 48.2% and 85.8% of native flavonoid pattern after digestion pancreatic^[37] (Figure 11). The bioavailability of flavonoids of the extract of *Citrus sinensis* was assessed using monolayers of Caco-2 cells as a model of absorption of the small intestine^[37,38]. The data reported in Table 2 showed a bioavailability in the range of 5.17 to 9.78% for the Neohesperidine, Eriocitrin, Narirutin, Neodiosmina, Hesperidin and Didymin. Instead, for the glycosidic flavonoids, such as Vicenin-2, Lucenina-2,4'-methyl ether and Isoquercetrin, the bioavailability was determined respectively 5.16%, 5.18% and 8.94%.

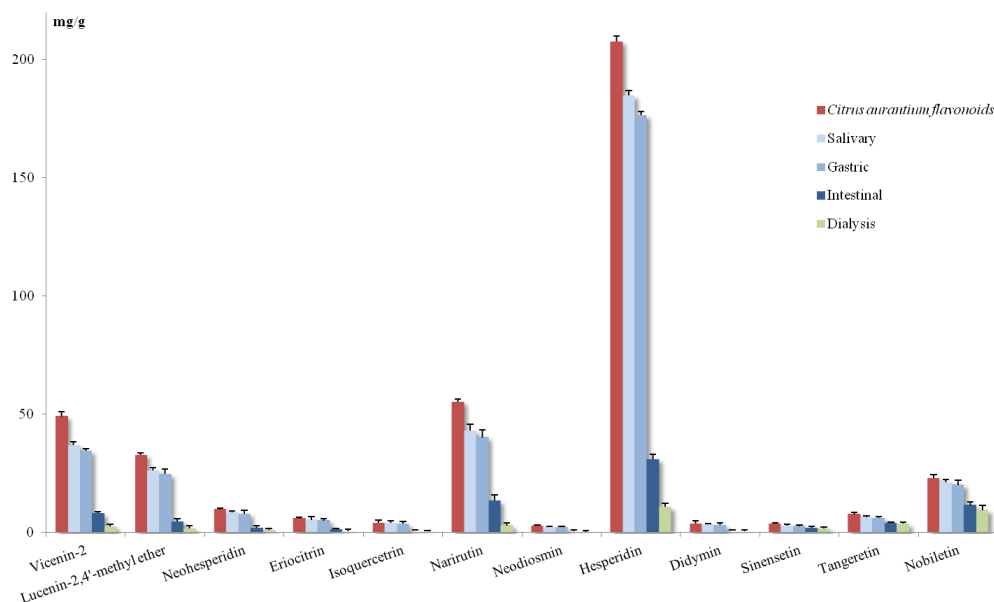


Figure 11: Comparison quantity flavonoids extract of *Citrus sinensis* following simulated digestion *in vitro*.

5. Conclusions

Although further studies will be necessary to evaluate the specific contribute of single flavonols to the antioxidant and antiinflammatory effects of *Citrus sinensis* juice on J774A.1 macrophages, we should consider the potential additive/synergic pharmacological activity of its constituents due to the contemporary presence of all of them together. Since the evaluated parameters in this study are critical mediators in inflammation and oxidative stress our evidences supported that the mixture of compounds contained in *Citrus sinensis* juice might have beneficial implication in the reduction of inflammatory conditions. The results obtained following the gastrointestinal digestion indicate a moderate permeation of flavonoids of the sweet and consequently an accumulation of intestinal polyphenols. Such molecules may exert an important local action by protecting the intestine by the action of oxidizing agents responsible for the onset of various pathological conditions (inflammation and tumors).

6. References

[¹] Manthey, J.A., Grohmann, K., & Guthrie, N. Biological properties of citrus flavonoids pertaining to cancer and inflammation, *Current Medicinal Chemistry*, **2001**, 8, 135-153.

[²] Benavente-Garcia, O., Castillo, J., Sabater, F., & Del Rio, J.A. Characterization of a S-adenosyl-L-methionine: Eriodictyol 4'-O-methyltransferase from *Citrus aurantium*. Developmental- Changes in the Levels of 4'-O-Methoxyflavonoids and S-Adenosyl- L-Methionine Eriodictyol 4'-O-Methyltransferase Activity, *Plant Physiology Biochemistry*, **1995**, 33, 263-271.

[³] Shiloh, M.U., Macmicking, J.D., Nicholson, S., Brause, J.E., Potter, S., Marino, M., Fang, F., Dinuer, M., & Nathan, C. Phenotype of mice and macrophages

deficient in both phagocyte oxidase and inducible nitric oxide synthase, *Immunity*, **1999**, 10, 29-38.

[⁴] Baeuerle, P.A. IkappaB-NF-kappaB structures: at the interface of inflammation control, *Cell*, **1998**, 95, 729-731.

[⁵] Popolo, A., Autore, G., Pinto, A., & Marzocco, S. Oxidative stress in patients with cardiovascular disease and chronic renal failure, *Free Radical Research*, **2013**, 47(5), 346–356.

[⁶] Braca, A., Dal Piaz, F., Marzocco, S., Autore, G., Vassallo, A., & De Tommasi, N. Triterpene derivatives as inhibitors of protein involved in the inflammatory process: Molecules interfering with phospholipase A(2), cyclooxygenase, and lipoxygenase, *Current Drug Targets*, **2011**, 12(3), 302–321.

[⁷] Huang, M., Lu, J. J., Huang, M. Q., Bao, J. L., Chen, X. P., & Wang, Y.T. Terpenoids: Natural products for cancer therapy, *Expert Opinion on Investigational Drugs*, **2012**, 21(12), 1801–1818.

[⁸] Ben Jemia, M., Kchouk, M.E., Senatore, F., Autore, G., Marzocco, S., De Feo, V., & Bruno, M. Antiproliferative activity of hexane extract from Tunisian *Cistus libanotis*, *Cistus monspeliensis* and *Cistus villosus*, *Chemistry Central Journal*, **2013**, 7, 47.

[⁹] Adesso, S., Popolo, A., Bianco, G., Sorrentino, R., Pinto, A., Autore, G., & Marzocco, S. The uremic toxin indoxyl sulphate enhances macrophage response to LPS, *PLoS One*, **2013**, 8(9), 776–778.

[¹⁰] Marzocco, S., Russo, R., Bianco, G., Autore, G., & Severino, L. Pro-apoptotic effects of nivalenol and deoxynivalenol trichothecenes in J774A.1 murine macrophages, *Toxicology Letters*, **2009**, 189 21-26.

[¹¹] Cianchi, F., Cuzzocrea, S., Vinci, M.C., Messerini, L., Comin, C.E., Navarra, G., Perigli, G., Centorrino, T., Marzocco, S., Lenzi, E., Battisti, N., Trallori, G., & Masini, E. Heterogeneous expression of cyclooxygenase-2 and inducible nitric

oxide synthase within colorectal tumors: correlation with tumor angiogenesis, *Digestive and Liver Disease*, **2010**, 42, 20-27.

[12] Sommella, E., Pepe, G., Pagano, F., Tenore, G.C., Marzocco, S., Manfra, M., Calabrese, G., Aquino, R.P., & Campiglia, P. UHPLC profiling and effects on LPS-stimulated J774A.1 macrophages of flavonoids from bergamot (*Citrus bergamia*) juice, an underestimated waste product with high anti-inflammatory potential, *Journal of Functional Foods*, **2014**, 7, 641-649.

[13] Pepe, G., Sommella, E., Manfra, M., De Nisco, M., Tenore, G.C., Scopa, A., Sofo, A., Marzocco, S., Adesso, S., Novellino, T., & Campiglia, P. Evaluation of anti-inflammatory activity and fast UHPLC–DAD–IT–TOF profiling of polyphenolic compounds extracted from green lettuce (*Lactuca sativa* L.; var. Maravilla de Verano), *Food Chemistry*, **2015**, 16, 153-161.

[14] Tenore, G.C., Campiglia, P., Stiuso, P., Ritieni, A., & Novellino, E. Nutraceutical potential of polyphenolic fractions from Annurca apple (*M. pumila* Miller cv Annurca), *Food Chemistry*, **2013**, 140, 614-622.

[15] Gomez-Monterrey, I., Campiglia, P., Bertamino, A., Aquino, C., Sala, M., Grieco, P., Dicitore, A., Vanacore, D., Porta, A., Maresca, B., Novellino, E., & Stiuso, P. A novel quinone-based derivative (DTNQ-Pro) induces apoptotic death via modulation of heat shock protein expression in Caco-2 cells, *British Journal Pharmacology*, **2010**, 160, 931-940.

[16] Raiola, A., Meca, G., Mañes, J., & Ritieni, A. Bioaccessibility of Deoxynivalenol and its natural co-occurrence with Ochratoxin A and Aflatoxin B1 in Italian commercial pasta, *Food and Chemical Toxicology*, **2012**, 50, 280–287.

[17] Kwang-Il, P., Hyeon-Soo, P., Mun-Ki, K., Gyeong-Eun, H., Arulkumar, N., Ho-Jeong, L., Silvia, Y., Won-Sup, L., Chung-Kil, W., Sung-Chul, S., & Gon-Sup, K. Flavonoids identified from Korean *Citrus aurantium* L. inhibit Non-Small Cell Lung Cancer growth in vivo and in vitro, *Journal of Functional Foods*, **2014**, 7, 287-297.

- [18] Tak, P.P., & Firestein, G.S. NF-kappaB: a key role in inflammatory diseases, *Journal of Clinical Investigation*, **2001**, 107, 7-11.
- [19] Brandon, E.F., Bosch, T.M., Deenen, M.J., Levink, R., van der Wal, E., van Meerveld, J.B., Bijl, M., Beijnen, J.H., Schellens, J.H., & Meijerman, I. Validation of in vitro cell models used in drug metabolism and transport studies: genotyping of cytochrome P450, phase II enzymes and drug transporters polymorphisms in the human hepatoma (HepG2), ovarian carcinoma (IGROV- 1) and colon carcinoma (CaCo-2, LS180) cell lines, *Toxicology and Applied Pharmacology*, **2006**, 211, 1-10.
- [20] Li, X., & Kushad, M.M. Correlation of glucosinolates content to myrosinase activity in horseradish (*Armoracia rusticana*), *Journal of Agricultural and Food Chemistry*, **2004**, 52, 6950-6955.
- [21] Ahmad, N., Chen, L.C., Gordon, M.A., Laskin, J.D., & Laskin, D.L. Regulation of cyclooxygenase-2 by nitric oxide in activated hepatic macrophages during acute endotoxemia, *Journal of Leukocyte Biology*, **2002**, 71, 1005-1011.
- [22] Thiemermann, C., Wu, C.C., Szabó, C., Perretti, M., & Vane, J.R. Role of tumour necrosis factor in the induction of nitric oxide synthase in a rat model of endotoxin shock, *British Journal of Pharmacology*, **1993**, 110, 177-182.
- [23] Brown, D.M., Donaldson, K., Borm, P.J., Schins, R.P., Dehnhardt, M., Gilmour, P., Jimenez, L.A., & Stone, V. Calcium and ROS-mediated activation of transcription factors and TNF-alpha cytokine gene expression in macrophages exposed to ultrafine particles, *American Journal of Physiology - Lung Cellular and Molecular Physiology*, **2004**, 286, 344-353.
- [24] Wu, M.L., Ho, Y.C., Lin, C.Y., & Yet, S.F. Heme oxygenase-1 in inflammation and cardiovascular disease, *American Journal of Cardiovascular Disease*, **2011**, 1, 150-158.
- [25] Wang, W.W., Smith, D.L., & Zucker, S.D. Bilirubin inhibits iNOS expression and NO production in response to endotoxin in rats, *Hepatology* **2004**, 40, 424-433.

- [26] Thorup, C., Jones, C.L., Gross, S.S., Moore, L.C., & Goligorsky, M.S. Carbon monoxide induces vasodilation and nitric oxide release but suppresses endothelial NOS, *American Journal of Physiology*, **1999**, 277, F882-889.
- [27] Hanhineva, K., Törrönen, R., Bondia-Pons, I., Pekkinen, J., Kolehmainen, M., Mykkänen, H., & Poutanen, K. Impact of dietary polyphenols on carbohydrate metabolism, *International Journal of Molecular Sciences*, **2010**, 11, 1365-1402.
- [28] Klover, P.J., & Mooney, R.A. Hepatocytes: critical for glucose homeostasis, *The International Journal of Biochemistry & Cell Biology*, **2004**, 36, 753-758.
- [29] Ha, S.K., Park, H.Y., Eom, H., Lim, Y., & Choi, I. Narirutin fraction from citrus peels attenuates LPS-stimulated inflammatory response through inhibition of NF- κ B and MAPKs activation, *Food and Chemical Toxicology*, **2012**, 50, 3498-3504.
- [30] Hirata, A., Murakami, Y., Shoji, M., Kadoma, Y., & Fujisawa, S. Kinetics of radical-scavenging activity of hesperetin and hesperidin and their inhibitory activity on COX-2 expression, *Anticancer Research*, **2005**, 25, 3367-3374.
- [31] Lin, N., Sato, T., Takayama, Y., Mimaki, Y., Sashida, Y., Yano, M., & Ito, A. Novel anti-inflammatory actions of nobiletin, a citrus polymethoxy flavonoid, on human synovial fibroblasts and mouse macrophages, *Biochemical Pharmacology*, **2003**, 65, 2065-2071.
- [32] Harada, S., Tominari, T., Matsumoto, C., Hirata, M., Takita, M., Inada, M., & Miyaura, C. Nobiletin, a polymethoxy flavonoid, suppresses bone resorption by inhibiting NF κ B-dependent prostaglandin E synthesis in osteoblasts and prevents bone loss due to estrogen deficiency, *Journal of Pharmacological Sciences*, **2011**, 115, 89-93.
- [33] Gonçalves, R., Mateus, N., & de Freitas, V. Inhibition of α -amylase activity by condensed tannins, *Food Chemistry*, **2011**, 125, 665–672.

[34] Manach, C., Scalbert, A., Morand, C., Rémésy, C., & Jiménez, L. Polyphenols: Food sources and bioavailability, *American Journal of Clinical Nutrition*, **2004**, 79, 727–747.

[35] Bouayed, J., Deußer, H., Hoffmann, L., & Bohn, T. Bioaccessible and dialysable polyphenols in selected apple varieties following in vitro digestion vs. their native patterns, *Food Chemistry*, **2012**, 131, 1466–1472.

[36] Zhu, Q. Y., Holt, R. R., Lazarus, S. A., Ensunsa, J. L., Hammerstone, J. F., Schmitz, H. H., et al. Stability of the flavan-3-ols epicatechin and catechin and related dimeric procyanidins derived from cocoa, *Journal of Agricultural and Food Chemistry*, **2002**, 50, 1700–1705.

[37] Bouayed, J., Hoffmann, L., & Bohn, T. Total phenolics, flavonoids, anthocyanins and antioxidant activity following simulated gastro-intestinal digestion and dialysis of apple varieties: Bioaccessibility and potential uptake, *Food Chemistry*, **2011**, 128, 14–21.

[38] Déprez, S., Mila, I., Huneau, J.-F., Tomé, D., & Scalbert, A. Transport of proanthocyanidin dimer, trimer and polymer across monolayers of human intestinal epithelial Caco-2 cells, *Antioxidants and Redox Signaling*, **2001**, 3, 957–967.

CHAPTER V

Beyond the skin of *Annurca* apple: An in depth analytical investigation of polyphenolic fingerprint

Abstract Annurca apple, a Southern Italian cultivar, possesses not only a particular taste and flavor, different from other types of apple, but also several healthy properties. With the aim to thoroughly elucidate the polyphenolic profile of this variety, listed as Protected Geographical Indication product, an extensive qualitative profiling of Annurca apple polyphenolic extract was carried out, by employing a combination of ultra high performance reversed phase (RP-UHPLC) and hydrophilic liquid chromatography (HILIC) coupled to ion trap-time of flight (IT-TOF) mass spectrometry. A total of 67 compounds were tentatively identified, some not reported so far, comprising of dihydrochalcones, hydroxycinnamic acids, flavonols, anthocyanins and procyanidins. Furthermore, thanks to the different selectivity obtained with the HILIC, in combination with accurate mass measurements, an improved separation and detection of procyanidins, was obtained. The presence of oligomers above degree of polymerization six, up to ten, was highlighted in detail for the first time in this kind.

Keywords : Annurca, profiling, HILIC, IT-TOF, Polyphenols

1. Introduction

There is an increasing interest in polyphenolic compounds, due to their claimed healthy activity, such as anticancer^[1], antioxidant, anti-inflammatory^[2] and hypoglycaemic effects^[3]. These compounds are more often included in nutraceutical formulations and functional foods, which are usually based on fruits or vegetables extracts, characterized by high polyphenolic content. Among widely consumed fruits, apple is one of the most important source of polyphenols in diet, and historically is considered a “healthy” food, since his regular consumption has been associated with lower onset of cardiovascular diseases^[4] and different type of cancer^[5]. Apples contain a wide variety of polyphenolic classes: hydroxycinnamic

acids, dihydrochalcones, flavonols, anthocyanins, and flavan-3-ols. Usually the peel contains the highest concentration of these bioactive compounds, with respect to flesh and core^[6]. Within the different classes of apples, “Annurca” is a typical cultivar of Southern Italy, in particular of Campania region, and has been listed as a Protected Geographical Indication (IGP) product from the European Council [Commission Regulation (EC) No. 417/2006]. It is characterized from a crispy flesh and a fragrant flavor^[7], the high acid/sugar ratio gives a different taste from other types of apples. This cultivar is subjected to a particular reddening treatment, with controlled exposure to sun and temperature^[8]. Many biological activities have been reported for the “Annurca” polyphenolic extract, such as: antioxidant^[9] anticancer^[10] and hypoglycaemic^[11]. Since apple extracts are often employed in nutraceutical products, it is important to possess a deep knowledge of their polyphenolic profile. In this regard, from an analytical perspective, the most popular technique to elucidate polyphenolic profile in natural products is high performance liquid chromatography (HPLC) coupled with diode array detection (DAD), and especially with mass spectrometry (MS)^[12]. Very recently, ultra high performance liquid chromatography (UHPLC) coupled to quadrupole-time of flight (Q-TOF) mass spectrometry have been reported for polyphenolic profiling of apple pomace and juices^[13] showing superior resolution with respect to conventional HPLC methods, and leading to the identification of 52 compounds in a very short run. Regarding the composition of Annurca apple, few methods have been reported^[14,15] carried out by employing C18 columns packed with conventional particles, coupled to low resolution MS instrumentations, such as ion trap (IT) and triple quadrupole (QqQ), and recently UHPLC with diode array detector (DAD)^[16]. The employment of high resolution mass spectrometers, capable of higher mass accuracy in both MS and tandem MS (MS/MS) stages is very helpful, for structure elucidation and identification of polyphenols^[17,18]. Furthermore, in these matrices, particularly challenging is the separation of condensed tannins or

proanthocyanidins, a class of phenols composed of flavan-3-ol monomeric units joined through interflavanoid linkages, divided into various subclasses with procyanidins, based on (epi)catechin units, and prodelphinidins, comprising (epi)gallocatechin units. Monomers are frequently linked through C4→C6 or C4→C8 bonds (B-type), or, more rarely, a second bond can occur from oxidative coupling of C2→O7 to form A-type oligomers. This class of compounds, especially those with high degree of polymerization (DP), tend co-elute in reversed phase liquid chromatography (RP-LC) in an unresolved “hump”^[19] which hamper their resolution and detection. Although UHPLC conditions, using sub-2 μm particle C18 columns, improve the resolution of procyanidins^[20], the separation of complex mixtures, containing both polymerized procyanidins and other polyphenolic molecules, still remains a challenge. A valid option, for procyanidins separation, is represented by normal phase liquid chromatography (NP-LC)^[19], and recently, by hydrophilic liquid chromatography (HILIC) as reported for cocoa procyanidins^[21,22], even if these techniques are not capable of resolve isomers. In HILIC, a polar stationary phase is used in combination with aqueous mobile phase in order to separate analytes according to polarity. The probable retention mechanism involve partitioning of analytes between the mobile phase and a water-layer immobilized on the stationary phase^[23]. During my PhD focused on a combined approach, based on ultra high performance reversed phase and hydrophilic liquid chromatography, has been developed for the detailed qualitative profiling of Annurca apple polyphenols. Both separation techniques were hyphenated with diode array detection (DAD) and with a hybrid ion trap-time of flight (IT-TOF) mass spectrometer. Good separation of flavonols, hydroxycinnamic acids and dihydrochalcones, was obtained in reversed phase, furthermore HILIC separation improved the resolution and detection of procyanidins, thanks to a different separation mechanism, and to the increased

sensitivity of electrospray (ESI) detection, due to the highly organic mobile phases used in HILIC. In this way the presence of oligomers above DP 6 up to DP 10 was described in detail for the first time in the Annurca extract. Was carried out a first comprehensive qualitative profiling of Annurca apple polyphenols, a total of 67 compounds were tentatively identified, marking an improvement in comparison with respect to previous observations, and representing a valid tool for the polyphenolic fingerprinting of apple extracts.

2. Materials and methods

2.1 Chemicals

Ultra pure water (H₂O) was obtained by a Milli-Q system (Millipore, Milan, Italy). The following chemicals have been all purchased from Sigma Aldrich (Milan, Italy) acetonitrile (ACN), and acetic acid LC-MS grade (CH₃COOH), methanol and hydrochloric acid (HCl). Unless stated otherwise all other reagents employed in the experimental sections below have been purchased from Sigma Aldrich. Two different columns were employed in this work: a Kinetex C18 150 × 2.1 mm, 2.6 μm (Phenomenex, Bologna, Italy) for the RP-UHPLC analysis, and a Luna HILIC 150 × 2.0 mm, 3.0 μm (Phenomenex), for the HILIC analysis.

2.2 Fruit collection and sample preparation

Annurca (*Malus pumila* Miller cv Annurca) apple fruits were acquired in a local store in Fisciano (SA, Campania, Italy). Fresh peels and flesh (10 g) of apple samples were homogenized by using an IKA Ultra-Turrax T-25 tissue homogenizer (IKA works Inc., Wilmington, NC, USA) and extracted in 30 mL methanol/water (80:20) with 0.1% HCOOH for 1 h at room temperature to extract phenolic

compounds. The mixture was centrifuged and the supernatants collected and filtered through 0.45 μm nylon membrane filters and injected for LC-MS analysis.

2.3 Instrumentation

RP-UHPLC and HILIC analyses were both performed on a Shimadzu Nexera UHPLC system (Shimadzu, Milano, Italy), consisting of a CBM-20A controller, four LC-30AD dual-plunger parallel-flow pumps, a DGU-20 A5 degasser, an SPD-M20A photo diode array detector (equipped with a semi-micro flow cell of 2.5 μL), a CTO-20A column oven, a SIL-30AC autosampler. The UHPLC system was coupled online to an LCMS-IT-TOF hybrid mass spectrometer through an ESI source (Shimadzu, Kyoto, Japan). LC-MS data elaboration was performed by the LCMSsolution® software (Version 3.50.346, Shimadzu).

2.4 RP-UHPLC and HILIC-PDA-ESI-IT-TOF conditions

For reversed phase ultra high performance liquid chromatography analyses the mobile phase employed was (A): 0.1% CH_3COOH in water v/v, (B) 0.1% CH_3COOH in ACN v/v, analysis was performed in gradient elution as follows: 0-5 min, 0-10 % B, 5-20 min, 10-20% B, 20-25 min, 20-50 % B, 25-26 min, 50-70 % B, 26-27 min, 70-95 % B. Flow rate was set at 0.5 mL/min. Column oven temperature was set to 40 °C. 2 μL of Annurca extract were injected. For the HILIC analyses the mobile phase employed was: (A) 0.1% CH_3COOH in water/ACN: 80W/20ACN, (B) ACN plus 0.1% CH_3COOH , analysis was performed in gradient elution as follows: 0-4 min, isocratic at 100% B, 4-60 min, 100-40 % B. Column oven temperature was set to 25 °C. 1 μL of extract was injected. The following PDA parameters were applied: sampling rate, 12.5 Hz; detector time constant, 0.160 s; cell temperature, 40 °C. Data acquisition was set in

the range 190-500 nm and chromatograms were monitored at 280 and 320 nm at the maximum absorbance of the compounds of interest. UHPLC system was coupled on-line to a hybrid IT-TOF instrument, in RP-UHPLC flow rate from LC was split 50:50 prior of the electrospray (ESI) source by means of a stainless steel Tee union (1/16 in., 0.15 mm bore, Valco HX, Texas U.S). Resolution, sensitivity, and mass number calibration of the ion trap and the TOF analyzer were tuned using a standard sample solution of sodium trifluoroacetate. MS detection was operated in negative ionization mode with the following parameters: detector voltage: 1.57 kV, Interface voltage: -3.5 kV, CDL (curved desolvation line) temperature: 250 °C, block heater temperature: 200 °C, nebulizing gas flow (N₂): 1.5 L/min, drying gas pressure: 100 kPa. Full scan MS data were acquired in the range of 200-1600 m/z, ion accumulation time: 25 ms, Ion trap repeat: 3. MS/MS experiments were conducted in data dependent acquisition, precursor ions were acquired in the range 300-1600 m/z; peak width, 3 Da; ion accumulation time: 50 ms, collision induced dissociation (CID) energy: 50%, collision gas: 50%, ion trap repeat: 1; execution trigger (BPC) intensity at 95% stop level. For the prediction of molecular formula the "Formula Predictor" software (Shimadzu) was used with the following settings: maximum deviation from mass accuracy: 5 ppm, fragment ion information, nitrogen rule.

3. Results and discussion

Annurca is an apple cultivar native to Southern Italy and its disciplinary of production identifies 137 municipalities in Campania region as the only places of production of the so called “Melannurca Campana” IGP^[24]. Beyond his particular taste and flavor, several observations have demonstrated that Annurca polyphenolic extracts reduce cholesterol accumulation^[3] and protect gastric cells against oxidative stress more than common apple cultivars^[25]. In this work we report a detailed qualitative profiling of Annurca polyphenols by a combination of RP-UHPLC and HILIC coupled with accurate MS detection.

3.1 RP-UHPLC-DAD-ESI-IT-TOF profiling of polyphenolic extract

As can be seen in figure 1 the entire separation was completed in less than 25 minutes, the chromatograms were recorded at 280 and 320 nm.

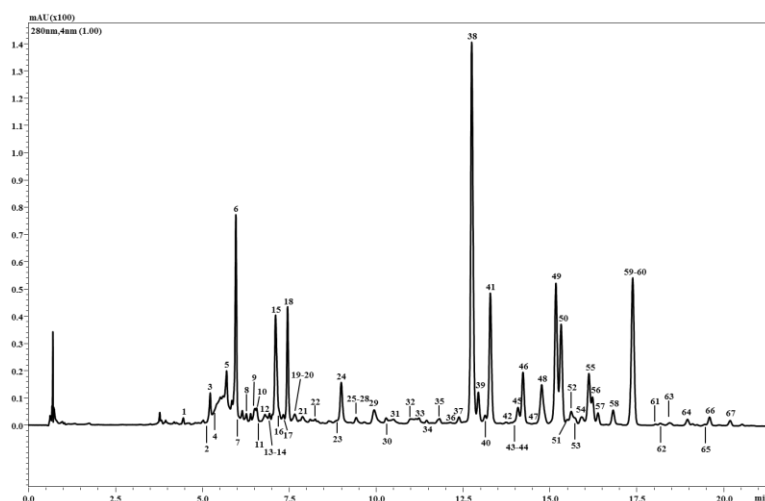


Figure 1: RP-UHPLC chromatogram recorded at 280 nm of Annurca extract. Column Kinetex C18 150 × 2.1 mm, 2.6 μm. Flow rate 0.5 mL/min. Column oven: 40°C.

Several parameters were investigated to obtain satisfactory resolution, such as flow rate, temperature, mobile phases. A flow rate of 0.5 mL/min and a column temperature of 40 °C gave the best results in terms of analysis time and peak overlap. Acetonitrile was used as organic modifier instead of methanol, resulting in lower backpressure, and acetic acid provided the better ionization efficiency compared to formic. MS ionization was operated in negative mode, since provided the highest sensitivity. The list of tentatively identified compounds by RP-UHPLC is reported in table 1. The compounds marked with a double asterisk are reported for the first time in the Annurca extract.

3.1.1 Hydroxycinnamic acids

Hydroxycinnamic acids eluted from 4 to 7.5 minutes, first eluting compound (tr 4.45) was tentatively identified as 4-hydroxybenzoic acid-4-O-glucoside m/z 299, as evident from the loss of glucose moiety $[M-H-C_6H_{12}O_6-H_2O]$ in MS2 spectrum. Compound 2 (tr 5.16) was identified as 3-p-coumaroylquinic acid, characterized from the fragment 191 m/z, typical of quinic acid moiety, the same fragmentation was observed for his isomer, compound 16, eluted at tr 7.34 and identified as 4-p-coumaroylquinic acid. Also characterized from the loss of quinic acid and from fragment at m/z 173, resulting from loss of water, were compounds 6 and 13 (tr 5.97, 6.94), possessing strong absorbance at 320 nm, identified as 5' caffeoylquinic acid (chlorogenic acid) and his 3' isomer. A fragment at 163 m/z was observed in the MS2 spectrum of compound 8 (tr 6.28), as result of loss of glucose, and was identified as 5-p-coumaroyl hexoside.

Table 1: List of polyphenolic compounds detected by RP-UHPLC-ESI-IT-TOF

*Detected as $[M-2H]^{2-}$; ** Reported for the first time in Annurca apple extract

Peak	Molecular Formula	[M-H] ⁻	[MS/MS]	Error (ppm)	Compound
1	C ₁₃ H ₁₆ O ₈	299.0758	//	-4.68	4-Hydroxybenzoic acid-4- <i>O</i> -glucoside **
2	C ₁₆ H ₁₈ O ₈	337.1122	191/163	-5.34	3- <i>p</i> -Coumaroylquinic acid **
6	C ₁₆ H ₁₈ O ₉	353.0873	191/173	-0.85	Chlorogenic Acid
8	C ₁₅ H ₁₈ O ₈	325.0924	183/163	-1.54	5- <i>p</i> -Coumaroyl hexoside **
13	C ₁₆ H ₁₈ O ₉	353.0846	191/173	-4.16	Chlorogenic Acid (isomer I)
17	C ₁₆ H ₁₈ O ₈	337.0942	191/173/163	-1.19	4- <i>p</i> -Cumaroylquinic acid b **
37	C ₂₆ H ₃₂ O ₁₅	583.1652	289/271/203	-2.23	3-Hydroxyphloretin-2- <i>O</i> -xylosyl-glucoside **
42	C ₂₇ H ₃₄ O ₁₅	597.1802	302/273	-1.51	Phloretin-dihexoside **

50	$C_{26}H_{32}O_{14}$	567.1738	273	1.94	Phloretin-2'- <i>O</i> -xylosyl-glucoside
53	$C_{26}H_{32}O_{14}$	567.1736	273	1.94	Phloretin-pentosyl-hexoside (isomer I)
59	$C_{21}H_{24}O_{10}$	435.1311	273/167	2.76	Phloridzin
60	$C_{25}H_{26}O_{14}$	549.1222	435/273	-5.10	Unknown Phloridzin derivate **
3	$C_{21}H_{22}O_{12}$	465.1055	285/241/199	3.66	Cyanidin-3- <i>O</i> -galactoside
10	$C_{21}H_{22}O_{12}$	465.1060	285/199	3.66	Cyanidin-3- <i>O</i> -glucoside **
14	$C_{21}H_{22}O_{12}$	465.1047	285/199	2.58	Cyanidin-3- <i>O</i> -hexoside isomer **
22	$C_{24}H_{38}O_{12}$	517.2329	223/205	3.09	Vomifoliol-9-[xylosyl-(1->6)-glucoside] **
4	$C_{21}H_{24}O_{11}$	451.1256	289/203	-5.01	Catechin-3- <i>O</i> -glucoside **
7	$C_{15}H_{14}O_6$	289.0702	245	-4.57	[+]-Catechin
18	$C_{15}H_{14}O_6$	289.0719	245	-4.57	[-]-Epicatechin
45	$C_{25}H_{26}O_{15}$	565.1167	451/289/271	-3.19	Catechin-3- <i>O</i> -glucoside derivate **
35	$C_{21}H_{22}O_{10}$	433.1128	271/177/151	-2.77	Naringin-4- <i>O</i> -glucoside **

33	C ₂₆ H ₂₈ O ₁₆	595.1308	301/271/255	0.50	Quercetin-3- <i>O</i> -glucosyl xyloside **
34	C ₂₆ H ₂₈ O ₁₆	595.1297	301/271/255	-1.34	Quercetin-3- <i>O</i> -glucosyl xyloside (isomer I) **
38	C ₂₁ H ₂₀ O ₁₁	463.0897	301/271/179	3.24	Quercetin-3- <i>O</i> -galactoside (Hyperoside)
39	C ₂₇ H ₃₀ O ₁₆	609.1465	301/271	-1.15	Rutin
41	C ₂₁ H ₂₀ O ₁₁	463.0890	301/271	1.73	Quercetin-3- <i>O</i> -glucoside (Isoquercetin)
44	C ₂₄ H ₂₂ O ₁₅	549.0884	505/463/301	-0.36	Quercetin-3- <i>O</i> -(6"-malonyl-glucoside) **
46	C ₂₀ H ₁₈ O ₁₁	433.0773	301/271	1.85	Quercetin-3- <i>O</i> -xyloside (Reynoutrin)
47	C ₂₀ H ₁₈ O ₁₁	433.0770	301/271	1.88	Quercetin-3- <i>O</i> -arabinopyranoside (Guajaverin)
48	C ₂₃ H ₂₂ O ₁₃	505.1003	301/271/179	2.38	Quercetin-3- <i>O</i> -β-D-Glucopyranosil-6'' acetate **
49	C ₂₀ H ₁₈ O ₁₁	433.0894	301/271/179	0.01	Quercetin-3- <i>O</i> -arabinofuranoside (Avicularin)
51	C ₂₇ H ₂₈ O ₁₆	607.1286	545/505/463/301	-3.13	Quercetin-3-[6''-(3-hydroxy-3-methylglutaryl)] galactoside **

52	$C_{20}H_{18}O_{11}$	433.0769	301/255/179	-1.62	Quercetin-3- <i>O</i> -pentoside
54	$C_{21}H_{20}O_{11}$	447.0931	301/255/179	1.94	Quercetin-3- <i>O</i> -rhamnoside (Quercitrin)
55	$C_{21}H_{20}O_{11}$	447.0937	301/271	-0.45	Quercetin-3- β -glucopyranoside (Isoquercitrin)**
56	$C_{22}H_{22}O_{12}$	477.1049	315/300/271	2.31	Isorhamnetin-3- <i>O</i> -galactoside **
57	$C_{28}H_{32}O_{16}$	623.1612	315/300/271	-3.37	Isorhamnetin-3- <i>O</i> -rutinoside (Narcissin) **
58	$C_{22}H_{22}O_{12}$	477.1047	315/300/271	2.30	Isorhamnetin-3- <i>O</i> -glucoside
61	$C_{23}H_{22}O_{12}$	489.1052	285/199	1.02	Luteolin-3- <i>O</i> -acetyl glucoside **
62	$C_{20}H_{18}O_{10}$	417.0841	285/255/183	0.01	Luteolin-3- <i>O</i> -xyloside **
63	$C_{28}H_{30}O_{16}$	621.1465	519/477/315/301	-0.97	Isorhamnetin-3-[6''-(3-hydroxy-3-methylglutaryl)] galactoside **
64	$C_{21}H_{20}O_{11}$	447.0934	315/300/271	0.22	Isorhamnetin-3- <i>O</i> -arafuranoside **
65	$C_{28}H_{30}O_{16}$	621.1465	477/315/300/271	-0.95	Isorhamnetin-3-[6''-(3-hydroxy-3-methylglutaryl)] glucoside **

66	$C_{21}H_{20}O_{11}$	447.0930	315/300/285/271	-0.67	Isorhamnetin-3- <i>O</i> -arafuranoside (isomer I) **
67	$C_{22}H_{22}O_{11}$	461.1103	315/300/285/271	1.52	Isorhamnetin-3- <i>O</i> -rhamnoside
5	$C_{30}H_{26}O_{12}$	577.1352	559/407/289	-0.69	Procyanidin B1
9	$C_{45}H_{38}O_{18}$	865.1967	739/695/577/407/287	-1.39	Epicatechin trimer (EC-3)
11	$C_{60}H_{50}O_{24}$	576.1231*	865/863/739/695/407/289	-5.55	Epicatechin tetramer (EC-4)
12	$C_{60}H_{50}O_{24}$	576.1241*	865/863/739/695/407/289	-5.55	Epicatechin tetramer (EC-4) (isomer I)
15	$C_{30}H_{26}O_{12}$	577.1357	559/407/289	0.87	Procyanidin B1 (isomer I)
16	$C_{45}H_{38}O_{18}$	865.1985	739/695/577/575/407/287	0.01	Epicatechin trimer (EC-3) (isomer II)
19	$C_{75}H_{62}O_{30}$	720.1570*	1153/865/863/739/577/575/ 407/287	2.22	Epicatechin pentamer (EC-5)
20	$C_{60}H_{50}O_{24}$	576.1235*	865/863/739/695/407/289	-5.21	Epicatechin tetramer (EC-4) (isomer II)
21	$C_{60}H_{50}O_{24}$	576.1243*	865/863/739/695/407/289	-4.69	Epicatechin tetramer (EC-4) (isomer III)

23	$C_{75}H_{62}O_{30}$	720.1568*	1153/865/863/739/577/575/407/287	2.20	Epicatechin pentamer (EC-5) (isomer I)
24	$C_{45}H_{38}O_{18}$	865.1968	739/695/577/407/289/287	-1.96	Epicatechin trimer (EC-3) (isomer III)
25	$C_{79}H_{78}O_{44}$	864.1890*	1153/695/577/575/407/287	3.74	Epicatechin esamer (EC-6)
26	$C_{75}H_{62}O_{30}$	720.1571*	1153/865/863/739/577/575/ 407/287	2.62	Epicatechin pentamer (EC-5) (isomer II)
27	$C_{105}H_{86}O_{42}$	1008.2226*	1153/865/739/575/407	-1.37	Epicatechin heptamer (EC-7) **
28	$C_{30}H_{26}O_{12}$	577.1345	559/407/289	-1.21	Procyanidin B1 (isomer II)
29	$C_{60}H_{50}O_{24}$	576.1240*	865/863/739/695/407/289	3.22	Epicatechin tetramer (EC-4) (isomer IV)
30	$C_{45}H_{38}O_{18}$	865.1967	739/695/577/575/407/289/ 287	-2.54	Epicatechin trimer (EC-3) (isomer IV)
31	$C_{75}H_{62}O_{30}$	720.1573*	1153/865/863/739/577/575/ 407/289	2.36	Epicatechin pentamer (EC-5) (isomer III)

32	$C_{75}H_{62}O_{30}$	720.1574*	1153/865/863/739/577/575/407/287	2.64	Epicatechin pentamer (EC-5) (isomer IV)
36	$C_{79}H_{78}O_{44}$	864.1892*	1151/695/575/407/287	3.70	Epicatechin esamer (EC-6) (isomer I)
40	$C_{30}H_{26}O_{12}$	577.1338	407/289/205	-2.43	Procyanidin B1 (isomer III)
43	$C_{45}H_{38}O_{18}$	865.1955*	695/577/407/289/287	0.12	Epicatechin trimer (EC-3) (isomer V)

3.1.2 Dihydrochalcones

Compound 37 (tr 12.36) showed MS2 fragments at 289 and 271 m/z, the first deriving from the consequential loss of an hexose and a pentose moiety, while m/z 271 denotes the possible loss of an hydroxyl group, and was tentatively assigned as 3-hydroxyphloretin-2-O-xylosyl-glucoside this observation is in accordance with previous Q-TOF data on apple extracts^[13]. Also detected was compound 42 (tr 13.77) identified as phloretin-di-hexoside, with a fragment at 273 m/z of the aglycone phloretin (C₁₅H₁₄O₅). An intense MS signal and absorbance at 280 nm was observed for compound 50 (tr 15.31), again, the aglycone at 273 m/z was the dominant fragment in MS2 spectrum, generated as for peak 37, from the cleavage of two sugar moieties, and was identified as phloretin-2'-O-xylosyl-glucoside, his isomer, peak 53, was detected at tr 15.72. Last compounds of this class, 59+60, co-eluted in an intense peak (tr 17.39), the compound with [M-H]⁻ 435, was easily identified as phloridzin, the loss of 162 amu represents the presence of glucose, this compound represents one of the most abundant compounds apples^[26]. The co-eluted compound, with [M-H]⁻ 549, shows in the MS2 spectrum both the phloridzin m/z 435 (C₂₁H₂₄O₁₀) and the phloretin m/z 273 signals, thus it is probably a phloridzin derivate, NMR and MSn experiments are necessary to confirm the structure.

3.1.3 Anthocyanins

Three anthocyanins were detected, even in a not suitable pH range for the separation of these compounds. Peaks 3 and 10 (tr 5.27, 6.54) showed a typical ionization profile of anthocyanins in negative mode, with the ions at 465 and 447 m/z corresponding to [M-2H]⁻ and [M-2H+H₂O]⁻^[27]. The fragment ion at 285 m/z [M-H-180]⁻ represents the aglycone cyanidin (C₁₅H₁₁O₆), and assumes the loss of

an hexose, finally leading to their identification as cyanidin-3-O-galactoside and cyanidin 3-O-glucoside, respectively. Peak 14 possesses the same precursor and fragment ion, and was recognized as a possible cyanidin-3-O-hexoside isomer.

3.1.4 Flavonols

A large number of flavonol glycosides were detected, as clearly visible from chromatograms recorded at 320 nm (Figure 2). Compounds 33 and 34 ($[M-H]^-$ at m/z 595) (tr 11.23, 11.44) possessed same fragment ion at m/z 301, typical of the sequential loss of a pentose and an hexose, and were tentatively assigned as quercetin-3-O-glucosyl xyloside. Peak 38 (tr 12.75) was the most intense in the profile, his fragment ion, again at m/z 301, points out the quercetin structure, and is the same observed for compound 41. These compounds were identified as quercetin-3-O-galactoside and quercetin-3-O-glucoside respectively, with the galactoside form that elutes first^[21]. The cleavage of a disaccharide $[M-H-C_{12}H_{22}O_{10}]^-$ was observed for peak 39 (tr 12.93) and was recognized as rutin. An in source fragmentation occurred for peak 44 (tr 13.99), with an ion at m/z 463, and a MS2 signal at m/z 301.

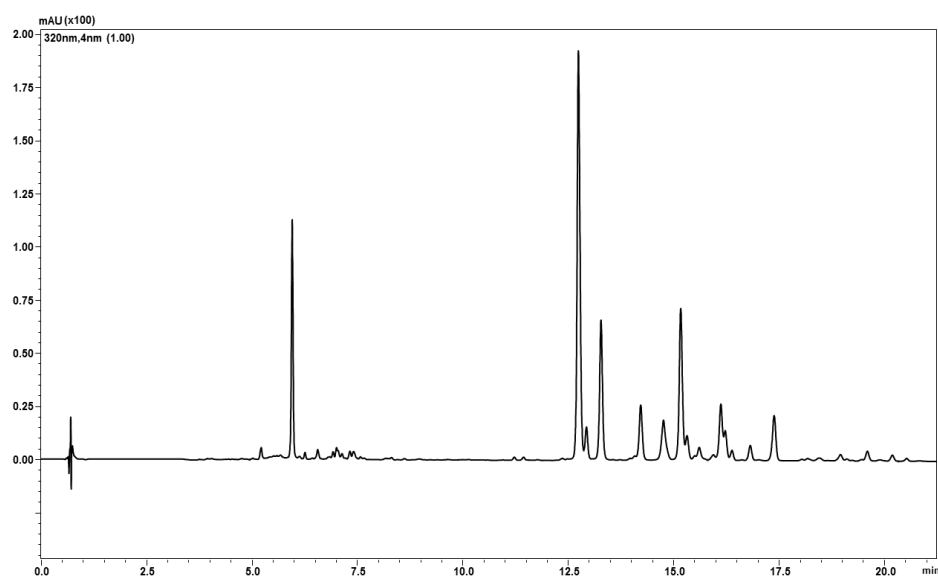


Figure 2: RP-UHPLC chromatogram recorded at 320 nm of Annurca extract. Column Kinetex C18 150 × 2.1 mm, 2.6 μm. Flow rate 0.5 mL/min. Column oven: 40 °C.

The mass difference (-87 amu) evidenced the cleavage of a malonyl residue followed by loss of glucose, and was proposed as quercetin 3-O-(6''-malonyl-glucoside). Compounds 46-47-49 (tr 14.25, 14.44, 15.18) were all characterized by same mass and fragmentation, hence, based on previous observation, regarding the elution order of quercetin glycosides in reversed phase^[28] they were identified as quercetin-3-O-xyloside, 3-O arabinopyranoside, and 3-O-arabinofuranoside respectively. Peak 48 (tr 14.78) gave two MS2 signals at 463 and 301 m/z, corresponding to the loss of an acetate group [M-H-42]⁻, and an hexose respectively, and was recognized as quercetin-3-O-β-D-Glucopyranosil-6'' acetate. A complex structure was hypothesized for peak 51 (tr 15.49) (Figure 3).

In this case the fragment at 463 m/z can be attributed to loss of a methylglutaryl moiety [M-H-144]⁻, while the ion at 505 m/z to a possible rearrangement into a 6''

acetate form, these information led to the tentative assignment as Quercetin-3-[6''-(3-hydroxy-3-methylglutaryl)] galactoside (C₂₇H₂₈O₁₆).

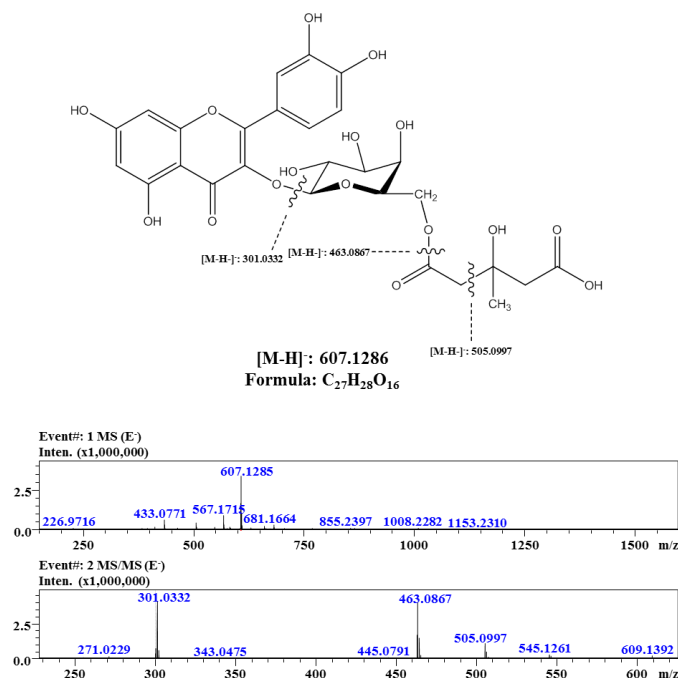


Figure 3: ESI-IT-TOF full scan MS and MS2 spectra for compound 51 (Quercetin-3-[6''-(3-hydroxy-3-methylglutaryl)] galactoside) and proposed structure and fragmentation pattern.

The difference of 150 amu of the fragment ion, suggests a pentose cleavage for peak 52 (tr 15.62). A loss of 146 amu was observed in the MS2 spectrum for peak 54 (tr 15.96), corresponding to a cleavage of rhamnose, and leading to identification of quercetin-3-O-rhamnoside, while peak 55 (tr 16.11) which possessed similar fragmentation pattern, was proposed as isoquercitrin. Peak 56 and 58 (tr 16.22, 16.81) exhibited the same precursor ion, and their main fragment ion, m/z 315, with molecular formula C₁₆H₁₂O₇, belongs to the aglycone isorhamnetin, hence they were finally identified as 3-O-galactoside and 3-O-

glucoside forms respectively. Peak 57 (tr 16.44) showed, in a similar manner to rutine, the loss of two sugar moieties, $[M-H-146-162]^-$, identifying the compound as isorhamnetin-3-O-rutinoside. Fragment ions of compound 61-62 (tr 18.07, 18.18), 285 m/z, revealed the presence of a luteoline aglycone ($C_{15}H_{10}O_6$), and were tentatively identified as luteolin-3-O-acetyl-glucoside and luteolin-3-O-xyloside. MS² spectra of peaks 63 and 65 (tr 18.53, 19.44) revealed a similar structure to compound 51, with a loss of methylglutaryl $[M-H-144]^-$ group, but in this case the ion at 315 m/z suggested the isorhamnetin structure, thus they were proposed as isorhamnetin-3-[6''-(3-hydroxy-3-methylglutaryl)] galactoside and glucoside respectively. The cleavage of a pentose (tr 18.97, 19.60) was observed for peaks 64 and 66, leading to their tentative identification as isorhamnetin-3-O-arafuranoside, and his isomer, respectively. As for peak 54, the loss of rhamnose, was observed, and last eluting peak, 67 (tr 20.22), was finally identified as isorhamnetin-3-O-rhamnoside.

3.1.5 Flavanones

One flavanone-glycoside was detected, peak 35 (tr 11.78), his main fragment ion, at 271 m/z, having molecular formula $C_{15}H_{12}O_5$, and was tentatively assigned as naringin-4-O-glucoside.

3.1.6 Flavan-3-ols

Peaks 7 and 18 (tr 6.01, 7.46) having same molecular formula ($C_{15}H_{14}O_6$) and fragments were identified as (+)-catechin and (-)-epicatechin. Peak 4 and 45 (tr 5.45, 14.08) both showed a fragment at 289 m/z with molecular formula $C_{15}H_{14}O_6$, evidencing the presence of catechin, and were recognized as catechin-3-O-glucoside, and his unknown derivate.

3.1.7 Other compounds

A non-polyphenolic compound was detected, peak 22 (tr 8.15). MS/MS data were in accordance with previous literature on apples extracts (cv. Jonathan), the compound, with formula $C_{24}H_{38}O_{12}$ was tentatively identified as vomifoliol-9-[xylosyl-(1>6)-glucoside]^[29].

3.1.8 Procyanidins

As can be observed from retention times in Table 1, the elution order of oligomeric procyanidins in reversed phase is not related on molecular mass. Multiple isomers were detected, in particular: four dimeric, five trimeric, five tetrameric, five pentameric, two esameric and one eptameric isomers were detected. Many isomers were not clearly visible in the UV profile, in this regard, fluorescence detection is more sensitive and commonly employed^[30]. Furthermore some compounds of this class are not fully resolved in these conditions. Several techniques have been developed for the analysis of procyanidins, such as matrix assisted laser desorption ionization (MALDI-TOF), which is a powerful technique but needs time consuming pre-fractionation of the extract prior analysis^[31]. Also commonly employed is thiolysis-RPLC, which provide information on the average degree of polymerization and type of constitutive units of procyanidins, but cannot provide any structural information for individual procyanidins molecules^[32]. For complex matrices, even RP-UHPLC does not possess an adequate resolving power, furthermore, exact structure elucidation of isomers up to dimer is difficult without suitable standards^[33]. As stated before the analysis of these molecules still remains a challenge.

3.1.9 HILIC-DAD-ESI-IT-TOF profiling of Annurca procyanidins

In the last years HILIC chromatography has been proposed as a valid alternative to RP for procyanidins separation^[34]. A variety of HILIC stationary phases are commercially available, an important application of this technique was the separation of cocoa and apple (Red Stark variety) procyanidins by off-line comprehensive two dimensional chromatography^[21], in which the authors used a diol stationary phase in the first dimension. Based on these observation we employed a HILIC column with cross-linked diol stationary phase. As well as for RP-UHPLC, several parameters, reported in section 2.4, were optimized in order to reach a satisfactory resolution. The HILIC chromatogram is reported in figure 4, non-procyanidins compound, like flavonols, hydroxycinnamic acids and dihydrochalcones were not well retained under these conditions, and tend to elute earlier in broad peaks.

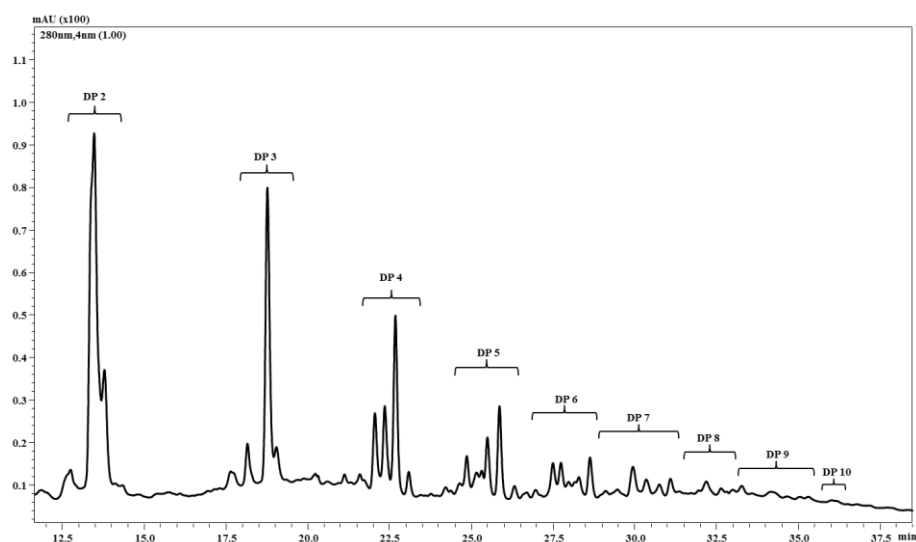


Figure 4: Expansion of HILIC chromatogram recorded at 280 nm of Annurca extract showing the separation of procyanidin oligomers from DP 2 to 10. Column HILIC 150 × 2.0 mm, 3 μm. Flow rate 0.3 mL/min. Column oven: 25 °C.

In contrast, an efficient separation of procyanidins from dimer to decamer was obtained. It is clearly visible that procyanidins are separated according to molecular weight under these conditions. With respect to the RP analysis, the separation and detection, by ESI-MS, of oligomers starting from degree of polymerization four (DP 4) is enhanced. The identification was based on MS spectra and comparison with literature data^[33]. As can be observed from Table 2, singly charged molecular ions $[M-H]^-$ were detected for oligomers with DP 2 to 4, whereas doubly charged ions $[M-2H]^{2-}$ were detected for DP 5 to 10. With respect to RP approach, the detection of oligomers with DP 6 and 7 was improved. In particular, from MS spectra in Figures 5a,b, can be appreciated how hexamers signals were covered by co-elutions in RPLC-MS (Figure 5a), but fully resolved and clearly detected with higher intensity in the HILIC-MS (Figure 5b).

Table 2: *Oligomeric procyanidins detected by HILIC-ESI-IT-TOF*

*** Oligomers described for the first time in Annurca apple extract*

DP	Molecular formula	HRMW	[M-H]⁻	[M-2H]²⁻	[MS/MS]	Error (ppm)	Compound
2	C ₃₀ H ₂₆ O ₁₂	578.1336	577.1331	-	407/289/205	-3.64	Epicatechin Dimer (Procyanidin B2)
3	C ₄₅ H ₃₈ O ₁₈	866.2058	865.1984	-	739/695/577/575/407/287	-0.12	Epicatechin trimer
4	C ₆₀ H ₅₀ O ₂₄	1154.2692	1153.2652	-	865/739/577/575/449	-1.47	Epicatechin tetramer
5	C ₇₅ H ₆₂ O ₃₀	1442.3284	-	720.1569	1151/865/577/575/407/287	-2.08	Epicatechin pentamer
6	C ₉₀ H ₇₄ O ₃₆	1730.3960	-	864.1870	1153/695/577/575/407/287	-2.55	Epicatechin hexamer
7	C ₁₀₅ H ₈₆ O ₄₂	2018.4594	-	1008.2226	1153/865/739/575/407	-1.39	Epicatechin eptamer **
8	C ₁₂₀ H ₉₈ O ₄₈	2306.5096	-	1152.2507	1008/865/768/695/577/575/407	-4.34	Epicatechin octamer **
9	C ₁₃₅ H ₁₁₀ O ₅₄	2594.5892	-	1296.2945	-	4.90	Epicatechin nonamer **
10	C ₁₅₀ H ₁₂₂ O ₆₀	2882.6568	-	1440.3191	-	5.00	Epicatechin decamer **

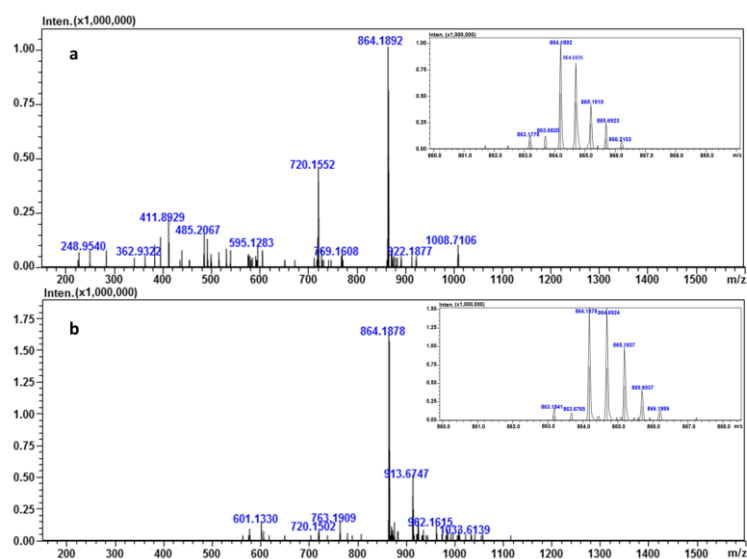


Figure 5 a,b: Comparison of full scan MS intensities for RP-UHPLC (5a) and HILIC (5b) in the detection of epicatechin examer.

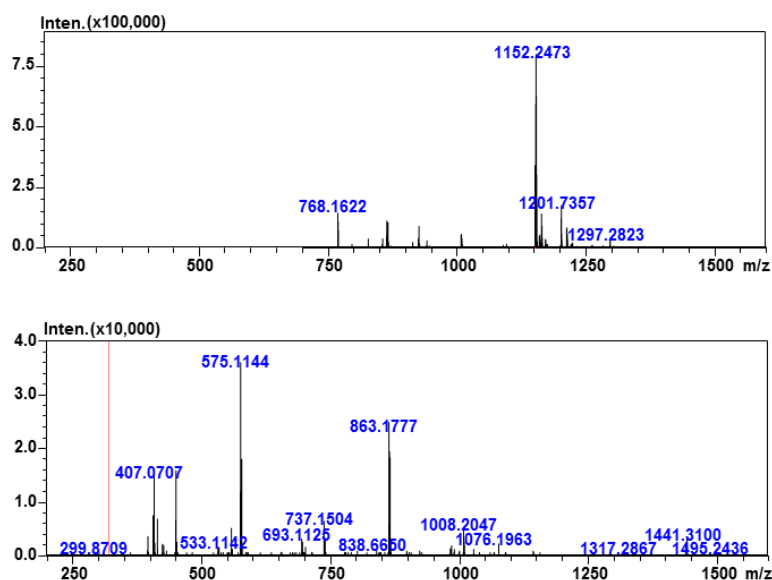


Figure 6: Full scan MS and MS2 spectra for epicatechin octamer (DP 8) detected only by HILIC-MS.

This is not only due to a better separation of these analytes, but also to the gain in ionization efficiency, since the highly organic mobile phase used enhanced the ESI sensitivity, as previously observed^[35,36]. Although present in traces, oligomers with DP 8 to 10, were detected only using HILIC-MS, as can be seen from Figure 6, showing MS and MS/MS spectra of the octamer. The resolution and detection decreases with increasing DP, and for highly molecular weight oligomers, with DP 9-10, extracted ion chromatogram were necessary for their identification, since these last eluting compound were present in very low concentration. Only B type procyanidins were detected in this variety of Annurca. Procyanidins are very interesting molecules for human health, but often overlooked^[37], thus it is important to extend the knowledge about their natural sources, even if their concentration can be low. In this regard the presence of oligomers over DP 6 has been only mentioned in Annurca^[38]. Furthermore, as reported previously^[39] DP of procyanidins can be directly related the taste and quality of apple ciders. To the best of our knowledge this is the first detailed description of procyanidins with DP > 6 in the Annurca extract.

4 Conclusions

The present research describes an extensive qualitative profiling of polyphenols in an Annurca apple extract, a typical cultivar of Southern Italy. The employment of two different separation techniques, such as RPLC and HILIC, in combination with a hybrid IT-TOF mass spectrometer, led to the tentative identification of 67 compounds, some not reported so far, which represent an improvement with respect to the previous observations. RP-UHPLC-MS was suitable for the analysis of dihydrochalcones, hydroxycinnamic acids, flavonols and anthocyanins, but not satisfactory for procyanidins. In this regard the employment of HILIC-MS improved the separation and detection of oligomeric procyanidins, and the presence

of oligomers with DP > 6 was described in detail for the first time in this apple variety. The proposed approach is a valid tool for polyphenolic fingerprinting and could be applied to other Annurca apple extracts, from different soils, to highlight the difference between different apple varieties, as well as in nutraceuticals based on Apple extracts.

5. References

- [1] Riboli, E., & Norat, T. Epidemiologic evidence of the protective effect of fruit and vegetables on cancer risk, *American Journal of Clinical Nutrition*, **2003**, 78, 559S–569S.
- [2] Pepe, G., Sommella, E., Manfra, M., De Nisco, M., Tenore, G.C., Scopa, A., Sofo, A., Marzocco, S., Adesso, S., Novellino, T., & Campiglia, P. Evaluation of anti-inflammatory activity and fast UHPLC–DAD–IT–TOF profiling of polyphenolic compounds extracted from green lettuce (*Lactuca sativa* L.; var. Maravilla de Verano), *Food Chemistry*, **2015**, 16, 153–161.
- [3] Tenore, G. C., Campiglia, P., Stiuso, P., Ritieni, A., & Novellino, E. Nutraceutical potential of polyphenolic fractions from Annurca apple (*M. pumila* Miller cv Annurca), *Food Chemistry*, **2013a**, 140 (4), 614–622.
- [4] Knekt, P., Jarvinen, R., Reunanen, A., & Maatela, J. Flavonoid intake and coronary mortality in Finland: A cohort study, *British Medical Journal*, **1996**, 312 (7029), 478–481.
- [5] Eberhardt, M. V., Lee, C. Y., & Liu, R. H. Antioxidant activity of fresh apples, *Nature*, **2000**, 405, 903–904.
- [6] Kalinowska, M., Bielawska, A., Lewandowska-Siwkiewicz, H., Priebe, W., & Lewandowski, W. Apples: Content of phenolic compounds vs. variety, part of apple and cultivation model, extraction of phenolic compounds, biological properties, *Plant Physiology and Biochemistry*, **2014**, 84, 169–188.

^[7] Fratianni, F., Sada, A., Cipriano, L., Masucci, A., & Nazzaro, F. Biochemical Characteristics, Antimicrobial and Mutagenic Activity in Organically and Conventionally Produced *Malus domestica*, Annurca, *The Open Food Science Journal*, **2007**, 1, 10–16.

^[8] D'Abrosca, B., Fiorentino, A., Monaco, P., Oriano, P., & Pacifico, S. Annurcoic acid: A new antioxidant ursane triterpene from fruits of cv. Annurca apple, *Food Chemistry*, **2006**, 98, 285–290.

^[9] Napolitano, A., Cascone, A., Graziani, G., Ferracane, R., Scalfi, L., Di Vaio, C., Ritieni, A., & Fogliano, V. Influence of variety and storage on the polyphenol composition of apple flesh, *Journal of Agricultural and Food Chemistry*, **2004**, 52 (21), 6526–6531.

^[10] Fini, L., Selgrad, M., Fogliano, V., Graziani, G., Romano, M., Hotchkiss, E., Daoud, Y. A., De Vol, E. B., Boland, C. R., & Ricciardiello, L. Annurca apple polyphenols have potent demethylating activity and can reactivate silenced tumor suppressor genes in colorectal cancer cells, *The Journal of Nutrition*, **2007**, 137 (12), 2622–2628.

^[11] Tenore, G. C., Campiglia, P., Ritieni, A., & Novellino, E. In vitro bioaccessibility, bioavailability and plasma protein interaction of polyphenols from Annurca apple (*M. pumila* Miller cv Annurca), *Food Chemistry*, **2013b**, 141 (4), 3519–3524.

^[12] De Rijke, E., Out, P., Niessen, W. M., Ariese, F., Gooijer, C., & Brinkman, U. A. Analytical separation and detection methods for flavonoids, *Journal of Chromatography A*, **2006**, 1112, 31–63.

^[13] Ramirez-Ambrosi, M., Abad-Garcia, B., Vilorio-Bernal, M., Garmon-Lobato, S., Berrueta, L. A., & Gallo, B. A new ultrahigh performance liquid chromatography with diode array detection coupled to electrospray ionization and quadrupole time-of-flight mass spectrometry analytical strategy for fast analysis

and improved characterization of phenolic compounds in apple products, *Journal of Chromatography A*, **2013**, 1316, 78–91.

^[14] Mari, A., Tedesco, I., Nappo, A., Russo, G. L., Malorni, A., & Carbone, V. Phenolic compound characterisation and antiproliferative activity of “Annurca” apple, a southern Italian cultivar, *Food Chemistry*, **2010**, 123 (1), 157–164.

^[15] Panzella, L., Petriccione, M., Rega, P., Scortichini, M., & Napolitano, A. A reappraisal of traditional apple cultivars from Southern Italy as a rich source of phenols with superior antioxidant activity, *Food Chemistry*, **2013**, 140 (4), 672–679.

^[16] Fratianni, F., Coppola, R., & Nazzaro, F. Phenolic composition and antimicrobial and antiquorum sensing activity of an ethanolic extract of peels from the apple cultivar annurca, *Journal of Medicinal Food*, **2011**, 14 (9), 957–963.

^[17] Sommella, E., Pepe, G., Pagano, F., Tenore, G. C., Dugo, P., Manfra, M., & Campiglia, P. Ultra high performance liquid chromatography with ion-trap TOF-MS for the fast characterization of flavonoids in Citrus bergamia juice, *Journal of Separation Science*, **2013**, 36 (20), 3351–3355.

^[18] Abu-Reidah, I. M., Ali-Shtayeh, M. S., Jamous, R. M., Arráez-Román, D., & Segura-Carretero, A. HPLC–DAD–ESI-MS/MS screening of bioactive components from *Rhus coriaria* L. (Sumac) fruits, *Food Chemistry*, **2015**, 166, 179–191.

^[19] Lazarus, S. A., Adamson, G. E., Hammerstone, J. F., & Schmitz, H. H. High-Performance Liquid Chromatography/Mass Spectrometry Analysis of Proanthocyanidins in Foods and Beverages, *Journal of Agricultural and Food Chemistry*, **1999**, 47 (9), 3693–3701.

^[20] Kalili, K. M., Cabooter, D., Desmet, G., & de Villiers, A. Kinetic optimisation of the reversed phase liquid chromatographic separation of proanthocyanidins on sub-2 μm and superficially porous phases, *Journal of Chromatography A*, **2012**, 1236, 63–76.

[21] Kalili, K. M., & de Villiers, A. Off-line comprehensive 2-dimensional hydrophilic interaction \times reversed phase liquid chromatography analysis of procyanidins, *Journal of Chromatography A*, **2009**, 1216 (35), 6274–6284.

[22] Kelm, M. A., Johnson, J. C., Robbins, R. J., Hammerstone, J. F., & Schmitz, H. H. High-performance liquid chromatography separation and purification of cacao (*Theobroma cacao* L.) procyanidins according to degree of polymerization using a diol stationary phase, *Journal of Agricultural and Food Chemistry*, **2006**, 54, 1571–1576.

[23] Nguyen, H. P., & Schug, K. A. The advantages of ESI-MS detection in conjunction with HILIC mode separations: Fundamentals and applications, *Journal of Separation Science*, **2008**, 31 (9), 1465–1480.

[24] Tenore, G. C., Calabrese, G., Stiuso, P., Ritieni, A., Giannetti, D., & Novellino, E. Effects of Annurca apple polyphenols on lipid metabolism in HepG2 cell lines: A source of nutraceuticals potentially indicated for the metabolic syndrome, *Food Research International*, **2014**, 63, 252–257.

[25] Graziani, G., D'Argenio, G., Tuccillo, C., Loguercio, C., Ritieni, A., Morisco, F., Del Vecchio Blanco, C., Fogliano, V., & Romano, R. Apple polyphenol extracts prevent damage to human gastric epithelial cells in vitro and to rat gastric mucosa in vivo, *Gut*, **2005**, 54, 193–200.

[26] Fromm, M., Bayha, S., Carle, R., & Kammerer, D. R. Characterization and quantitation of low and high molecular weight phenolic compounds in apple seeds, *Journal of Agricultural and Food Chemistry*, **2012**, 60 (5), 1232–1242.

[27] Sun, J., Lin, L. Z., & Chen, P. Study of the mass spectrometric behaviors of anthocyanins in negative ionization mode and its applications for characterization of anthocyanins and non-anthocyanin polyphenols, *Rapid Communications in Mass Spectrometry*, **2012**, 26, 1123–1133.

[28] Schieber, A., Hilt, P., Conrad, J., Beifuss, U., & Carle, R. Elution order of Quercetin glycosides from apple pomace extracts on a new HPLC stationary phase

with hydrophilic endcapping, *Journal of Separation Science*, **2002**, 25(5-6), 361–364.

[29] Schwab, W., & Schreier, P. Vomifoliol 1-O- β -D-xylopyranosyl-6-O- β -D-glucopyranoside: A disaccharide glycoside from apple fruit, *Phytochemistry*, **1990**, 29 (1), 161–164.

[30] Gu, L., Kelm, M., Hammerstone, J. F., Beecher, G., Cunningham, D., Vannozzi, S., & Prior, R. L. Fractionation of polymeric procyanidins from lowbush blueberry and quantification of procyanidins in selected foods with an optimized normal-phase HPLC-MS fluorescent detection method, *Journal of Agricultural and Food Chemistry*, **2002**, 50 (17), 4852–4860.

[31] Monagas, M., Quintanilla-López, J. E., Gómez-Cordovés, C., Bartolomé, B., & Lebrón-Aguilar, R. MALDI-TOF MS analysis of plant proanthocyanidins, *Journal of Pharmaceutical and Biomedical Analysis*, **2010**, 51 (2), 358–372.

[32] Kalili, K. M., Vestner, J., Stander, M. A., & de Villiers, A. Toward unraveling grape tannin composition: application of online hydrophilic interaction chromatography \times reversed-phase liquid chromatography-time-of-flight mass spectrometry for grape seed analysis, *Analytical Chemistry*, **2013**, 85 (19), 9107–9115.

[33] Lin, L. Z., Sun, J., Chen, P., Monagas, M. J., & Harnly, J. M. UHPLC-PDA-ESI/HRMSn profiling method to identify and quantify oligomeric proanthocyanidins in plant products, *Journal of Agricultural and Food Chemistry*, **2014**, 62 (39), 9387–9400.

[34] Karonen, M., Liimatainen, J., & Sinkkonen, J. Birch inner bark procyanidins can be resolved with enhanced sensitivity by hydrophilic interaction HPLC-MS, *Journal of Separation Science*, **2011**, 34 (22), 3158–3165.

[35] Kallio, H., Yang, W., Liu, P., & Yang, B. Proanthocyanidins in Wild Sea Buckthorn (*Hippophaë rhamnoides*) Berries Analyzed by Reversed-Phase, Normal-

Phase, and Hydrophilic Interaction Liquid Chromatography with UV and MS Detection, *Journal of Agricultural and Food Chemistry*, **2014**, 62 (31), 7721–7729.

[36] Periat, A., Boccard, J., Veuthey, J. L., Rudaz, S., & Guillarme, D. Systematic comparison of sensitivity between hydrophilic interaction liquid chromatography and reversed phase liquid chromatography coupled with mass spectrometry, *Journal of Chromatography A*, **2013**, 1312, 49–57.

[37] Cos, P., De Bruyne, T., Hermans, N., Apers, S., Berghe, D. V., & Vlietinck, A. J. Proanthocyanidins in health care: Current and new trends, *Current Medicinal Chemistry*, **2004**, 11 (10), 1345–1359.

[38] Lamperi, L., Chiuminatto, U., Cincinelli, A., Galvan, P., Giordani, E., Lepri, L., & Del Bubba, M. Polyphenol levels and free radical scavenging activities of four apple cultivars from integrated and organic farming in different Italian areas, *Journal of Agricultural and Food Chemistry*, **2008**, 56 (15), 6536–6546.

[39] Sanoner, P., Guyot, S., Marnet, N., Molle, D., & Drilleauthe, J. P. Polyphenol Profiles of French Cider Apple Varieties (*Malus domestica* sp.), *Journal of Agricultural and Food Chemistry*, **1999**, 47 (12), 4847–4853.

CHAPTER VI

***Vitis vinifera* (cv. Aglianico): healthy properties and polyphenolic profile of berry skin, wine and grape juices**

Abstract Red grapes are rich in phenolics, flavonoids, anthocyanins and resveratrol, all substances which have been suggested as having nutraceutical and health benefits. The berry skin and wine of grape cultivar *Vitis vinifera* L. (cv. Aglianico), grown in Basilicata (Southern Italy) were examined to determinate the presence of the above mentioned compounds as well as to establish the inorganic cation profile. HPLC analysis coupled with LC–ESI/MS/MS detected high contents of total flavonols and anthocyanins in grape juice, berry skin and wine. The wine made with the same grape used for berry skin assays showed a notable presence of quercetin-3-O-glucoside (39.4% of total flavonols), and malvidin and petunidin derivatives (63.9% and 10.8% of total anthocyanins, respectively). The processed grape juice (lioRGJ) was tested on cardiac-derived H9C2 myocytes to ascertain its effects on reactive oxygen species(ROS) generation and caspase-3 activity incubating cardiomyocytes with lioRGJ at increasing doses (0.01–1 µg). The strong antioxidant ROS-scavenging activity, determined by both DPPH and FRAP assays, and the high resveratrol content confer high sensory characteristics resulted to be associated with positive nutraceutical properties of these grapes and wine. The level of cis-resveratrol was lower than trans-resveratrol in both berry skin and wine reaching 44.1 mg/kg and 0.3 mg/l, respectively. The cation profile presents low levels of Ca, Cu, K, Fe, Zn and Cd compared to numerous, important red wines, such as Monastrell and Tempranillo.

Keywords: Aglianico Antioxidant activity, Anthocyanins, Flavonoids, Resveratrol, Multi-element analysis, Red grape juice, Lyophilization, Cardiomyocytes, Radical-scavenging activity.

1. Introduction

An increasing body of experimental evidence has shown the health benefits of polyphenols, a large family of natural compounds widely distributed in dietary plants which need phenolic compounds for pigmentation, growth, reproduction, and for many other functions, such as radical scavenging, signalling and defence from pathogen and parasitic attack. In grapes, four classes of flavonoids are commonly detected: flavonols, anthocyanins, flavan-3-ols and their polymeric forms, and condensed tannins^[1]. They are often leached out by grapes during the maceration period of wine making and endow characteristics to grape varieties and wines. While anthocyanins are water-soluble pigments located in grape skins and seeds, which appear red, purple or blue, according to pH, flavonols are yellow pigments generally considered to act as UV protectants and free-radical scavengers^[2]. Resveratrol (3,5,4'-trihydroxystilbene), the main stilbene synthesised in grape skin cells, is a non-flavonoid polyphenol that acts as a phytoalexin, being part of plant's defence system. Indeed, it is produced in plants in response to invading fungus, stress, injury, infection, or UV irradiation. Red wines contain high levels of resveratrol, as do grapes, raspberries, peanuts, and other plants^[3]. Wine flavonoids show beneficial effects on coronary heart disease, atherosclerosis, and some metabolic disorders, and they can inhibit carcinogenesis due to their antioxidant capacity^[4]. Generally, it has been established that an oxidation process is involved in the initial development steps of these disease, since an excess of reactive oxygen species (ROS) naturally formed during normal metabolism can damage biological macromolecules, such as proteins, lipids and nucleic acids^[5]. Resveratrol has also been shown to reduce tumour incidence in animals by affecting one or more stages of cancer development. The strong antioxidant and radical-scavenging properties of resveratrol and flavonols, such as of quercetin, have been intensively studied in both grapes and wines^[6]. This wide range of

health-promoting compounds suggests that several different and interrelated mechanisms of action are involved in the enhancement of the total antioxidant effects of the polyphenol family present in grape and wine. Recently, grape seed proanthocyanidins, a group of polyphenolic bioflavonoids ubiquitously found in the lignified portions of grape clusters, were found to possess cardioprotective abilities by acting as *in vivo* antioxidants and by their ability to directly scavenge ROS including hydroxyl and peroxy radicals^[7-9]. However, their pro-oxidant toxicity at higher doses (100–500 µg/mL) was also reported, particularly their ability to cause apoptosis in cardiomyocytes induced by ROS generation^[10-12]. The effects on cardiomyocytes by directly testing the whole grape juice are unknown. The study of the components present in wine and in grapes, as flavonols and anthocyanins, may also contribute to wine grape taxonomic characterisation and for certifying wine quality and origin^[13]. Grape and wine ionome, which describes the content of all mineral nutrients and trace elements, is today a poorly studied sector. The minerals, taken up by the grape and wine from the soil usually make up approximately 0.2–0.6% of the fresh weight of the fruit. K mineral cations, including, Na and Fe, are essential to the human organism and, together with Ca, Co, Cu, Fe, Mn, Se, Zn, play a crucial role for their nutraceutical properties. Consumption of wine in moderate quantities may significantly cover metal physiological needs. Numerous of these inorganic cations, naturally present in must and wine at non-toxic concentrations (e.g., K, Fe and Cu), play a major role both in winemaking and wine quality. Heavy metals as Pb, Hg and Cd, naturally present as sulphides in trace concentrations in the fruit, usually precipitate during fermentation, and their presence is important for grape and wine toxicology purposes. On the bases of these study, during my PhD we investigated the presence of the above cited compounds in the berry skins and wine of Aglianico (*Vitis vinifera* L.). The antioxidant profile of a commercial red grape juice was studied before (RGJ) and after lyophilization (lioRGJ) to evaluate its stability to

processing; to test the processed sample on cardiomyocytes to ascertain its effects on the physiological and doxorubicin-induced oxidative stress.

2. Materials and methods

2.1 Reagents and standards

All chemicals and reagents were analytical-reagent at HPLC grade. DPPH(1,1-diphenyl-2-picrilhydrazyl), 2,4,6-tris-2,4, 6-tripiridyl-2-triazine (TPTZ), iron (III) chloride (dry), 6-hydroxy- 2,5, 7,8-tetramethylchroman-2-carboxylic acid (Trolox), (+)-catechin hydrate, gallic acid monohydrate, aluminium chloride (dry), malvin (malvidin-3-O-glucoside) chloride, resveratrol (cis/trans isomers), Folin & Ciocalteu's phenol reagent, were purchased from Sigma Chemical Co. (St. Louis, MO, USA). Methyl alcohol (RPE) was purchased from Carlo Erba (Milano, Italy). HNO₃ (Suprapur grade) and multielemental standard stock solutions (1000 mg/L) were purchased from Merck (Darmstadt, Germany). Tris-HCl buffer, sodium dodecyl sulfate, diethylenetriaminepentaacetic acid, catalase, nitroblue tetrazolium, xanthine, bathocuproinedisulfonic acid, and bovine serum albumin (BSA) were purchased from Sigma Chemical Co. (St. Louis, MO, USA). Syringetin-3-O-galactoside was purchased from Extrasynthese (Lyon, France). Dulbecco's modified Eagle's medium (DMEM), penicillin, streptomycin, fetal bovine serum, and Dulbecco's phosphate-buffered saline (PBS) were purchased from Gibco-Invitrogen (Carlsbad, CA, USA). Tissue culture flasks and 24-well tissue culture plates were purchased from Corning (Corning, NY, USA).

2.2 Experimental vineyard, plant material, grapes and grape juice

The experiment was carried out in 2008 on a 5-year-old vineyard of Aglianico (VCR11) grafted onto 1103 Paulsen and located in Montegiordano Marina (42°02'N, 16°35'E; Southern Italy). All juices were manufactured during the same year. Purple juices were heat-extracted (approximately 50 °C) using pulp, seeds, and skin, with a subsequent pressing, and then submitted to pasteurization (at 85 °C). The juice was packaged and stored at 4 °C until the beginning of the analyses. According to the Winkler classification, this production area falls within climatic region 5, very hot. During the experiment, the temperature ranged between 0 and 38.5 °C, while cumulative rainfall of the period was 245 mm. The experimental plot, of about 0.30 ha, consisted of ten rows of spur-pruned vines to a permanent horizontal unilateral cordon. Each vine, decked at 0.60 m above the ground, was characterised by about 8 spurs of 2 to 3 buds each. The distance between the vines was of 2.5×1.0 m, with a final plant density of 4000 vines ha⁻¹. Rows were north-south oriented. The rows were oriented in a north-south direction. The soil was classified as a clay-loam. The plants were irrigated weekly from 9 June to 1 August (from fruit set to veraison) using a water amount equal to 100% of cultural evapotranspiration (ET_c). The value of ET_c was calculated using $ET_o \times K_c$, where ET_o is the reference evapotranspiration calculated according to Hargreaves method, and K_c is the cultural coefficient during the experimental period, equal to 0.6 for grapevine^[14]. The seasonal irrigation volume was of 960 m³ ha⁻¹ (240 L plant⁻¹). Each vine was irrigated by two drip emitters per plant discharging 4 L h⁻¹ each.

2.3 Lyophilization

A 10 mL aliquot of each RGJ of the four batches was lyophilized for 24 h (Edwards High Vacuum, West Sussex, UK). The residue (2.5 g) was stored in anhydrous atmosphere, at 4 °C in the dark, until the beginning of the analyses. Then, the sample was diluted to 10 mL with ultrapure water.

2.4 Total Phenolic Content

An aliquot (20 µL) of RGJ, lioRGJ, and calibration solutions of gallic acid (20, 40, 60, 80, and 100 mg/L) was added to a 25 volumetric flask containing 9 mL of ultrapure water (ddH₂O)^[15]. A reagent blank using ddH₂O was prepared. One milliliter of Folin–Ciocalteu’s phenol reagent was added to the mixture and shaken. After 5 min, 10 mL of Na₂CO₃ aqueous solution (7 g/100 mL) was added with mixing. The solution was then immediately diluted to volume with ddH₂O and mixed thoroughly. After incubation for 90 min at 23 °C, the absorbance versus prepared blank was read at 765 nm. Total phenolic content was expressed as milligrams of gallic acid equivalents (GAE) per 100 mL.

2.5 Total Flavonol Content

50 µL aliquot of RGJ, lioRGJ, and calibration solutions of quercetin-3-O-glucoside (20, 40, 60, 80, and 100 mg/L) was added to a 5 mL volumetric flask containing 2 mL of ddH₂O^[16]. At zero time, 0.15 mL of NaNO₂ aqueous solution (5 g/100 mL) was added to the flask. After 5 min, 0.15 mL of AlCl₃ aqueous solution (10 g/100 mL) was added. At 6 min, 1 mL of 1 M NaOH was added to the mixture. Immediately, the reaction flask was diluted to volume with the addition of 1.2 mL of ddH₂O and thoroughly mixed. Absorbance of the mixture, pink in color, was

determined at 510 nm versus prepared water blank. Total flavonol content was expressed as milligrams of quercetin-3-O-glucoside equivalents (QE)/ per 100 mL.

2.6 Total Monomeric Anthocyanin

An aliquot of 1 mL of RGJ, lioRGJ, and calibration solutions of malvin (0.1–10 mg/100 mL) was added to two vials containing 10 mL of acetate buffer (pH 3.6) and 1 N HCl, respectively^[17]. The difference between the absorbances read at 530 nm was calculated. Total anthocyanin content was expressed as milligrams of malvin equivalents (ME) per 100 mL.

2.7 Flavonol and anthocyanin extractions from berry skin and wine of Aglianico grapes

At harvest, on 27 September 2008, three clusters per plant were randomly sampled in the central and well-irradiated area of the canopy of five plants (n = 5) located in the central part of the row, where microclimatic conditions and soil physico-chemical characteristics were similar. From the clusters of each plant (n = 5), the berries were immediately detached, weighted and pooled together, and immediately stored at 4 °C in sterile plastic bags. Immediately after the transportation in the laboratory, the berries with a weight between 0.60 and 1.25 g (the most abundant and representative weight class) were rapidly stored at -80 °C in sterile polyethylene containers before the following analyses. Successively, frozen berries were peeled with a scalpel and the skins collected. This operation was carried out in an efficient way, as at low temperature the skin is easily removed by the rest of the berry. From each sample (n = 5), five grams of berry skin were placed in a 100 mL methanol–HCl 0.75% (w/w) solution at room temperature. The extraction was monitored for 24 h. Furthermore, the wine coming from nine chosen plants located

in the central part of the row (nine samples of one-year-old wine; n = 9) was bottled in glass bottles previously purged with gaseous nitrogen. The bottles were closed with corks and stored in the dark at 15 °C until analyses.

2.8 Identification and quantification of flavonols and anthocyanins

Separation of the flavonols and anthocyanins from berry skin, wine and grape juice (RGJ) was performed by high performance liquid chromatography (HPLC) and the analysis of crude extracts was performed after filtration with nylon filters of 0.45 mm (Teknokroma, Barcelona, Spain) to remove any solid residue. The structural identification was carried out by comparison of UV and retention times of our samples with authentic commercial samples according to a methodology reported in a previous paper^[2]. These data were validated by the LC–ESI/MS/MS analysis. The HPLC analysis were carried out by a Finnigan HPLC system (Thermo Electron Corporation, San Jose, CA, USA), a photodiode array detector (DAD). For detection of compounds, the chromatograms were recorded at 260, 353 and 520 nm in the photodiode detector. The different phenol compounds analysed were tentatively identified according to their order of elution, retention times of standard pure compounds, characteristics of the UV–Vis or fluorescence spectra, and by comparison with a bibliographic data. A complete UV–Vis spectrum database of all extracts and wine components was build and used to assess peak identification. Elution conditions consisted in 10% formic acid in water (Solvent A) and 10% formic acid in methanol (Solvent B) gradient at a flow rate of 1.0 mL/min. The column used was a C-18 Zorbax (150 mm × 4.6 mm, 5 µm packing; Agilent, USA) protected by an Agilent C-18 guard column. The elution conditions were: 0 min, 18% B; 14 min, 29% B; 16 min, 32% B; 18 min, 41% B; 18.1 min, 30% B; 29 min, 41% B; 32 min, 50% B; 34.5 min, 100% B; 35–38 min, 18% B. Calibration curves consisted in 0.001–1 mg/mL catechin and 0.05–1 mg/mL malvidin-3-glucoside

standard solutions. The identification of anthocyanins and flavonols was confirmed by a liquid chromatography electrospray ionization tandem mass spectrometry (LC–ESI/MS/MS) analysis using a HP1100 HPLC system (Agilent Technologies Inc., CA, USA) coupled to PE-Sciex API-2000 triple-quadrupole mass spectrometer (Warrington, Cheshire, UK) equipped with a Turbospray (TSI) source. MS detection was carried out in positive ion mode for anthocyanins and negative ion mode for flavonols at unit resolution using a mass range of 150–1500 m/z and a mass peak width of 0.7 ± 0.1 . Selected ion monitoring (SIM) experiments were carried out using the following operational parameters: vaporiser, 350 °C; heated capillary, 150–200 °C; carrier gas, nitrogen, at a sheath pressure of 70 psi; auxiliary gas, nitrogen, to assist in nebulisation, at a pressure of 30 psi; de-clustering potential, 44.0 eV; focusing potential, 340.0 eV; entrance potential, 10.0 eV; collision energy, 33.0 eV for ion decomposition in the collision cell at 0.8 mTorr.

2.9 Determination of cis- and trans-resveratrol

The quantification of cis- and trans-resveratrol in skin extracts and wine samples was carried out on the Finnigan HPLC equipment reported above. Separation was achieved using a Zorbax C-8 column (150 × 4.6 mm, 5 µm packing; Agilent, USA) and a mobile phase of 0.1% aqueous formic acid (solvent A) and acetonitrile (solvent B) delivered in isocratic elution mode at 25% B (v/v) at a flow rate of 1 mL/min. Calibration curves were plotted from 0.005 to 10 mg/mL. Wine samples (20 µl) were directly injected after filtration through a 0.45 µm membrane filter. A photodiode array detector was used, and quantification was done at 285 nm for cis- and trans-resveratrol.

2.10 Total antioxidant capacity

For each antioxidant assay, a Trolox aliquot was used to develop a 50–500 $\mu\text{mol/L}$ standard curve. All data were expressed as Trolox Equivalents ($\mu\text{mol TE}/100 \text{ mL}$). Spectrophotometric analyses were performed using a Jasco V-530 UV–vis spectrophotometer (Tokyo, Japan) set at appropriate wavelengths to each assay. The ability of the berry skin, wine and red grape juice (RGJ and lioRGJ) samples to scavenge the DPPH radical was measured^[18]. Aliquots (20 μL) of samples were added to 3 mL of DPPH solution ($6 \times 10^{-5} \text{ mol/L}$) and the absorbance was determined at λ 515 nm every 5 min until the steady state. The anti-oxidant potential of berry skin extracts, wines and RGJ was also determined using a FRAP assay, Ferric Reducing Ability of Plasma, as a measure of antioxidant power. A solution of 10 mmol/L TPTZ in 40 mmol/L HCl and 12 mmol/L FeCl_2 was diluted in 300 mmol/L sodium acetate buffer (pH 3.6) at a ratio of 1:1:10. Aliquots (20 μL) of samples were added to 3 mL of the FRAP solution and the absorbance was determined at 593 nm every 5 min until the steady state was reached.

2.11 Metal determination

Determination of the main metals in both berry skin extracts and wine samples was performed by quadrupole based inductively coupled plasma mass spectrometry, ICP-QMS (Elan DRC II, Perkin- Elmer SCIEX, CT, USA). Operational parameters were the following: sample uptake rate, 1 mL/min; sample introduction, Meinhard nebulizer with cyclonic spray chamber; gas flow rates (L min^{-1}): plasma, 15; auxiliary, 1.0; nebuliser, 0.85; dwell time, 50 ms; No. of replicate, 5; interface, Pt cones; extraction lens voltage, optimized for maximum I (56Fe). High purity He (99.9999% He) and H_2 (99.9995% H_2) were used, in order to minimise the potential problems caused by unidentified reactive contaminant species in the cell.

The high radio frequency power (1500 W) helped to maintain stable plasma in the presence of ethanol. Before use, all glassware and plastic containers were cleaned by washing with 10% ultrapure grade HNO₃ for at least 24 h, and then rinsed with copious quantities of ultra-pure water obtained with a Milli-Q purification system (Millipore Inc., Bedford, MA, USA). The wine samples were collected from the glass bottles by cautiously removing the corks, conditioning the necks by 5% HNO₃, and then aspirating the liquid with no contaminating pipettes. The plasma instability, related to the ethanol content in wine^[19], were minimised by a simple 1:5 dilution with 1% HNO₃. A 2.5% ethanol matrix for standards and blanks was used to approximate the 1:5 diluted wine matrixes. The calibration solutions were prepared from multi-elemental standard stock solutions of 1000 mg/L. The calibration curves were obtained by using at least 6 calibration solutions. Reagent blanks containing ultra-pure water were additionally analysed in order to control the purity of reagents and laboratory equipment. Standards and blanks were subjected to the same treatment as the wine samples.

2.12 Cell Culture and Viability Test

Cell Culture and Viability Test. Rat cardiac H9C2 cells (ATCC, Manassas, VA, USA) were cultured in DMEM supplemented with 10% fetal bovine serum, 100 U/mL of penicillin, and 100 µg/mL of streptomycin in 150 cm² tissue culture flasks at 37 °C in a humidified atmosphere of 5% CO₂. The cells were fed every 2–3 days and subcultured once they reached 70–80% confluence. Cell viability and proliferation were assessed by incubating the culture with lioRGJ (0.01–1 µg) and 1 µM doxorubicin for 72 h.

2.13 Preparation of Cell Extract

Cardiac H9C2 cells were collected by centrifugation and then resuspended in ice-cold 50 mM potassium phosphate buffer (pH 7.4), containing 2 mM EDTA. The cells were sonicated, followed by centrifugation at 13000g for 10 min at 4 °C. The resulting supernatants were collected and kept on ice for immediate measurements.

2.14 Measurement of Intracellular ROS Accumulation

2',7'- Dichlorodihydrofluorescein diacetate (DCF-DA, 5 µM) was used to detect intracellular ROS levels in H9C2 cells^[20] DCF-DA is cell membrane permeable. Once inside the cells, DCF-DA is hydrolyzed by cellular esterases to form DCF, which is trapped intracellularly due to its membrane impermeability. DCF then reacts with intracellular ROS to form the fluorescent product, 2',7'-dichlorofluorescein. Then, the cells were washed once with PBS and lysed in 3 mL of ice-cold 10 mM Tris-HCl buffer (pH 7.4) containing 0.2% sodium dodecyl sulfate. The cell lysates were collected and centrifuged at 2000g for 5 min at 4 °C. The fluorescence of the supernatants was measured using a Perkin- Elmer luminescence spectrometer (LS50B) at an excitation wavelength of 495 nm and an emission wavelength of 525 nm.

2.15 Measurement of Cellular Superoxide Dismutase (SOD)

A reaction mixture contained 50 mM potassium phosphate buffer (pH 7.8), 1.33 mM diethylenetriaminepentaacetic acid, 1.0 U/ mL catalase, 70 μ M nitroblue tetrazolium, 0.2 mM xanthine, 50 μ M bathocuproinedisulfonic acid, and 0.13 mg/mL BSA^[21]. A 0.8 mL aliquot of the reaction mixture was added to each cuvette, followed by the addition of 100 μ L of lysate. The cuvettes were prewarmed at 37 °C for 3 min. The formation of formazan blue was monitored at 560 nm and 37 °C for 5 min. The sample total SOD activity was calculated using a concurrently run SOD (Sigma) standard curve and expressed as units per milligram of cellular protein. Cellular protein content was quantified with Bio-Rad protein assay dye (Hercules, CA, USA) on the basis of the method that makes use of BSA as the standard.

2.16 Measurement of Caspase-3 Activity

Caspase-3 activity was measured using the BD ApoAlert Caspase-3 Fluorogenic Assay (BD Biosciences Clontech, Palo Alto, CA, USA). Briefly, protein lysates were collected from cells that had been incubated with IioRGJ (0.01–1 μ g) for 8 h, as per protocol. Activity was measured using a fluorescent microplate reader (PerSeptive Biosystems, Farmington, MA, USA).

2.17 Statistics

Unless otherwise stated, all of the experimental results were expressed as mean \pm standard deviation of measurements from independent samples ($n = 5$ for berry skin and $n = 9$ for wine). A one-way ANOVA was performed on the means to

determine whether they differed significantly. Significant differences were determined at $P \leq 0.05$, according to Fisher's LSD test.

3. Results and discussion

3.1 Flavonols and anthocyanins

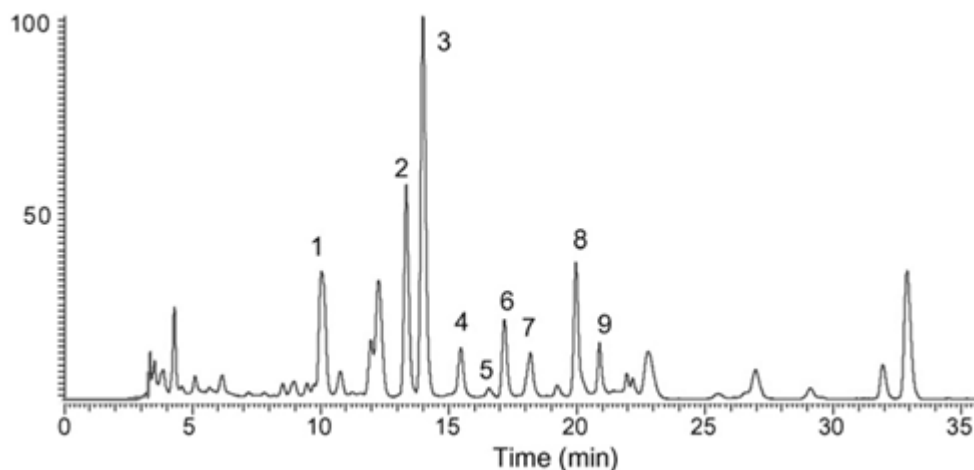
The data of flavonols present in berry skin, wine, RGJ and lioRGJ of Aglianico grapes, are reported in Tables 1-4, respectively. The flavonol content of berry skins (1036.7 mg/kg fresh weight) was 15-fold higher than in the corresponding wine (69.5 mg/l). Our sample showed a higher concentration of flavonols than other more widely consumed red grape juices and wines. Among the nine flavonols detected in Aglianico grape and wine, quercetin-3-O-glucoside and, to a lesser extent, quercetin-3-O-glucuronide, were the most abundant flavonols both in berry skin and wine, in agreement with previous works^[22]. These compounds are involved in the longterm colour stability of red wines and in the improvement of organoleptic properties. It has long been known that the increased biosynthesis of polyphenols, especially flavonols, is greatly influenced by sunlight exposure and temperature, so it is expected that the grapes which are grown in warmer, sunnier areas have a higher level of flavonols. In addition, industrial processing in which the juice is submitted to a heat treatment to obtain a product characterized by much better conditions for storage, transport, and preservation can increase the flavonol content due to more exhaustive extraction processes and digestion mechanisms^[23]. Moreover, they are associated to numerous positive nutraceutical properties and health benefits. Myricetin-3-O-glucoside, largely present in berry skin and grape juice, decreased in wine, indicating a lowering of its bioavailability during the winemaking process. Generally, wine samples have shown an important peak corresponding to free myricetin suggesting that this flavonol seems to be

easily hydrolysed^[24]. Isorhamnetin-3-O-glucoside and kaempferol-3-O-caffeoylate reverse the common flavonol content by doubling their presence in the wine when compared to the berry skin. Isorhamnetin inhibits adipogenesis through down-regulation of PPAR-gamma and C/EBP-alpha in 3T3-L1 Cells^[25]. Kaempferol seems to prevent arteriosclerosis by inhibiting the oxidation of low density lipoprotein and the formation of platelets in the blood. Current evidence indicates that kaempferol not only protects LDL from oxidation but also prevents atherogenesis through suppressing macrophage uptake of oxLDL.

Table 1: Flavonol content (\pm standard deviation) of berry skin ($n = 5$) and wine ($n = 9$) of Aglianico grapes.

Compound	Berry skin		Wine	
	(mg/kg fresh weight)	%	(mg/L)	%
Myricetin-3- <i>O</i> -glucoside	142.1 \pm 1.2	13.7	7.70 \pm 0.9	11.1
Quercetin-3- <i>O</i> -glucuronide	170.6 \pm 1.1	16.5	9.07 \pm 0.8	13.1
Quercetin-3- <i>O</i> -glucoside	441.3 \pm 7.4	42.6	27.39 \pm 1.5	39.4
Laricitrin-3- <i>O</i> -galactoside	38.7 \pm 0.9	3.7	2.14 \pm 0.8	3.1
Kaempferol-3- <i>O</i> -glucoside	27.2 \pm 1.1	2.6	1.40 \pm 0.7	2.0
Laricitrin-3- <i>O</i> -rhamnose-7- <i>O</i> -trihydroxycinnamic acid	56.1 \pm 0.7	5.4	3.90 \pm 0.3	5.6
Kaempferol-3- <i>O</i> -caffeoylate	46.5 \pm 0.9	4.5	5.44 \pm 0.6	7.8
Isorhamnetin-3- <i>O</i> -glucoside	67.0 \pm 0.8	6.5	8.69 \pm 0.5	12.5
Syringetin-3- <i>O</i> -galactoside	47.2 \pm 0.4	4.6	3.74 \pm 0.4	5.4
Total	1036.7		69.47	

Table 2: Mass chromatogram and mass spectrometry data of the flavonols detected in Aglianico berry skin and wine.



Peak	Compound	m/z [M-H] ⁻	MS ^{2a}	MS ^{3a}	MS ^{4a}
1	Myricetin-3- <i>O</i> -glucoside	479	<u>316</u> /317	242, 270/ <u>271</u> , 287	171, 199, 227
2	Quercetin-3- <i>O</i> -glucuronide	477	301	151, <u>179</u> , 193, 257, 273	151
3	Quercetin-3- <i>O</i> -glucoside	463	301	151, <u>179</u> , 193, 257, 273	151
4	Laricitrin-3- <i>O</i> -galactoside	493	330, <u>331</u>	151, 179, 193, <u>316</u> , 317	151, 164, <u>179</u> , 219, 244, 270/ <u>271</u> , 287/288
5	Kaempferol-3- <i>O</i> -glucoside	447	255, <u>284</u> /285, 327, 401, 419, 429	227, 239, <u>255</u> /256	212, 227
6	Laricitrin-3- <i>O</i> -rhamnose-7- <i>O</i> -trihydroxycinnamic acid	655	303, 314, <u>329</u> , 347, 475, 501, 509	314	299
7	Kaempferol-3- <i>O</i> -caffeoylate	447	<u>284</u> /285	227, 239, <u>255</u> /256	212, 227
8	Isorhamnetin-3- <i>O</i> -glucoside	477	271, 285, <u>314</u> /315, 357	243, 257, 271, <u>285</u> /286, 299/300	241/270
9	Syringetin-3- <i>O</i> -galactoside	507	<u>344</u> /345, 387, 479, 489	330	

^a Base peak (100%) is underlined

Table 3: LC/MS data of flavonols in *Vitis vinifera* L. cv. Aglianico N. red grape juice before (RGJ) and after lyophilization (lioRGJ) and their quantitative analysis using DAD at 353 nm.

Peak	Compound	mg QE/100 mL*		m/z [M-H] ⁻	MS ^{2a}
		GJ	lioGJ		
1	Myricetin-3-O-glucoside	93.1 ± 0.3	91.7 ± 0.2	479	316/317
2	Quercetin-3-O-glucuronide	75.6 ± 0.2	73.5 ± 0.3	477	301
3	Quercetin-3-O-glucoside	79.8 ± 0.07	78.4 ± 0.08	463	301
4	Laricitrin-3-O-galactoside	13.3 ± 0.08	11.9 ± 0.06	493	330, 331
5	Kaempferol-3-O-glucoside	5.6 ± 0.02	5.6 ± 0.01	447	255, 284/285, 327, 401, 419, 429
6	Laricitrin-3-O-rhamnose-7-O-trihydroxycinnamic acid	18.2 ± 0.1	16.8 ± 0.2	655	303, 314, 329, 347, 475, 501, 509
7	Kaempferol-3-O-caffeoylate	16.8 ± 0.02	16.8 ± 0.02	447	284/285
8	Isorhamnetin-3-O-glucoside	24.5 ± 0.03	23.1 ± 0.04	477	271, 285, 314/315, 357
9	Syringetin-3-O-galactoside	19.6 ± 0.05	20.3 ± 0.03	507	344/345, 387, 479, 489

Numerous studies showed kaempferol may have health benefits for people at risk of cancer^[26]. Wine content of laricitrin-3-O-rhamnose, laricitrin-3-O-galactoside, syringetin-3-O-galactoside and kaempferol-3-O glucoside retain proportionality with the total flavonoid content in berry skin. The main flavonol glycosides in red grape juices and wines are derivatives of myricetin and quercetin^[27,28] namely, myricetin-3-O-glucoside, quercetin-3-O-glucoside, and quercetin-3-O-glucuronide (Table 3). In contrast to the literature, low levels of kaempferol derivatives were found. During the ripening of the grapes, flavonols are accumulated in the berry skin and their absolute and relative content can be influenced by many abiotic factors, including water availability and temperature^[2]. Considering that water

supplies in this experiment were not a limiting factor, we compared the levels of flavonols and anthocyanins with those found in grapevines grown under similar cultivation and environmental conditions. From this comparison, it appears that total quercetin content detected in Aglianico berry skin (441.3 and 170.6 mg/kg for quercetin-3-O-glucuronide and quercetin-3-O-glucoside, respectively), as well as the levels of other flavonols detected, are higher than those found in some of the most important red grape varieties^[29]. The same difference was found considering wines, where Aglianico ranks at the first places for quercetin derivatives and total flavonols, with levels comparable to wines produced from high-quality red wine varieties such as Cabernet Sauvignon, Sangiovese, Primitivo, Merlot, and Zinfandel. The anthocyanin levels and the mass spectrometry parameters of the berry skin, wine and grape juice samples are shown in Tables 4, 5, 6, respectively. Among the fruits and vegetables commonly consumed, grapes and their associated products are regarded as the most important source of our dietary anthocyanins. These compounds have been shown to contribute to the strong protection of the red grape and wine against low-density lipoprotein oxidation^[30]. Recent studies have demonstrated that the long-term intake of anthocyanins, which were administered as food matrix or enriched fractions, changed the markers for the oxidative status in some tissues and affected antioxidant enzyme expression levels and activities when compared with animals that did not receive polyphenols in the diet^[31]. Thus, considering the dietary intake of anthocyanins (approximately 100 mg/die) and their potential health benefits, the grape and wine samples could be regarded as a valuable anthocyanin source suitable for use as dietary supplement. Malvidin-3-O-glucoside was found to be the main anthocyanin present along with its coumaroyl derivative, accounting for 87% and 59% of total content in berry skin and wine, respectively (Table 4).

Malvidin-3-O-glucoside is found to be the most abundant compound both before and after lyophilization (Table 6). Besides the malvidin-3-O-glucoside and trans

malvidin-3-(6-O-coumaroyl)-glucoside, differences between anthocyanin present in berry skin, wine and RGJ were found for peonidin derivatives, malvidin-3-O-acetyl-glucoside and trans petunidin-3-(6-O-coumaroyl)-glucoside, with percentages significantly higher in wine than in berry skin and RGJ (Table 4). Total anthocyanin content in berry skin was approximately 14-fold of the corresponding value found in wine (9996.1 mg/kg and 716.3 mg/L, respectively), a proportion not differing greatly from that found in Spanish variety Jumilla-Monastrell^[32]. Generally, Aglianico wine appeared to have a high anthocyanin content (716.3mg/L) in comparison with the profiles of other high-quality red wines^[33]. Furthermore, the concentration of malvidin and petunidin derivatives (63.9% and 10.8% of total anthocyanins, respectively), in Aglianico wine, is comparable with their presence in other well-known red wines, such as Tempranillo^[34], Cabernet Sauvignon^[32], Monastrell-J, Shiraz, and Pinot Noir and Muscat Rouge^[35]. In particular, the high levels of acetylated anthocyanins detected in Aglianico wine (e.g., peonidin-3-O-acetylglucoside and petunidin-3-O-acetylglucoside), represent another positive sensory parameter as they confer a deep red colour and organoleptic attributes^[36].

Table 4: Anthocyanin content (\pm standard deviation) of the berry skin ($n = 5$) and wine ($n = 9$) of Aglianico grapes. ND = not detected.

Compound	Berry skin		Wine	
	(mg/kg fresh weight)	%	(mg/L)	%
Delphinidin-3- <i>O</i> -glucoside	369.5 \pm 6.2	3.7	40.8 \pm 1.6	5.7
Cyanidin-3- <i>O</i> -glucoside	353.8 \pm 3.2	3.5	37.3 \pm 0.9	5.2
Petunidin-3- <i>O</i> -glucoside	504.6 \pm 1.1	5.0	27.7 \pm 1.2	3.9
Peonidin-3- <i>O</i> -glucoside	33.5 \pm 0.9	0.3	21.2 \pm 0.6	3.0
Malvidin-3- <i>O</i> -glucoside	5613.7 \pm 9.1	56.2	344.2 \pm 1.5	48.1
Delphinidin-3- <i>O</i> -acetyl-glucoside	222.5 \pm 2.1	2.2	2.1 \pm 0.8	0.3
Cyanidin-3- <i>O</i> -acetyl-glucoside	173.2 \pm 1.2	1.7	0.9 \pm 0.7	0.1
Petunidin-3- <i>O</i> -acetyl-glucoside	84.4 \pm 0.7	0.8	19.9 \pm 0.9	2.8
Peonidin-3- <i>O</i> -acetyl-glucoside	140.7 \pm 2.2	1.4	54.6 \pm 1.2	7.6
Petunidin-(6- <i>O</i> -caffeoyl)-glucoside	34.2 \pm 0.6	0.3	ND	ND
Malvidin-3- <i>O</i> -acetyl-glucoside	57.0 \pm 0.8	0.6	34.6 \pm 0.7	4.8
Malvidin-(6- <i>O</i> -caffeoyl)-glucoside	112.6 \pm 1.9	1.1	0.7 \pm 0.2	0.1
Cyanidin-3-(6- <i>O</i> -coumaroyl)-glucoside (<i>trans</i> isomer)	63.8 \pm 0.8	0.6	0.4 \pm 0.1	0.0
Petunidin-3-(6- <i>O</i> -coumaroyl)-glucoside (<i>trans</i> isomer)	140.9 \pm 0.7	1.4	29.2 \pm 1.2	4.1
Peonidin-3-(6- <i>O</i> -coumaroyl)-glucoside (<i>trans</i> isomer)	106.5 \pm 1.2	1.1	24.6 \pm 0.9	3.4
Malvidin-3-(6- <i>O</i> -coumaroyl)-glucoside (<i>trans</i> isomer)	1985.2 \pm 8.5	19.9	78.1 \pm 0.8	10.9
Total	9996.1		716.3	

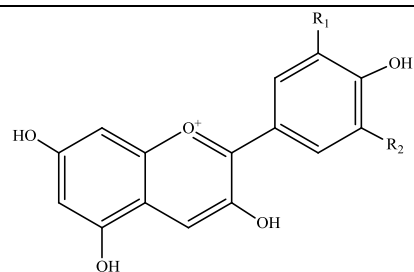
Table 5: Mass spectrometry data of anthocyanins detected in Aglianico berry skin and wine.

Peak	Compound	<i>m/z</i> [M+H] ⁺	MS ^{2a}	MS ^{3a}	MS ^{4a}
1	Delphinidin-3- <i>O</i> -glucoside	465	303	229, 257, <u>303</u>	229, 257
2	Cyanidin-3- <i>O</i> -glucoside	449	287	213, 231, 241, 259, <u>287</u>	213, 231, 241, 259, <u>287</u>
3	Petunidin-3- <i>O</i> -glucoside	479	317	257, 274, <u>302</u> , 317	218, 228, 246, <u>274</u>
4	Peonidin-3- <i>O</i> -glucoside	463	301	286	230, 258, 268
5	Malvidin-3- <i>O</i> -glucoside	493	331	179, 242, 270, 287, 299, <u>315/316</u>	213, 257, 285, 287, 313, 315
6	Delphinidin-3- <i>O</i> -acetyl-glucoside	507	303	229, 257, <u>303</u>	229, 257, <u>303</u>
7	Cyanidin-3- <i>O</i> -acetyl-glucoside	491	287	213, 231, 259, <u>287</u>	213, 231, 259, <u>287</u>
8	Petunidin-3- <i>O</i> -acetyl-glucoside	521	<u>302</u> , 317	218, 228, 246, 256, <u>274</u>	135, <u>149</u> , 153, 163, 181
9	Peonidin-3- <i>O</i> -acetyl-glucoside	505	301	286	230, 258, 268
10	Petunidin-(6- <i>O</i> -caffeoyl)-glucoside	641	317	302	218, 228, 246, 274
11	Malvidin-3- <i>O</i> -acetyl-glucoside	535	331	179, 242, 270, 299, <u>315</u> , 331	257, 285, 287, 313, 315
12	Malvidin-(6- <i>O</i> -caffeoyl)-glucoside	655	331	179, 242, 270, 287, 299, <u>315/316</u> , 331	257, 285, 287, 313, 315
13	Cyanidin-3-(6- <i>O</i> -coumaroyl)-glucoside (<i>trans</i> isomer)	595	287	213, 231, 259, <u>287</u>	213, 231, 259, <u>287</u>
14	Petunidin-3-(6- <i>O</i> -coumaroyl)-glucoside (<i>trans</i> isomer)	625	317	274, <u>302</u>	218, 228, 246, <u>274</u>
15	Peonidin-3-(6- <i>O</i> -coumaroyl)-glucoside (<i>trans</i> isomer)	609	301	286	230, 258, 268
16	Malvidin-3-(6- <i>O</i> -coumaroyl)-glucoside (<i>trans</i> isomer)	639	331	179, 242, 270, 287, <u>299</u> , <u>315/316</u> , 331	225, 253, <u>281</u> , 299

^a Base peak (100%) is underlined.

Table 6: LC/MS data of tentatively identified anthocyanins in *Vitis vinifera* L. cv. Aglianico N. red grape juice before (RGJ) and after lyophilization (lioRGJ) and their quantitative analysis using DAD at 520 nm.

Peak	Compound	mg ME/100 mL*		<i>m/z</i> [M+H] ⁺	MS ^{2a}
		GJ	lioGJ		
1	Delphinidin-3- <i>O</i> -glucoside	34.78 ± 1.1	34.87 ± 1.3	465	303
2	Cyanidin-3- <i>O</i> -glucoside	21.63 ± 1.2	21.63 ± 1.1	449	287
3	Petunidin-3- <i>O</i> -glucoside	25.63 ± 1.4	25.68 ± 1.0	479	317
4	Peonidin-3- <i>O</i> -glucoside	31.24 ± 1.0	31.15 ± 0.9	463	301
5	Malvidin-3- <i>O</i> -glucoside	114.63 ± 1.9	114.50 ± 1.7	493	331
6	Delphinidin-3- <i>O</i> -acetylglucoside	10.38 ± 1.5	10.40 ± 0.3	507	303
7	Cyanidin-3- <i>O</i> -acetylglucoside	5.08 ± 0.9	5.01 ± 0.4	491	287
8	Malvidin-3-(6- <i>O</i> -coumaroyl)glucoside (<i>cis</i> isomer)	12.38 ± 0.8	12.21 ± 0.4	639	331
9	Malvidin-(6- <i>O</i> -caffeoyl)glucoside	52.99 ± 1.2	53.00 ± 0.6	655	331
10	Peonidin-3-(6- <i>O</i> -coumaroyl)glucoside (<i>trans</i> isomer)	4.32 ± 1.0	4.32 ± 0.2	609	301
11	Malvidin-3-(6- <i>O</i> -coumaroyl)glucoside (<i>trans</i> isomer)	14.66 ± 0.8	14.35 ± 0.1	639	331



Name	R ₁	R ₂
Cyanidin	OH	H
Peonidin	OCH ₃	H
Delphinidin	OH	OH
Petunidin	OCH ₃	OH
Malvidin	OCH ₃	OCH ₃

3.2 Resveratrol and total antioxidant capacity

The content of trans-resveratrol in wine was significantly higher than that of cis-resveratrol^[37] (Table 7) and lower in wine than in berry skin because of the scarce stability of stilbenes during winemaking processes^[38]. The wine total resveratrol presence (5.88 mg/L) was higher than that found in many red wines usually assessed as 1.9 ± 1.7 mg/L and comparable to the level found in some wines, Pinot Nero and Merlot, famous for the high concentration of the trans isomer. The results show that resveratrol was present in Aglianico wine at higher concentrations than in the common red wines.

Table 7: *trans- and cis-Resveratrol content (\pm standard deviation) of the berry skin ($n = 5$) and wine ($n = 9$) from Aglianico grapes.*

Samples	Berry skin (mg/kg fresh weight)	Wine (mg/L)
<i>trans</i> -resveratrol	441.41 ± 2.1	3.79 ± 0.9
<i>cis</i> -resveratrol	163.63 ± 1.6	2.09 ± 1.1

3.3 Polyphenolic composition and antioxidant capacity

The results obtained for RGJ polyphenolic composition (Figure 1) were generally higher than those reported elsewhere for other commercial samples^[39]. It has been shown that sun-exposed grapes can contain up to 10 times more total phenolics than grapes cultivated in the shade^[40]. Moreover, thermal treatments employed during grape processing for grape juice production may be responsible for a more exhaustive extraction of polyphenols^[30]. Particularly, RGJ high flavonol levels may be ascribed to hydrolysis processes, which would increase the monomeric compound content in the final product^[23].

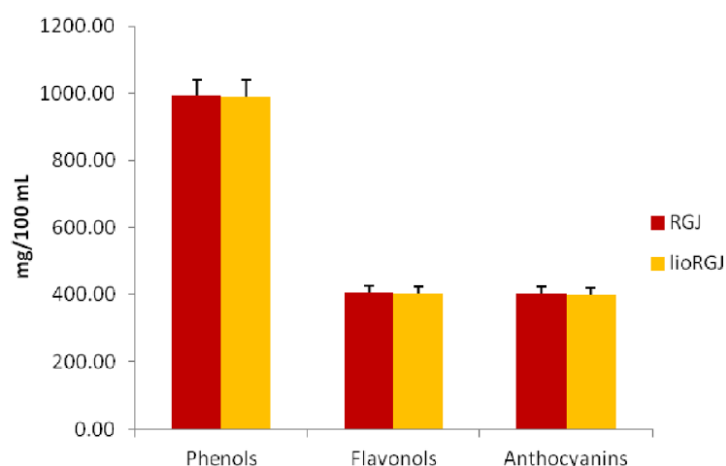


Figure 1: Polyphenolic contents in Aglianico red grape juice before (RGJ) and after lyophilization (lioRGJ). Phenol contents are expressed as mg GAE/100 mL \pm SD; Flavonol contents are expressed as mg QE/100 mL \pm SD; Anthocyanin contents are expressed as mg ME/100 mL \pm SD

This method, based on complex formation with aluminum chloride^[16], is rather specific to flavonols, because the aluminum complexation requires a 4-keto group and at least one neighboring (3- or 5-) hydroxyl group, which are common features of flavonols. Interestingly, the almost identical RGJ and lioRGJ polyphenolic contents indicated a good stability of the juice to the lyophilization process^[41]. These samples have a variety of bioactivity related to its antioxidant properties, such as cardioprotective, anti-cancer, anti-inflammation, anti-ageing and anti microbial activities. Moreover, some studies supported Sinclair's hypothesis that the effects of resveratrol are indeed due to the activation of the Sirtuin 1 gene which is involved in life extension^[42]. Owing to the complex reactivity of phytochemicals, the antioxidant activities of food and food extracts cannot be evaluated by only a single method, but at least two test systems have been recommended for the determination of antioxidant activity to establish authenticity^[43]. For this reason, the antioxidant activity was determined by two

spectrophotometric methods, DPPH and FRAP tests, and expressed as trolox equivalents (TEs). The reduction of DPPH absorption is indicative of the capacity of the samples to scavenge free radicals, while the FRAP method is used to determine the capacity of reductants in a sample. The total antioxidant capacity, evaluated by FRAP and DPPH tests, was higher for wine than for berry skin extracts (about 2- to 4-fold) (Table 8), due to the increased presence of malvidin, peonidin, cyanidin, delphinidin and petunidin derivatives in wine^[44]. RGJ and lioRGJ showed quite comparable antioxidant activities when tested by both assays. These results confirmed that the quali-quantitative polyphenolic composition of the freeze-dried sample remained almost unchanged. Results revealed for the juice samples a good antioxidant activity when compared with that of authentic standards chosen as widely employed food preservatives and strong hydrophilic or lipophilic antioxidants (Figure 2).

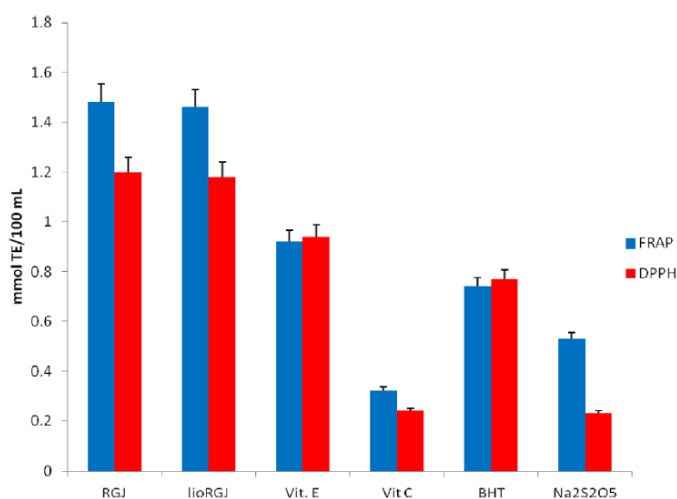


Figure 2: Reducing capacity (FRAP test) and radical-scavenging activity (DPPH test) of Aglianico red grape juice (RGJ and lioRGJ) versus antioxidant standards. Values are expressed \pm SD ($P < 0.001$).

Table 8: Total antioxidant capacity expressed as Trolox of the extracts from the berry skin ($n = 5$) and wine ($n = 9$) of Aglianico grapes determined by DPPH and FRAP assays at the steady state (DPPH, 45 min; FRAP, 55 min).

Sample	DPPH [•]	Assay method	FRAP
		($\mu\text{mol/L}$)	
Berry skin	443.6		1095.7
Wine	1550.0		2200.0

3.4 Effects of grape juice after lyophilization on Cardiomyocytes.

We examined the effect on free radical and manganese superoxide dismutase levels in cardiac-derived H9C2 myocytes exposed to increasing doses (0.01–1 μg) of lioRGJ (Table 9). The data demonstrated that antioxidants in the juice sample at a maximum sample dose of 0.01 μg were able to directly scavenge free radicals (with the exception of RNS) without interfering with cell antioxidant defensive system involving enzymes and proteins for cardioprotection. Nevertheless, exposure to increasing concentrations of lioRGJ resulted in pro-oxidant effects as demonstrated by the increase in ROS, RNS, and antioxidant enzyme levels at a sample dose of 0.05 μg (Table 9).

Table 9: *Effect of lyophilized Aglianico red grape juice on free radicals generated and manganese superoxide dismutase activity in lysate of H9C2 cardiomyocytes.*

	Control	0.01 µg lioRGJ	0.05 µg lioRGJ	Dox 1 µM	Dox 1 µM + 0.01 µg lioRGJ	Dox 1 µM + 0.05 µg lioRGJ
TBARS µM/µg protein	0.0043	0.0035	0.0047	0.0068	0.0021	0.005
NO ₂ ⁻ nmol/µg protein	0.0010	0.0039	0.008	0.0065	0.0052	0.024
MnSOD U/µg protein	0.01	0.010	0.018	0.008	0.008	0.035

lioRGJ: lyophilized red grape juice

Dox: doxorubicin

TBARS: Thiobarbituric Acid Reactive Substances

MnSOD: manganese superoxide dismutase

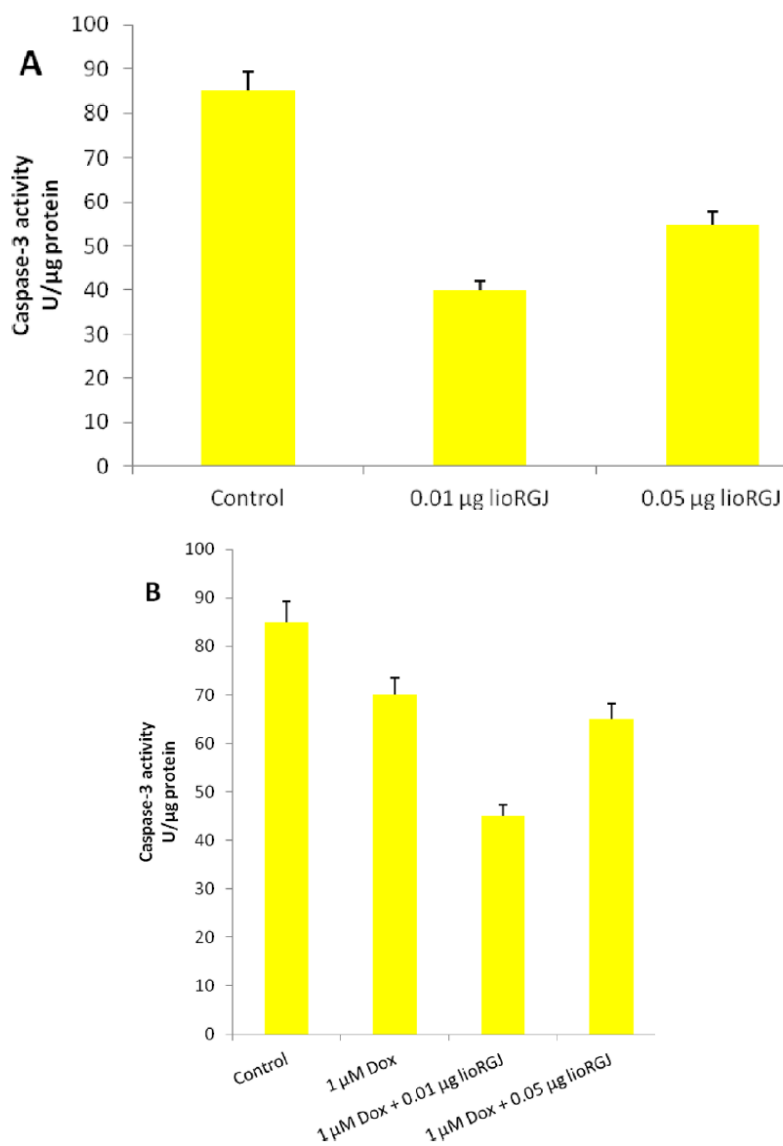


Figure 3: (A) Effect of increasing doses (0.01-1 μg) of lyophilized *Vitis vinifera* L. cv. Aglianico N. red grape juice before (lioRGJ) on proliferation of H9C2 cardiomyocytes. (B) Effect of lyophilized *Vitis vinifera* L. cv. Aglianico N. red grape juice before (lioRGJ) on caspase-3 activity in lysate of H9C2 cardiomyocytes. (C) Effect of lyophilized *Vitis vinifera* L. cv. Aglianico N. red grape juice before (lioRGJ), doxorubicin (Dox) and their combination on proliferation of H9C2 cardiomyocytes.

These results would suggest what has already been stated in the literature for grape seed proanthocyanidin extract that higher doses of antioxidants occurring in the juice sample may cause apoptotic cell injury via effector caspase-3 activation and subsequent induction of ROS and RNS generation^[10-12]. To confirm such a hypothesis, the influence of lioRGJ on caspase-3 activity in cardiac-derived H9C2 myocytes was tested (Figure 3). Among the many known regulators and effectors of apoptosis, caspases are a family of cytoplasmic proteases that play an important role in the execution phase of apoptosis. Cells were incubated with lioRGJ (0.01–1 µg) in medium for 8 h and then lysed to measure caspase-3 activity using a fluorogenic assay. The best result was achieved with a dose of 0.01 µg that made the caspase-3 activity decrease by about 47% (Figure 3). An increase in lioRGJ dose (from 0.01 to 0.05 µg) exposure to cardiomyocytes seemed to be less effective in reducing caspase-3 activity. Collectively, these data suggested that higher doses of lioRGJ caused cell death via the caspase-3-mediated apoptotic pathway. To ascertain the potential effects of lioRGJ on the doxorubicin-induced oxidative stress in cardiac cells, H9C2 cardiomyocytes were exposed to 1 µM doxorubicin and a combination of doxorubicin and different doses of lioRGJ for 72 h (Table 10)^[45]. A sample aliquot of 0.01 µg provided an appreciable radical-scavenging activity as indicated by the decrease in the free radical levels (especially ROS species, about 31%) and the unchanged antioxidant defense system activity (Table 10). Interestingly, the association of doxorubicin with higher lioRGJ doses (from 0.01 to 0.05 µg) led to the enhancement of cardiac cell oxidative stress, probably due to sample pro-oxidant effects, as indicated mainly by the increase in RNS and antioxidant enzyme levels (Table 10).

Table 10: ^aValues are expressed as means \pm SD of at least three experiments ($P < 0.001$ compared to the control). *lioRGJ*, lyophilized red grape juice; *Dox*, doxorubicin; *TBARS*, thiobarbituric acid reactive substances; *MnSOD*, manganese superoxide dismutase; *control*, untreated cell lines.

	Control	1 μ M Dox	1 μ M Dox + 0.01 μ g of <i>lioRGJ</i>	1 μ M Dox + 0.05 μ g of <i>lioRGJ</i>
TBARS μ M/ μ g protein	0.0043 \pm 0.05	0.0068 \pm 0.09	0.0021 \pm 0.02	0.0050 \pm 0.05
NO ₂ nmol/ μ g protein	0.0010 \pm 0.02	0.0065 \pm 0.08	0.0052 \pm 0.07	0.0240 \pm 0.21
MnSOD, U/ μ g protein	0.0100 \pm 0.12	0.0080 \pm 0.05	0.0080 \pm 0.10	0.0350 \pm 0.35

To confirm such a hypothesis, the influence of 1 μ M doxorubicin and a combination of doxorubicin with different doses of *lioRGJ* on caspase-3 activity in cardiomyocytes was assayed (Figure 3). Data showed that doxorubicin significantly up-regulated caspase-3 activity, whereas its combination with maximum sample aliquot of 0.01 μ g seemed to effectively depress (by about 60%) the activity of this apoptotic factor. The means of the results from all of the above experiments were different at a significance level of $P < 0.001$. In conclusion, our results showed a good antioxidant stability of the juice sample to lyophilization that may be reasonably regarded as a suitable process for the formulation of food supplements. In vitro experiments on cardiomyocyte cell culture indicated that low doses of *lioRGJ* were able to confer protection against both physiological reactive oxygen species (ROS) and doxorubicin-induced oxidant injury. It would be difficult to draw direct comparisons of our in vitro study, in which cardiomyocytes were directly exposed to *lioRGJ*, with animal models. Our data suggest for the juice sample the possibility to be employed as a food supplement with prospective cardioprotective benefits, although further studies are needed to optimize its dosages to avoid harmful pro-oxidant effects.

3.5 Metals

Excess of Fe and Cu cations in wine, determines turbidity and causes significant instability owing to catalysing oxidative reactions which modify taste characteristics. Furthermore, wine haziness induction (commonly called ‘casse’) is due to unstable colloid formation arising from reaction between Fe, Cu, proteins and other wine components. For all these reasons, a high level of these minerals is undesirable as is the presence of poorly soluble Ca which contributes to colloid flocculation and salt precipitation. If compared to the mean values of Fe, Cu and Ca detected in a broad range of Southern Italian red wines^[46] and American red wines^[47], the Aglianico wine samples presented low levels of these three elements (190.51, 1.60 and 8.34 mg/L for Fe, Cu and Ca, respectively) (Table 11). While the mean value of K concentration in wine is approximately 1 mg/L^[48], Aglianico wine samples resulted to have a mean concentration of 0.691 mg/L (Table 11). This is a positive feature, as a high K level negatively affects wine quality, colour, stability and taste, depending on potassium bitartrate formation. Some of the heavy metals present into the wine, such as Cd, Pb and Zn may be derived from soil contaminants, fungicidal residues, or winery equipments, and could represent a danger for human health if present in high concentrations. In our wine samples, the levels of Cd and Zn (0.20 and 4.55 µg/L, respectively) were markedly low if compared to the levels usually detected in red wines^[46]. The Pb concentration (61.96 µg/L), under the limit fixed by the Organization Internationale de la Vigne et du Vin^[49] is not negligible. Among heavy metals, Mn was present at a low level (17.34 µg/L) in wine (Table 11), and this could be related to its greater presence in grape seeds than in berry skin^[48]. Finally, the optimal balance of macro- and micro-elements in Aglianico grape and wine can give a definitive contribution to defining

the organoleptic and nutraceutical profile of this important but poorly studied grape variety.

Table 11: Macro- and micro-element content of berry skin ($n = 5$) and wine ($n = 9$) from Aglianico grapes. ND = not detected.

Element	Berry skin (mg/kg dry weight)	Wine ($\mu\text{g/L}$)
Ag	0.22 ± 0.04	2.16 ± 0.95
Al	8.10 ± 0.94	176.51 ± 0.02
Ca	332.99 ± 1.12	8.34 ± 0.15^a
Cd	0.02 ± 0.06	0.20 ± 0.01
Co	0.51 ± 0.07	9.42 ± 0.85
Cu	23.82 ± 0.79	1.60 ± 0.90^a
Fe	28.59 ± 0.73	190.51 ± 0.91
Ga	0.15 ± 0.05	9.35 ± 1.05
K	62.40 ± 0.21	691.00 ± 0.05
Mg	60.40 ± 2.53	6.12 ± 0.03
Mn	0.81 ± 0.03	17.34 ± 0.22
Mo	0.77 ± 0.02	17.75 ± 0.85
Na	1.16 ± 0.91	9.31 ± 0.20
Pb	1.76 ± 0.09	61.96 ± 0.96
Pt	0.01 ± 0.002	0.32 ± 0.04
Ru	3.67 ± 0.91	50.71 ± 1.23
Se	0.58 ± 0.09	ND
Sn	1.27 ± 0.75	16.27 ± 1.12
V	1.74 ± 0.87	29.94 ± 1.12
Zn	47.11 ± 1.11	4.55 ± 0.95

^a concentration in (mg/l).

4. References

- [1] Clarke, R. J.; Bakker, J. Wine Flavour Chemistry; Blackwell Publishing: Oxford, UK, **2004**.
- [2] Downey, M. O., Dokoozlian, N. K., & Krstic, M. P. Cultural practice and environmental impacts on the flavonoid composition of grape and wine: A review of recent research, *American Journal of Enology and Viticulture*, **2006**, 57, 257–268.
- [3] Goldberg, D. M., & Soleas, G. J. Resveratrol: Biochemistry, cell biology and the potential role in disease prevention. In M. Sandler & R. Pinder (Eds.), Wine. A scientific exploration New York: Taylor & Francis, **2003** (pp. 160–198).
- [4] Vermerris, W., & Nicholson, R. Phenolic compound biochemistry. Dordrecht: Springer. **2006**.
- [5] García-Alonso, M., Pascual-Teresa, S., Santos-Buelga, C., & Rivas Gonzalo, J. C. Evaluation of the antioxidant properties of fruits, *Food Chemistry*, **2004**, 84, 13–18.
- [6] Davalós, A., & Lasunción, M. A. Health-promoting effects of wine phenolics. In M. V. Moreno-Arribas & M. C. Polo (Eds.), Wine chemistry and biochemistry, New York: Springer, **2009**, (pp. 571–591).
- [7] Shao, Z.-H.; Becker, L. B.; Vanden Hoek, T. L.; Schumacker, P. T.; Li, C.-Q.; Zhao, D.; Wojcik, K.; Anderson, T.; Qin, Y.; Dey, L.; Yuan, C.-S. Grape seed proanthocyanidin extract attenuates oxidant injury in cardiomyocytes. *Pharmacological Research*, **2003**, 47, 463–469.
- [8] Shao, Z.-H.; Wojcik, K. R.; Dossumbekova, A.; Hsu, C.; Mehendale, S. R.; Li, C.-Q.; Qin, Y.; Sharp, W. W.; Chang, W.-T.; Hamann, K. J.; Yuan, C.-S.; Vanden Hoek, T. L. Grape seed proanthocyanidins protect cardiomyocytes from ischemia

and reperfusion injury via Akt-NOS signaling, *Journal of Cellular Biochemistry*, **2009**, 107, 697–705.

[9] Baydar, N. G.; Özkan, G.; Yaşar, S. Evaluation of the antiradical and antioxidant potential of grape extracts, *Food Control*, **2007**, 18, 1131–1136.

[10] Shao, Z.-H.; Vanden Hoek, T. L.; Xie, J.; Wojcik, K.; Chan, K. C.; Li, C.-Q.; Hamann, K.; Qin, Y.; Schumacker, P. T.; Becker, L. B.; Yuan, C.-S. Grape seed proanthocyanidins induce pro-oxidant toxicity in cardiomyocytes. *Cardiovascular Toxicology*, **2003**, 3, 331–339.

[11] Shao, Z. H.; Hsu, C. W.; Chang, W. T.; Waypa, G. B.; Li, J.; Li, D.; Li, C. Q.; Anderson, T.; Qin, Y.; Schumacker, P. T.; Becker, L. B.; Vanden Hoek, T. L. Cytotoxicity induced by grape seed proanthocyanidins: role of nitric oxide. *Cell Biology and Toxicology*, **2006**, 22, 149–158.

[12] Lluís, L.; Muñoz, M.; Nogués, M. R.; Sánchez-Martos, V.; Romeu, M.; Giralt, M.; Valls, J.; Solà, R. Toxicology evaluation of a procyanidin-rich extract from grape skins and seeds, *Food and Chemical Toxicology*, **2011**, 49, 1450–1454.

[13] Ribéreau-Gayon, P., Glories, Y., Maujean, A., & Dubourdieu, D. Dry extract and minerals. Handbook of enology: The chemistry of wine and stabilization and treatments, West Sussex, UK: John Wiley & Sons, Ltd, **2006**, (Vol. 2).

[14] Allen, R. G., Pereira, L. S., Raes, D., & Smith, M. Crop evapotranspiration. Guidelines for computing crop water requirements. FAO Irrigation and Drainage Paper No. 56. Rome, Italy: Food and Agriculture Organization of the United Nations, **1998**,

[15] Singleton, V. L.; Rossi, J. A., Jr. Colorimetry of total phenolics with phosphomolybdic-phosphotungstic acid reagents, *American Journal of Enology and Viticulture*, **1965**, 16, 144–158.

- [16] Zhishen, J.; Mengcheng, T.; Jianming, W. The determination of flavonoid contents in mulberry and their scavenging effects on superoxide radicals. *Food Chemistry*, **1999**, 64, 555–559.
- [17] Giusti, M. M.; Wrolstad, R. E. Characterization and measurement of anthocyanins by UV-visible spectroscopy.; Wrolstad, R. E., Acree, T. E., An, H., Decker, E. A., Penner, M. H., Reid, D. S., Schwartz, S. J., Shoemaker, C. F., Sporns, P., Eds.; Wiley: New York, *In Current Protocols in Food Analytical Chemistry*, **2001**; pp F1.2.1–F1.2.13.
- [18] Brand-Williams, W., Cuvelier, M. E., & Berset, C. Use of free radical method to evaluate antioxidant activity, *Lebensmittel-Wissenschaft und Technologie*, **1995**, 28, 25–30.
- [19] Taylor, V. N., Longrich, H. P., & Greenough, J. D. Multielement analysis of Canadian wines by inductively coupled plasma mass spectrometry (ICP-MS) and multivariate statistics, *Journal of Agricultural and Food Chemistry*, **2003**, 51, 856–860.
- [20] Vanden Hoek, T. L.; Shao, Z. H.; Li, C. Q.; Schumacker, P. T.; Becker, L. B. Mitochondrial electron transport can become a significant source of oxidative injury in cardiomyocytes, *Journal of Molecular and Cellular Cardiology*, **1997**, 29, 2441–2450.
- [21] Kirshenbaum, L. A.; Singal, P. K. Changes in antioxidant enzymes in isolated cardiac myocytes subjected to hypoxiareoxygenation, *Laboratory Investigation*, **1992**, 67, 796–803.
- [22] Gawel, R. Red wine astringency: A review, *Australian Journal of Grape and Wine Research*, **1998**, 4, 74–95.
- [23] Bermúdez-Soto, M. J.; Tomás-Barberán, F. A. Evaluation of commercial red fruit juice concentrates as ingredients for antioxidant functional juices, *European Food Research and Technology*, **2004**, 219, 133–141.

- [24] Castillo-Muñoz, N., Gómez-Alonso, S., García-Romero, E., & Hermosín Gutiérrez, I. Flavonol profiles of *Vitis vinifera* red grapes and their single-cultivar wines, *Journal of Agricultural and Food Chemistry*, **2007**, 55, 992–1002.
- [25] Lee, J., Jung, E., & Lee, J. Isorhamnetin represses adipogenesis in 3T3-L1 cells, *Obesity*, **2009**, 17, 226–232.
- [26] Zhang, Y., Chen, A. Y., Li, M., Chen, C., & Yao, Q. Ginkgo biloba extract kaempferol inhibits cell proliferation and induces apoptosis in pancreatic cancer cells, *Journal of Surgical Research*, **2008**, 148, 17–23.
- [27] Talcott, S. T.; Lee, J. H. Ellagic acid and flavonoid antioxidant content of Muscadine wine and juice, *Journal of Agricultural and Food Chemistry*, **2002**, 50, 3186–3192.
- [28] Gawel, R. Red wine astringency: a review, *Australian Journal of Grape and Wine Research*, **1998**, 4, 74–95.
- [29] Makris, D. P., Kallithraka, S., & Kefalas, P. Flavonols in grapes, grape products and wines: Burden, profile and influential parameters, *Journal of Food Composition and Analysis*, **2006**, 19, 396–404.
- [30] Frankel, E. N., Bosanek, C. A., Meyer, A. S., Silliman, K., & Kirk, L. L. Commercial grape juices inhibit the in vitro oxidation of human low-density lipoproteins, *Journal of Agricultural and Food Chemistry*, **1998**, 46, 834–838.
- [31] Hassimotto, N. M. A., & Lajolo, F. M. Antioxidant status in rats after longterm intake of anthocyanins and ellagitannins from blackberries, *Journal of the Science of Food and Agriculture*, **2011**, 91, 523–531.
- [32] Romero-Cascales, I., Ortega-Regules, A., López-Roca, J. M., Fernández-Fernández, J. I., & Gómez-Plaza, E. Differences in anthocyanin extractability from grapes to wines according to variety, *American Journal of Enology and Viticulture*, **2005**, 56, 212–219.

- [33] Gómez-Alonso, S., Fernández-González, M., Mena, A., Martínez, J., & García-Romero, E. Anthocyanin profile of Spanish *Vitis vinifera* L. red grape varieties in danger of extinction, *Australian Journal of Grape and Wine Research*, **2007**, 13, 150–156.
- [34] Revilla, E., García-Beneytez, E., & Cabello, F. Anthocyanin fingerprint of clones of Tempranillo grapes and wines made with them, *Australian Journal of Grape and Wine Research*, **2009**, 15, 70–78.
- [35] Boss, P. K., Davies, C., & Robinson, S. P. Anthocyanin composition and anthocyanin pathway gene expression in grapevine sports differing in berry skin colour, *Australian Journal of Grape and Wine Research*, **1996**, 2, 163–170.
- [36] Santos-Buelga, C., & de Freitas, V. Influence of phenolics on wine organoleptic properties. In M. V. Moreno-Arribas & M. C. Polo (Eds.), *Wine chemistry and biochemistry* **2009**, (pp. 529–570). New York: Springer.
- [37] Feijóo, O., Moreno, A., & Falqué, E. Content of trans- and cis-resveratrol in Galician white and red wines, *Journal of Food Composition and Analysis*, **2008**, 21, 608–613.
- [38] Stervbo, U., Vang, O., & Bonnesen, C. A review of the content of the putative chemopreventive phytoalexin resveratrol in red wine, *Food Chemistry*, **2007**, 101, 449–457.
- [39] Landbo, A. K.; Meyer, A. S. Ascorbic acid improves the antioxidant activity of European grape juices by improving the juices' ability to inhibit lipid peroxidation of human LDL in vitro, *International Journal of Food Science & Technology*, **2001**, 36, 727–735.
- [40] Spayd, S. E.; Tarara, J. M.; Mee, D. L.; Ferguson, J. C. Separation of sunlight and temperature effects on the composition of *Vitis vinifera* cv. Merlot berries, *American Journal of Enology and Viticulture*, **2002**, 53, 171–182.

- [41] Michalczyk, M.; Macura, R.; Matuszak, I. The effect of airdrying, freeze-drying and storage on the quality and antioxidant activity of some selected berries, *Journal of Food Processing and Preservation*, **2009**, 33, 11– 21.
- [42] Wood, J. G., Rogina, B., Lavu, S., Howitz, K., Helfand, S. L., Tatar, M., et al. Sirtuin activators mimic caloric restriction and delay ageing in metazoans, *Nature*, **2004**, 430, 686–689.
- [43] Schlesier, K., Harwat, M., Bohm, V., & Bitsch, R. Assessment of antioxidant activity by using different in vitro methods, *Free Radical Research*, **2002**, 36, 177–187.
- [44] Radovanovi, A., Radovanovi, B., & Jovanievi, B. Free radical scavenging and antibacterial activities of Southern Serbian red wines, *Food Chemistry*, **2009**, 117, 326–331.
- [45] Picq, M.; Dubois, M.; Munari-Silem, Y.; Prigent, A. F.; Pacheco, H. Flavonoid modulation of protein kinase C activation, *Life Sciences*, **1989**, 44, 1563–1571.
- [46] Volpe, M. G., La Cara, F., Volpe, F., De Mattia, A., Serino, V., Petitto, F., et al. Heavy metal uptake in the enological food chain, *Food Chemistry*, **2009**, 117, 553–560.
- [47] Bentlin, F. R. S., Pulgati, F. H., Dressler, V. L., & Pozebon, D. Elemental analysis of wines from South America and their classification according to country, *Journal of the Brazilian Chemical Society*, **2011**, 22, 327–336.
- [48] Conde, C., Silva, P., Fontes, N., Dias, A. C. P., Tavares, R. M., Sousa, M. J., et al. Biochemical changes throughout grape berry development and fruit and wine quality, *Food*, **2007**, 1, 1–22.
- [49] O.I.V. Office International de la Vigne et du Vin. Compendium of International methods of wine and must analysis. Paris, **2011**.